

THESIS

EVALUATING THE LONG-TERM DURABILITY OF FIBER REINFORCED
POLYMERS VIA FIELD ASSESSMENTS OF REINFORCED CONCRETE
STRUCTURES

Submitted by

Douglas Gregory Allen

Department of Civil and Environmental Engineering

In partial fulfillment of the requirements

For the degree of Master of Science

Colorado State University

Fort Collins, Colorado

Fall 2011

Master's Committee:

Advisor: Rebecca Atadero

Paul R. Heyliger

Don Radford

UMI Number: 1503551

All rights reserved

INFORMATION TO ALL USERS

The quality of this reproduction is dependent on the quality of the copy submitted.

In the unlikely event that the author did not send a complete manuscript and there are missing pages, these will be noted. Also, if material had to be removed, a note will indicate the deletion.



UMI 1503551

Copyright 2011 by ProQuest LLC.

All rights reserved. This edition of the work is protected against unauthorized copying under Title 17, United States Code.



ProQuest LLC.
789 East Eisenhower Parkway
P.O. Box 1346
Ann Arbor, MI 48106 - 1346

ABSTRACT

EVALUATING THE LONG-TERM DURABILITY OF FIBER REINFORCED POLYMERS VIA FIELD ASSESSMENTS OF REINFORCED CONCRETE STRUCTURES

Fiber Reinforced Polymer Composites (FRP) are an attractive repair option for reinforced concrete structures, however their long term performance in field environments is not well understood. Laboratory durability tests have indicated that FRP generally performs quite well, but these laboratory tests cannot model the synergistic effects that occur when the FRP is in-service on a bridge (or other structure). Field assessments of FRP properties are very rare in the literature. This thesis describes an effort to collect in-situ data about a FRP repaired concrete arch bridge.

The Castlewood Canyon Bridge on Colorado state highway 83 was reconstructed in 2003. The reconstruction included replacement of the deck and spandrel columns and repair of the existing concrete arches with externally bonded FRP. The FRP had been in service for 8 years when its condition was assessed for this project.

Assessment efforts started with collection of as much information as possible about the materials and techniques used for repair. Unfortunately only limited amounts of initial or baseline data were recovered. Based on available information a tentative plan for site assessment activities was prepared, including testing locations at the base and crest of the arch.

The field assessment of the bridge was completed on location during July, 2011. The complete extrados of the east arch was inspected for voids between the concrete and FRP using acoustic sounding and thermalgraphic imaging. Voids that were previously identified during a routine bridge inspection in 2007 had grown significantly larger by the 2011 assessment. Pull-off tests were used to test the bond strength at the base and top of the arch. Pull-off strengths were on average lower and represented different failure modes from pull-off tests conducted at the time of repair. Large debonded regions of FRP were cut from the structure to use in laboratory testing. Damaged regions were repaired with new FRP.

Materials brought back from the bridge were used for tensile and Differential Scanning Calorimetry (DSC) testing. The tensile tests showed that the FRP strength was well below the specified design strength, but the lack of initial data makes it difficult to tell if the material has deteriorated over time, or if the material started off with lower strengths due to field manufacture techniques. The DSC tests showed that the glass transition temperature of the composites was near the value suggested by the manufacturer.

The field assessment was used as a case study in collecting durability data about FRP. From this case study numerous recommendations are made to improve the available information about the durability of FRP repairs in field environments. A specific process to be followed in collecting this data is also proposed.

ACKNOWLEDGEMENTS

I would like to thank my advisor, Dr. Atadero, for her guidance and assistance with Oscar Mata physically completing the case study portion of this thesis at the Castlewood Canyon Bridge. Also instrumental in the field assessment at the bridge were CDOT's personnel Thomas Moss and David Weld. Other CDOT personnel that helped shape the project through meetings and feedback were Mike Mohseni, Aziz Khan, Trevor Wang, Matt Greer, Eric Prieve, and William Outcalt. Steve Olsen and Stephen Henry provided the instruction and use of the thermal camera, and Bill Schiebel and Roman Jauregui coordinated to provide the box of files from the project. Nickolas Dickens graciously provided a special use permit. Dr. Radford's instruction and guidance in regard to differential scanning calorimetry and glass transition temperature interpretation were deeply appreciated. I would also like to thank Steve Nunn and Olley Scholer for providing the FRP materials for the repair of the damaged areas caused during the case study and their participation to smoothly accommodate our needs and inquiries of material properties etc. Janice Barman and JR Santos provided their services in acquiring materials and the manufacturing of the aluminum pucks used for the pull-off tests. I am grateful for the participation of Dr. Heyliger, Dr. Radford, and Dr. Atadero as members of my committee. Lastly, I feel forever indebted to my lovely wife, Emilie, for her continued love and support through my toils.

CONTENTS

1 Introduction	1
1.1 Overview	1
1.1.1 Failing Infrastructure and Bridges and Fiber Reinforced Polymers (FRP) as a Repair Material	1
1.1.2 A Closer Look at FRP	4
1.2 Objective and Method	6
1.3 Organization of Thesis	7
2 Literature Review	9
2.1 Durability of FRP	9
2.1.1 Accelerated Ageing	13
2.2 Field Assessments	16
2.2.1 Macedonia, 2008	16
2.2.2 Northwest Region of U.S., 2005	18
2.2.3 New York, 2004	19
2.2.4 Utah, 2004	21
2.2.5 Summary of Field Evaluations of Durability	24
2.3 Nondestructive Evaluation Methods	26
2.3.1 Acoustic Sounding	27
2.3.2 Thermalgraphic Imaging	28
2.4 Tests	29
2.4.1 Pull-off Tests	29
2.4.2 Differential Scanning Calorimetry (DSC)	31
3 Case Study	34
3.1 The Castlewood Canyon Bridge	34
3.2 Renovation in 2003	37
3.2.1 Replacement of Spandrel Columns, Pier Caps, and Bridge Deck	37
3.2.2 Repair of Arches and Struts	39
3.2.3 Initial Values and Quality Control of the Renovation in 2003	42
3.2.3.1 Tensile Properties of CFRP	42

3.2.3.2 Bond Strength of CFRP	44
3.3 Biannual Bridge Inspections	47
3.4 Field Assessment of the Castlewood Canyon Bridge	51
3.4.1 Planning Tests and Locations	51
3.4.2 Preliminary Site Visit	54
3.4.3 Void Detection	59
3.4.4 Pull-off Tests	61
3.4.5 Collecting Specimens for Laboratory Testing	75
3.4.6 CFRP Repair	80
3.5 Laboratory Tests at Colorado State University	84
3.5.1 Tensile Tests	84
3.5.2 Differential Scanning Calorimetry (DSC)	94
3.6 Summary of Field Assessment and Laboratory Testing	104
4 Developing a Durability Model of FRP	106
4.1 Durability of FRP in Field Environments	107
4.1.1 What was learned in the Case Study?	108
4.1.2 Mock Example	114
5 Summary, Conclusion, and Additional Areas of Research	123
5.1 Summary	123
5.2 Conclusions	124
5.3 Additional Areas of Research	127
References	130
Appendices	136
Appendix A: Voids, Defects, and Thermal Images	136
Appendix B: Pull-off Tests	152
Appendix C: Tensile Tests	162
Appendix D: DSC	165

LIST OF FIGURES

3.1 Castlewood Canyon Bridge location indicated by the red star.....	34
3.2 Castlewood Canyon Bridge (Mohseni, CDOT).....	35
3.3 Castlewood Canyon Bridge prior to the 2003 repair (Mohseni, CDOT).....	36
3.4 Castlewood Canyon Bridge after the 2003 repair (Mohseni, CDOT).....	36
3.5 Plan view of the arches, struts, and column pedestals showing the bay labeling Scheme.....	37
3.6 Systematically replacing the bridge deck (Mohseni, CDOT).....	38
3.7 Placing the new spandrel columns adjacent to the existing columns (Mohseni, CDOT).....	38
3.8 Concrete spalling on arch section prior to repair (Mohseni, CDOT).....	39
3.9 Concrete spalling on arch section prior to repair (Mohseni, CDOT).....	39
3.10 Removal of loose concrete using 6.8 kg (15 lbs.) jackhammer (Mohseni, CDOT).....	39
3.11 Restoring the cross section with shotcrete (Mohseni, CDOT).....	39
3.12 Fyfe’s Tyfo® S Epoxy resin (likely with glass fibers as a filler) being applied to the extrados of an arch (Mohseni, CDOT).....	41
3.13 Installation of saturated unidirectional CFRP fabric, Tyfo® SCH-41 (Mohseni, CDOT).....	41
3.14 Longitudinal and transverse CFRP wraps at the base of an arch (Mohseni, CDOT).....	41
3.15 Void injected with resin during 2003 renovation (Mohseni, CDOT).....	45
3.16 Pull-off test locations from 2003 denoted in red.....	46
3.17 Outlined in permanent marker are identified areas of debonding between the FRP and the substrate developed in the structure between inspections in 2007 and 2011. Faintly denoted in the bottom of the photographs (enclosed in red circles) are previously found voids identified with “DELAM 07” and lines distinguishing the boundaries of the voids.....	49
3.18 Outlined in permanent marker are identified areas of debonding between the FRP and the substrate developed in the structure between inspections in 2007 and 2011. Faintly denoted in the bottom of the photographs (enclosed in red circles) are previously found voids identified with “DELAM 07” and lines distinguishing the boundaries of the voids.....	49

3.19 Enclosed in permanent marker are identified areas of debonded areas between the FRP and the substrate from 2011 and June, 2007. Notice in this more protected bay of the structure the markings from 2007 are more clearly visible	50
3.20 Crack identified in 2007	50
3.21 Thermal image from an infrared camera of two voids, (appearing yellow), found in 2011 on the 1 st bay on the north side of the east arch	59
3.22 Photograph of two voids, found in 2011 on the 1 st bay on the north side of the east arch	59
3.23 Two identified voids during the 2011 inspection, visible cracks in CFRP	60
3.24 Pull-off test locations highlighted in red	62
3.25 Damage caused by core bit without the use of the jig	63
3.26 Starting a core hole using a wooden jig	64
3.27 The core drilling location that failed due to torsional stresses during the core drilling process, bay 1NW	65
3.28 The core drilling location that failed due to torsional stresses during the core drilling process, bay 1NW	65
3.29 Removing water and debris from core cuts	65
3.30 Removing the acrylic paint later before adhering the aluminum pucks	66
3.31 Prepared areas for the adhesion of aluminum pucks for pull-off tests and a close-up of a prepared surface	66
3.32 Prepared areas for the adhesion of aluminum pucks for pull-off tests and a close-up of a prepared surface	66
3.33 Aluminum pucks before and after sanding with 40 grit sandpaper	67
3.34 Preparing the aluminum pucks way up high on the arch	67
3.35 Adhered aluminum pucks for pull-off tests	68
3.36 Spherical headed bolt threaded into puck	68
3.37 Placing the pull-off tester to engage the spherical headed bolt	68
3.38 Conducting a pull-off test with the digital manometer reading	69
3.39 Removing the tested puck from the pull-off tester	69
3.40 Failure Mode A: bonding adhesive failure at loading fixture	69
3.41 Failure Mode E: Adhesive failure at CFRP/substrate adhesive interface	69
3.42 Failure Modes B and F: cohesive failure in FRP laminate, and mixed cohesive failure in substrate and adhesive failure at the adhesive/substrate interface, respectively	70
3.43 Failure Mode G: cohesive failure in concrete substrate	70
3.44 Failure Modes of Pull-off Tests from 2003 and 2011	71
3.45 Histogram of Pull-off Test Strength	74
3.46 PDF of Pull-off test results	74
3.47 Areas removed are highlighted in green	76
3.48 Void in CFRP with transverse crack identified with red arrows	77
3.49 Cutting the perimeter of the void in the CFRP	77
3.50 Water exiting the void area directly after the lower cut through the CFRP was completed	78

3.51 Cracks in the substrate were transmitted through the CFRP and notice the smooth texture and blue and white color of the underside of the CFRP	78
3.52 Cracks in the substrate were transmitted through the CFRP and notice the smooth texture and blue and white color of the underside of the CFRP	78
3.53 Voids found in the 3 rd bay on the north end of the east arch	79
3.54 Removal of the CFRP of the largest void	79
3.55 Epoxy filled holes following the pull-off tests	80
3.56 Applying a primer coat to the areas for repair	81
3.57 Allocating fabric for repair	83
3.58 Applying the second layer of CFRP to the area of pull-off tests on the east arch	83
3.59 The repaired sections on the north end of the arches	83
3.60 The repaired sections on the north end of the arches	83
3.61 The rough contour of a tensile test strip of CFRP	85
3.62 Failed tensile test specimens from the large void removed from bay 3NE, note the oatmeal appearance	86
3.63 Failed tensile test specimens from the small void removed from bay 1NE, note the milky appearance	87
3.64 Distribution of Tensile Strength Results	87
3.65 Distribution of Modulus of Elasticity Results	88
3.66 Probability Density Function of the Two Samples, Tensile Strengths	90
3.67 Probability Density Function of All Tensile Tests	90
3.68 Probability Density Function of the two samples, Modulus of Elasticity	91
3.69 Probability Density Function of All Modulus of Elasticity Samples	91
3.70 Probability Density Function of the Rupture Strain of All Tensile Tests	93
3.71 Ground CFRP, Diced CFRP, and Diced Filler Resin	95
3.72 DSC Specimen Chamber	96
3.73 DSC with Liquid Nitrogen	96
3.74 Temperature vs. Time of the DSC Analysis for the Ground CFRP1 Specimen ..	97
3.75 Ground CFRP Specimen	98
3.76 Ground CFRP1A	99
3.77 Heat-Cool-Reheat-Cool of the Same Specimen	100
3.78 Ground CFRP2	100
3.79 Ground and Diced CFRP DSC Results	101
3.80 Filler Resin DSC Results	102
A1 Bay 1NW, 2 of the 3 small voids and rust spot	139
A2 Photograph and thermal image of rust spot	139
A3 Bay 1NE, 5 voids	140
A4 Bay 1NE, 4 of the 5 voids; Crack exists, enclosed in red oval, in the top of the largest void	140
A5 Photograph and thermal image of two voids in Bay 1NE	141
A6 Bay 2NE, 3 Voids	141
A7 Bay 2NE, Crack enclosed in red oval was identified in 2007	142

A8 Previously identified in 2007, a crack enclosed in the red oval, no debonding at the location of the crack.....	142
A9 Bay 3NE with 1 of the 2 defects found in 2007 shown.....	143
A10 4 of the 5 voids found in 2011.....	143
A11 Enclosed in the red circle is 1 of the 2 voids found in 2007.....	144
A12 Photograph and thermal image of a seam in the CFRP sheets, no void present.....	144
A13 Bay 4NE, V-shaped silicone bead water diverter.....	145
A14 Bay 5NE.....	145
A15 Bay 5SE.....	146
A16 Bay 4SE.....	147
A17 Void from 2007 has grown and a new void developed.....	147
A18 Bay 3SE.....	148
A19 Thermal image of cracks previously identified in 2007.....	148
A20 Bay 2SE.....	149
A21 Photograph and thermal image of two voids.....	149
A22 Photograph and thermal image of two voids, the black color in the photograph is left over strain gauges from the work done by Colorado University of Boulder.....	150
A23 Bay 1SE, 1 void.....	150
A24 Photograph and thermal image of a defect found in Bay 1SW.....	151
B1 Test No.1.....	156
B2 Test No. 2.....	156
B3 Test No.3.....	156
B4 Test No.5, note puck slid off of center while epoxy was setting.....	156
B5 Test No. 6.....	156
B6 Test No.7.....	157
B7 Test No.8, weak bond strength.....	157
B8 Test No.9, weak bond strength.....	157
B9 Test No.10, weak bond strength.....	158
B10 Test No.12, weak bond strength.....	158
B11 Test No.13, weak bond strength.....	158
B12 Test No.14, weak bond strength.....	159
B13 Test No.15, weak bond strength.....	159
B14 Test No.17.....	159
B15 Test No.18.....	159
B16 Test No.19.....	160
B17 Test No.20.....	160
B18 Test No.21.....	160

B19 Test No.22.....	160
B20 Test No.23, weak bond strength (poorly mixed concrete?).....	161
B21 Test No.24.....	161
B22 Test No.25.....	161
B23 Test No.26 note very weak bond strength (poorly mixed concrete?).....	161
B24 Test No.27.....	161
D1 Differential Scanning Calorimetry Curves.....	165
D2 Close up of T_g Regions.....	165
D3 Close up of T_g Regions.....	166

LIST OF TABLES

3.1	ASTM D7522 Failure Modes.....	46
3.2	Failure Modes of the pull-off tests conducted in 2003.....	47
3.3	Summary of Failure Modes for the Pull-off Tests.....	70
3.4	Pull-off Test Results of Failure Mode G Tests.....	72
3.5	Material Properties of the Existing and Repair Materials.....	82
3.6	ASTM D3039 Letter Codes for Failure Modes.....	86
3.7	Material Properties of 2003 CFRP.....	88
3.8	Statistics from the Tensile Samples.....	89
3.9	Tyfo SCH-41 Rupture Strain Values.....	92
3.10	Rupture Strain Values from the 2011 Tensile Tests.....	93
3.11	Glass Transition Temperatures of CFRP and Filler Resins.....	103
4.1	Quantities of Samples and Specimens.....	121
4.2	Specific Amounts for Mock Example.....	121
A1	Summary of Voids on the Extradoses of the Entire East Arch and One Bay of the West Arch.....	137
A2	Summary of Cracks on the Extradoses of the Entire East Arch.....	138
A3	Summary of Rust on the Extradoses of the Entire East Arch and One bay of the West Arch.....	138
B1	Pull-off Test Results from 2011.....	152
B2	Pull-off Test Results from 2003.....	153
B3	Average Values of Bond Strength.....	155
C1	2011 Tensile Tests.....	162
C2	Average Values for each Sample.....	164

CHAPTER 1: INTRODUCTION

1.1 Overview

1.1.1 Failing Infrastructure, Bridges and Fiber Reinforced Polymers (FRP) as a Repair Material

In 2009, the American Society of Civil Engineers (ASCE) published an assessment of the United States' infrastructure in the form of a report card. The infrastructure was differentiated into the following categories: Water and Environment, Transportation, Public and Facilities, and Energy. The bridge section, within the Transportation category, earned a grade of "C" requiring approximately "\$17 Billion of annual investment to substantially improve current bridge conditions" (ASCE 2009). It is estimated that "more than 26%, or one in four, of the nation's bridges are either structurally deficient or functionally obsolete" (ASCE, 2009). A political awareness of the precarious state of US bridges has sprouted due to the recent tragic structural failure of the I-35W bridge in Minneapolis in 2007, in which 13 people died (Sofge, 2009). This reckoning has spurred on funding of infrastructure with approximately \$50 billion announced by President Obama on Labor Day of 2010 (Huffpost, 2010). In order to maximize the return on this investment, it is critical that an efficient approach is implemented in the maintenance, repair, and replacement of our bridges.

A proactive and preventative management approach proves to be more cost effective considering life cycle costs of structures such as bridges. In *"Too Big to Fall"*, Barry LePatner (2010) recognizes the need for well managed resources by emphasizing W.R. De Sitters "law of fives", which estimates that "when maintenance is neglected, repairs when they become essential will generally equal five times maintenance costs; if repairs are not made even then, rehabilitation costs will be five times repair costs."

Coomarasamy and Goodman (1999) compare FRP with steel as repair materials stating "the main advantages of FRP over steel for this application are that the FRP materials do not corrode, have better electromagnetic properties, and have a higher ratio of strength to mass density." Tan et al. (2011) adds "Due to the lightweight and high-strength, low costs, and convenience of construction, the strengthening method of using bonded FRP has gradually taken the place of the traditional steel-encased method and bonding steel method."

Though FRP has potential as being an excellent solution to many of the structurally deficient reinforced concrete bridges, this relatively recent innovation has limited history (especially in field applications) and therefore its durability needs to be verified. Chin et al. (1997) describes the need for and importance of conducting durability studies on FRP materials:

"With the continuous deterioration of the world's infrastructure, it has become increasingly urgent to determine the feasibility of using high-performance polymer composite materials in fabricating new structures as well as rehabilitating existing ones."

Moreover, “The durability of polymer composites is one of the primary issues limiting the acceptance of these materials in infrastructural applications” (Chin et al., 1997).

In an effort to satisfy the durability concerns, multiple durability studies have been conducted in laboratories. The durability of FRP has been evaluated with accelerated ageing through varying exposures to environments, solutions, and temperatures. In some cases specimens have been aged on-site and/or with control specimens. Inspiring a principle objective of this thesis, Karbhari et al. (2003) determined “It is well established that durability data generated through laboratory experiments can differ substantially from field data.” Similarly, Byars et al. (2003) contributed “accelerated exposure data and real-time performance are unlikely to follow a simple linear relationship and the relationships have yet to be confidently determined”. Through field assessments additional information can be gathered, “data that is invaluable to the establishment of appropriate durability based design factors” (Karbhari et al. 2003).

A field assessment was conducted on the Castlewood Canyon Bridge as the case study for this thesis to contribute to the long-term durability evaluation of fiber reinforced polymer (FRP) materials used as externally bonded reinforcement for existing reinforced concrete structures. Castlewood Canyon Bridge, built in 1946 and repaired in 2003, is a reinforced concrete arch bridge that spans Cherry Creek in Castlewood Canyon State Park on Highway 83, south of Franktown, CO. Externally applied FRP provided additional tensile reinforcement after the steel reinforcement had endured

corrosion. A comprehensive field assessment was conducted to evaluate the 2003 FRP installation and identify the presence, location and severity of damage. By collecting field data, the development of degradation can be further understood. As a result, the process of collecting and documenting field data from conducting a field assessment was established and refined.

1.1.2 A Closer Look at FRP

Fiber reinforced polymers are manufactured into bars or a fabric that is saturated with resin in a “wet layup” process and are applied externally or “near surface mount” (NSM) to provide tensile reinforcement to structures or structural members. Repair and strengthening, terms used interchangeably throughout this paper, in shear and/or flexure with wet layup of carbon fiber reinforced polymers (CFRP) on reinforced concrete substrates are the main focus in this durability study.

Bakis et al. (2002) described FRP as a “combination of high-strength, high-stiffness structural fibers with lightweight, environmentally resistant polymers” creating “composite materials with mechanical properties and durability better than either of the constituents alone.” The performance of FRP is dependent on the ability to transfer stresses which relies on maintaining its material properties, bond strength, and the strength of its substrate. Similar to the development length of rebar, Hu et al. (2004) describes the importance of bond to the performance of the composite, “The usual strengthening method is to bond the FRP laminates on the surface of concrete structures, so the effect of strengthening is dependent on the bond behavior between FRP laminates and concrete substrate.”

FRP has significant advantages to consider when compared with the strengthening alternatives of using external steel plates or rebuilding large sections. Strengthening reinforced concrete structures with FRP adds very little dead weight to the structure and can be conducted relatively quickly, inexpensively, and with minimal impact on traffic of lane closures or delays (Holloway, 2011). Holloway (2011) adds “Manufacturing technologies allow optimization and control of the structure of the composite, e.g. fiber-matrix interactions, the fiber/volume ratio, degree of cure and fiber arrangement.” These technologies provide the ability to “optimize the formation process in terms of economics, productivity, product performance, quality, and reproducibility” (Holloway, 2011). Fiber reinforced polymers offer a much needed solution to an overwhelming concern of safety that is our degrading infrastructure.

Environmental exposure and the quality of the on-site manufacturing process (wet layup) can adversely affect the durability of FRP. Karbhari et al. (2003) identifies the following environmental conditions of primary importance pertaining to the durability of FRP composites: “moisture/solution, alkali, thermal (including temperature cycling and freeze-thaw), creep and relaxation, fatigue, ultraviolet, and fire.” Saenz et al. (2004) similarly identifies from Harries et al. (2003) findings “In 2002, ACI Subcommittee 440-D recognized that the most critical need for additional research is environmental durability of FRP composite materials in concrete applications. ACI Subcommittee 440-L established that the most critical and unique civil engineering environments to evaluate are moisture, salt, and freezing and thawing, because these environments are typically found in highway infrastructure.”

1.2 Objective and Method

The initial intention of this work was to conduct a field assessment to provide some of the much needed data on the durability of FRP in field environments. In initiating the process of conducting a field assessment many difficulties were encountered which in turn further shaped and defined the goal and objectives of this thesis. The more robust goal also includes establishing a procedure starting at the time of FRP repair that will facilitate field assessments over the service life of the composite to evaluate its durability. In order to reach this goal, the following objectives are pursued:

- Conduct a field assessment of an FRP repair and establish limitations or weaknesses of current procedures followed at the time of repair and information available for assessment.
- Evaluate the durability of the FRP application to the extent possible with the field assessment data
- Propose enhanced procedures that would facilitate and improve the quality of future assessments and lead to more usable durability data.
- Provide an example demonstrating the feasibility of the proposed procedures.

To achieve the objectives previously explained, a case study was developed. An FRP repaired reinforced concrete bridge, Castlewood Canyon Bridge on Highway 83 in Colorado, was identified as a candidate for a field assessment. Inspection, evaluation, and testing techniques that could identify the presence, location, and severity of damage were chosen. The inspection, evaluation, and testing techniques were

conducted on the case study bridge. Values from the inspection, evaluation, and testing techniques were compared to baseline values, previous values, and/or design minimums to apply judgment as to how the structures response is affected.

The process described here as the method was then evaluated and areas of potential improvement or optimization were identified. Improving the field assessment process consists of causing less damage to the inspected structure while recovering valuable data that can be more meaningful due to consistent and thorough documentation.

1.3 Organization of Thesis

This thesis is comprised of five chapters. This chapter is Chapter 1: Introduction, which begins with an overview of the condition of infrastructure and proceeds to narrower in focus on bridges and FRP repairs. Following the overview, the objective of the thesis is explained as well as the method in which the objective is attained. Concluding the Introduction is this section on the organization of the thesis.

Chapter 2: Literature Review provides the background and additional information on topics of significance to the remainder of the thesis. The topics that are addressed include: durability of FRP, needs for data from field assessment and previously conducted field assessments, and available evaluation and testing methods.

The actual process taken to satisfy the previously mentioned need of acquiring data from field assessments is found in Chapter 3: Methods, Case Study. This chapter describes the inspections and a test conducted on the Castlewood Canyon Bridge and presents the results from the procedures. Chapter 3 also describes the procedure and

results of the tests conducted in the laboratories with specimens that were taken from the bridge.

Chapter 4, Developing a Durability Model for FRP, was established from the undertakings within Chapter 3. The difficulties posed by Chapter 3 became elements of ways to improve the existing practices to accommodate a more streamline and robust process of field assessments.

The final chapter, Chapter 5, is a summary and conclusion of the thesis and describes additional areas of research.

Chapter 2: Literature Review

2.1 Durability of FRP for Repair

Tan et al. (2011) explains that “though the main factors affecting durability and failure mechanism of concrete have been fully investigated, few studies on the durability of FRP reinforced structures have been taken” and “factors affecting the durability of FRP reinforced structures should be analyzed.” Tan et al. (2011) defines the term “durability” as:

“the given structure under conditions of normal designing, constructing, serving and maintaining can continue to perform its intended functions during the specified or traditionally expected service life, in spite of structural performance deteriorating with time.”

Similarly, the Civil Engineering Research Foundation (CERF) and the Market Development Alliance (MDA) of the FRP Composites Industry in collaboration with Karbhari et al. (2000) defined the term “durability” with respect to fiber reinforced polymer composites as “the ability to resist cracking, oxidation, chemical degradation, delamination, wear, and/or, the effects of foreign object damage for a specified period of time, under the appropriate load conditions, under specified environmental conditions” in their study of “Critical Gaps in Durability Data for FRP Composites in Civil Infrastructure.” The term “durability” used throughout this thesis will be inclusive of both definitions provided above by Tan et al. (2011) and Karbhari et al. (2000).

FRP materials have potentially high overall durability, however, Karbhari et al. (2000) notes that “there is evidence of rapid degradation of specific types of FRP composites when exposed to certain environments” and “actual data on durability is sparse, not well documented, and in cases where available – not easily accessible to the civil engineer.” Karbhari et al. (2000) continues that there is a “wealth of contradictory data published in a variety of venues” resulting from the “reporting of data without sufficient detail of the actual materials used, use of different forms of materials and processing techniques, and even changes in the materials systems with time” (Karbhari et al. 2000). Seven years later, Chen et al. (2007) agrees “although a number of durability studies on FRP have been reported by various researchers, no general conclusions are possible as researchers used different testing procedures and conditions. In some cases, even conflicting results have been reported.”

The durability of an FRP composite is compromised if the material properties of the FRP appreciably change or if the bond between layers of FRP or between the FRP and its substrate becomes weak or is lost all together. Karbhari and Ghosh (2009) identify the critical components of the performance of externally applied FRP, stating “since the composite element is bonded onto the concrete substrate the efficacy of the rehabilitation scheme depends on the combined action of the entire system with emphasis on the integrity and durability of the bond between the FRP and concrete.” Karbhari and Ghosh (2009) add “the performance characteristics of the substrate, FRP, adhesive/resin forming the bond and the interfaces can all be deteriorated by environmental exposure and hence there is a need to assess its effect on these

materials and on the bond itself.” Byars et al. (2003) agrees contributing “changes in mechanical properties such as Young’s modulus, tensile and interlaminar shear strengths and bond strength are the best indicators of changes in the performance of FRP.”

Manufacturing, material components (fiber and resin types), environmental conditions, and the quality of the application process all contribute to the durability of an FRP composite. Prefabrication and wet layup are the two primary manufacturing processes for strengthening applications of FRP. The wet layup process utilizes an “ambient temperature cure resin system” (Karbhari and Ghosh, 2009) which has the advantage of conforming to irregular shapes or areas of uneven geometry reducing unbonded areas, but it may deteriorate faster than prefabricated bars or strips. As described by Karbhari and Ghosh (2009) these prefabricated materials are based on “well characterized high-temperature and controlled condition cure resin/adhesive systems used for long-term durable bonds in the aerospace industry.” Durability of FRP depends intrinsically on the choice of constituent materials, methods and conditions of processing, and surrounding environmental conditions through their service lives (Karbhari, 2003).

Karbhari et al. (2000) and Karbhari et al. (2003) identify identical environmental conditions of primary importance pertaining to the durability of internal and external applications of FRP: “moisture/solution, alkali, thermal (including temperature cycling and freeze-thaw), creep and relaxation, fatigue, ultraviolet, and fire.” Coinciding with Karbhari et al., Byars et al. (2003) considered similar environmental conditions that may

affect the durability of FRP: “moisture, chlorides, alkali, stress, temperature, UV actions, carbonation and acid attack.” Numerous laboratory tests of the durability of FRP have been conducted.

Previous laboratory studies have investigated the durability of both glass fiber reinforced polymers (GFRP) and carbon fiber reinforced polymers (CFRP). From these studies, it has been identified that different fiber types are susceptible or vulnerable to different conditions. Karbhari and Ghosh (2009) found that “glass fiber reinforced system undergoes slightly greater moisture initiated deterioration than the carbon fiber reinforced system.” Fiber types can be optimized depending on the requirements of the FRP application such as in Stallings (2000) study where GFRP was used for shear strengthening and CFRP was used for flexural strengthening of bridge girders in Alabama. The stronger, more expensive CFRP was used where durability was more critical because the flexural strength was controlling, while the weaker, less expensive GFRP plates were used to confine the flexural cracks and to add stiffness, reducing deflections. Carbon fibers are less vulnerable than glass and will be the primary focus in this thesis when discussing FRP.

The durability of fiber types alone is unfortunately not a comprehensive study of the durability of FRP. Karbhari (2003) addresses this complexity stating “Although carbon fibers are generally considered to be inert to most environmental influences likely to be faced in civil infrastructure applications the inertness does not apply to the fibre-matrix bond and the matrix itself, both of which can in fact be significantly deteriorated by environmental exposure.”

2.1.1 Accelerated Ageing

Through rigorous durability studies Karbhari (2000) anticipates “appropriately designed and fabricated, these systems can provide longer lifetimes and lower maintenance than equivalent structures fabricated from conventional materials.” To further understand the development of degradation, multiple lab tests have been conducted to determine the effects of various conditions on the durability of GFRP and CFRP composites. Externally bonded FRP applications are typically subject to certain environmental exposures in which CFRP has proven to be much more durable than GFRP. A multitude of lab tests have been conducted in which the normal ageing process is sped up called accelerated ageing. The following are a few examples.

Typical accelerated aging techniques include exposing specimens, sometimes alternating exposures, to varying solutions and temperatures. As an example, Chen et al. (2007) conducted accelerated aging tests by elevating the temperatures of specimens while cycling wet and dry (WD) and freezing and thawing (FT) in solutions representative of expected environments. Chen et al. (2007) used 5 different solutions in their study consisting of: tap water “to simulate high humidity and used as a reference environment,” solutions with varying amounts of sodium hydroxide, potassium hydroxide, and calcium hydroxide with pH values of 13.6 and 12.7, a simulation of ocean water consisting of sodium chloride and sodium sulfate, and finally a solution emulating concrete pore water contaminated with deicing agents containing sodium chloride and potassium hydroxide with a pH of 13. “Elevated temperatures of 40 °C and 60 °C were used to accelerate the attack of simulated environments on FRP bars, since the

degradation rate mainly depends on diffusion rate and chemical reaction rate, both of which can be accelerated by elevated temperatures” (Chen et al., 2007). The first four solutions were subject to nine WD cycles which “consisted of four days of immersion at 60 °C followed by four days of drying at 20 °C” (Chen et al., 2007). All five solutions were subject to FT cycles which “consisted of 30 min of soaking at 20 °C, 90 min of ramping from 20 to -20 °C, 30 min of soaking at -20 °C, and finally 90 min of ramping from -20 to 20 °C” (Chen et al., 2007). Durability performance was measured by the change in tensile and interlaminar shear strengths after exposures. Bond strengths were also evaluated through use of pullout tests. Chen (2007) concluded “strength loss resulted from the accelerated exposure of both bare and embedded GFRP bars, including bond strength, especially for solutions at 60°C. In contrast CFRP bars displayed excellent durability performance.”

Hu et al. (2007) conducted a study exposing specimens to the aggressive environmental conditions of: fast freeze-thaw cycling, alkaline immersion, water immersion, and wet-thermal exposure. This study also concluded: “CFRP specimens subjected to aggressive environments showed good durability with no significant degradation in tensile strength and modulus, however, GFRP specimens exhibited a little decrease in mechanical property after aggressive environments exposure.”

Ghosh et al. (2005) also used 5 different exposures in the evaluation of bond strength durability by the use of pull-off tests. “Eleven different composite systems, six carbon fabric systems, one glass fabric system and four pultruded carbon strip systems, were bonded to the surface of concrete blocks using epoxy resin systems” (Ghosh,

2005). Five different exposure conditions in addition to a set of specimens kept at room temperature were evaluated at 6, 12, and 18 months. Ghosh (2005) concluded “only two systems showed susceptibility to these exposure conditions. In terms of overall performance, two carbon fabric/epoxy resin composite systems showed good bond strength retentions under all the exposure conditions studied.” Confirming what Karbhari (2000) ascertained Ghosh (2005) advised “a judicious selection of the composite system based on its performance specific to its application condition will be necessary for optimization and long-term integrity of such strengthening/rehabilitation.”

Durability tests conducted in laboratories using accelerated aging techniques and extreme exposures to determine the long-term durability of FRP composites have often shown promising results. Though useful, these efforts have not satisfied the concern about the long-term performance, or durability, of FRP strengthened reinforced concrete structures in the field. This difference was explained by Karbhari (2003) as an “apparent dichotomy between ‘real-world’ applications and laboratory data” that is currently accounted for through the use of safety factors in design. Moreover, perhaps providing some of the reasoning why this dichotomy exists Karbhari et al. (2003) states “synergistic effects (i.e., effects resulting from the combination of multiple environmental conditions, both in the absence and presence of load) are known to exacerbate individual effects.”

Reay et al. (2006) pointed out “Studies on field applications of FRP materials have been limited, and many of those that have been performed have not provided the

type of real-time, long-term durability data needed to better understand the effects of environmental conditions on FRP materials.”

2.2 Field Assessments

From a collaborative study sponsored by the Civil Engineering Research Foundation and the Federal Highway Administration, Karbhari et al. (2003) addresses the need for field assessment in their summary “Implementation of Plans for Field Assessment” below:

“It is well established that durability data generated through laboratory experiments can differ substantially from field data. The determination of actual durability under field conditions over extended periods of time is essential for the optimal design of FRP composites for use in civil infrastructure. It is thus critical that steps be taken to collect, on an ongoing basis, data from field implementations. This data is invaluable to the establishment of appropriate durability based design factors, and the opportunity of having new projects from which such data could be derived in a scientific manner should not be wasted.”

Even though the reference above was published in 2003, very little evidence of field data was found in the published literature. Below are the only examples found related to field assessments of the durability of FRP applications.

2.2.1 Macedonia, 2008

Nineteen highway bridges were repaired with 11,000 meters of bonded FRP plates in the Republic of Macedonia in 2001 and 2002. American Concrete Institute (ACI) 440.2R (2000) was used for the design of the FRP repair. Crawford (2008) summarizes the objective of this study:

“identify a relationship between bridge deterioration factors and the rate of change in FRP durability and to establish a correlation with bridge performance. The overall goal is to provide bridge owners procedures to maintain FRP-strengthened bridges, to optimize service life, and to sustain original FRP-

designed bridge performance. The evaluation of the FRP strengthened bridges in the Republic of Macedonia will establish a baseline for defining long-term FRP-structural system durability applied to concrete bridges” (Crawford, 2008).

Load tests were conducted on 3 of the bridges prior to and following the repair.

These load tests were considered “trial testing” and were done to confirm and verify mathematical models, the FRP repair, and to provide data for comparison with future tests. The trial test consisted of static and dynamic load of a 102 ton, 9 axle heavy commercial vehicle. Strain gauges on reinforcing steel prior to the repair were replaced with strain gauges on the FRP in similar locations following the repair. The trial test was a success and “strongly supported the provisions of ACI 440 (2000),” and “fully justified the suitability of FRP system for strengthening of bridges” (Crawford, 2008). The study developed a valuable model for FRP system inspection which is outlined below:

- Define bridge performance standards and criteria
 - Establish base-line condition for the bridges, i.e. at completion of FRP application
 - Define bridge performance (loading) standard
- Inspection
 - Establish inspection criteria, procedures, protocols
 - Set inspection frequency, measuring points, data collection requirements
- Data Collection and Analysis
 - Collect inspection data, record in national data base
 - Perform data analysis to identify types of deterioration and rate of deterioration
- FRP-System Bridge Maintenance
 - Set maintenance criteria and standards for bridges and FRP systems
 - Prescribe FRP-maintenance protocols and procedures
- Load Testing and Certification
 - Perform bridge load testing, up to 100 tons, every 8-10 years
 - Certify bridge load capacity for national authorities

Crawford (2008) identified “the next step is to develop specific inspection and testing procedures for measuring and collecting data” which motivated Chapter 4 of this

thesis with a mock example following the model provided above. The focus of this thesis diverges from Crawford's in that load testing is not included. Load tests could however be a significant way to evaluate how the development of degradation affects the performance of the structure as a whole.

Crawford (2008) did an excellent job describing durability, environments that threaten durability, debonding mechanisms, and design, but this study provided no data other than the initial values from the load tests prior to and following the repair. This study does not provide any inspection criteria, procedure, or protocol nor does it recommend inspection frequency, measuring points, or data collection methods. In addition, this paper has failed to describe how to set maintenance criteria or maintenance protocols and procedures. This study has presented a large group of bridges with known baseline values of load tests, and have set the stage for a durability study, but neglected to give any specific guidance as to how or what future durability studies should consist of other than load tests "up to 100 tons, every 8-10 years."

2.2.2 Pacific Northwest Region of U.S., 2005

Barlow (2005) outlines the history of the use of FRP with five case studies in the northwest region of the United States. In 1993, "the northwestern United States spearheaded the bold use of these materials" despite the fact that "initial research was done in other states and parts of the world" (Barlow, 2005). The case studies included 2 bridges, a library, a courthouse, and a treatment plant. Quality control of the FRP applications on the bridges as well as the courthouse and library were monitored by tension test panels that were made simultaneous to the installation. In the cases of the

bridges, the test panels were retained by their respective agencies, WSDOT and ODOT. Independent testing prior to the repair provided the quality assurance of the projects. The owner of the courthouse retained the test panels and an independent testing laboratory performed “periodic special inspection.” The application on the courthouse also included pull-off tests in accordance with ASTM D4541 to verify the bond strength of the FRP to the substrate.

The anticipation of test panels with these projects was innovative and much needed. From this study, no information in regard to degradation over time or durability was provided. It is unknown as to whether or not subsequent pull-off tests were conducted or if the test panels were used. It was also unclear as to what conditions or environments the test panels were stored. Perhaps the test panels are intended to be tested in the future, but without utilizing these samples with premeditated frequency it is uncertain as to how helpful, if at all, the resulting data will be to understanding the durability of FRP. To fully understand the development of degradation it is necessary to collect more data points over time with additional samples and their respective environments.

2.2.3 New York, 2004

Hag-Elsafi et al. (2004) conducted an “in-service evaluation” of an FRP repaired bridge in New York. In November, 1999, a T-beam bridge, Wynantskill Creek Bridge was strengthened to increase the shear and flexural capacities using the FRP wet layup process. The FRP repair was also intended to contain freeze-thaw cracking. Prior to and directly following the FRP repair, instrumentation was installed and load tests were

conducted to find the change in stiffness or performance of the repaired bridge. The bridge was in service for approximately 2 years before an additional load test was conducted in November, 2001. There was no detection of deterioration of the strengthened bridge in the 2 years of service through measures of strain caused from the load test or from infrared thermography. Figures were included of the repaired T-beam bridge as well as a figure of an infrared Thermographic image of the repaired bridge (Hag-Elsafi et al., 2004).

The ability to detect damage using infrared thermography is questionable at distances such as in the figure provided which is a “typical thermalgraphic image” according to Hag-Elsafi et al. (2004). Assuming closer inspection was used than that shown in this study, Hag-Elsafi et al. (2004) reported “Upon close observation, only small bubbles were detected in some of the camera images.”

“The changes in beam stiffness during the three tests are very small,” however smaller strains were consistently recorded for the 2001 test, “although some of the strains were within the variations normally associated with instrumentation” (Hag-Elsafi et al., 2004). Hag-Elsafi et al. (2004) concluded that from the data collected and subsequent analysis considering transverse load distribution, effective flange width and neutral axis locations established from strain gauge measures and thermographic imaging that there was “absence of any signs of deterioration in the retrofit system after two years in service.”

It is reasonable to believe that the repaired T-beam bridge could be in service until 2030 or longer. This study confirms that the FRP repaired bridge proved to be

durable and resilient to the conditions between November, 1999 and November, 2001. It did not however, anticipate any follow up evaluations in which further valuable data and information of performance could be gathered. It is unreasonable to forecast 30 years of durability based on two years of exposure, especially considering the variance of conditions the bridge can be exposed from year to year.

2.2.4 Utah, 2004

Saenz et al. (2004) conducted a durability study of FRP composites exposed to “single, dual and multi-variable environmental exposures.” The study combined GFRP and CFRP with epoxy-resin and urethane-resin matrices for a total of 4 combinations of FRP composites. The single exposure specimens were isolated in a dry dark environment to undergo “natural aging” or non-accelerated exposure evaluated at 450 and 900 days. The dual exposures were subject to the combination of “accelerated freeze-thaw cycling in salt water” for 112 and 162 cycles of exposure. The multi-variable environmental exposure, also considered “naturally exposed” consisted of aging the specimens at the State Street Bridge location on I-80 in Salt Lake City, Utah and evaluated at 365 and 730 days of exposure. The purpose of the single and dual environmental exposures was to decouple the degradation due to natural aging with the degradation due to the accelerated freeze-thaw cycles in the saline solution. The purpose of the specimens “naturally exposed” was to identify degradation due to typical environmental exposures at bridge locations. Zhang (2002) also contributed a durability study of FRP aged in a natural setting.

Tensile, ring, and lap slice tests were conducted and it was determined that the “naturally exposed” units showed no degradation after the 365 days of exposure. The specimens with urethane-resin matrix showed “significant loss in interlaminar shear strength after freezing and thawing exposure” while specimens with epoxy-resin matrix “showed a significant increase after freezing and thawing exposure.”

Reay and Pantelides (2006) conducted a similar durability study in regard to the State Street Bridge and considered the CFRP retrofit “effective after 3 years of service.” Following 3 years of exposure, “nondestructive evaluation was conducted through strain gauges, tiltmeters, thermocouples, and humidity sensors installed on the bridge bents for real-time health monitoring.” “Destructive tests were performed to determine the ultimate tensile strength, hoop strength, concrete confinement enhancement, and bond-to-concrete capacity of the CFRP.” In addition, thermography was used to detect voids, or unbonded areas, between the FRP and the concrete substrate.

During the repairs (east bents in August of 2000 and west bents in June of 2001), three types of tests were conducted as quality assurance measures: tensile tests, fiber volume tests, and glass transition temperature tests. Specimens were also created at the time of the FRP repair for future tests consisting of tensile tests, composite rings, confined concrete cylinders, and pull-off tests. The specimens were stored in 3 different locations: “on top of the cap beam at the State Street Bridge, inside a cage located at ground level between two columns of the State Street Bridge, and in an isolated area of the Structures Laboratory at the University of Utah” (Reay and Pantelides, 2003). The specimens were tested at approximately six month intervals of 18, 24, and 30 months.

In addition to the specimens created at the time of repair a section of the side of the cap beam was prepared with a patch for future tensile tests. Half of the patch was covered with an “ultraviolet protective coating” (Reay and Pantelides, 2003) and the other half unprotected. Some degradation of the FRP due to the environment was found through the destructive tests. Reay and Pantelides (2003) concluded “Destructive tests of CFRP composite tensile coupons, rings, and CFRP composite-to-concrete bond specimens have shown that specimens stored in the laboratory, generally give higher ultimate strength capacity than those stored at the bridge.”

Both of these studies were innovative in sample selection and storage, but it is unclear as to why the Saenz et al. (2004) study evaluated specimens at differing times. It makes the comparison more difficult when the “single exposure” specimens were evaluated at 450 and 900 days, while the other specimens were evaluated at 365 and 730 days. It is also difficult to compare the exposures when the environment at the bridge was not quantified in ways such as number of freeze/thaw cycles, precipitation, applications of deicing agents etc.

In reading these two studies it is also unclear as to whether or not the carbon fiber/epoxy resin specimens were used for both studies or if the studies were entirely independent. There were specimens mentioned in Saenz et al. (2004) study, specimens exposed for 730 and 900 days, that were not included in the results. Perhaps the Reay et al. (2006) study was a follow up study making different comparisons focusing on degradation over time of CFRP with epoxy resin for each storage location as opposed to Saenz et al. (2004) focusing more on the combination of fiber and resin types.

In addition to the destructive and non-destructive tests, in June of 2003, multiple voids of varying shapes and sizes were located on the southeast bent of the State Street Bridge using thermographic imaging. Because no thermographic images were taken directly after the retrofit, it was not possible to determine whether the voids or bond flaws existed at the time of the repair or if they developed during service. Six months later in December, 2003 thermographic images were taken and compared with the images collected in June, 2003 and no significant changes in size or shape were found. Reay and Pantelides (2003) concluded “More sophisticated methods are required to determine quantitatively the size and any enlargements of the voids.”

Thermographic imaging at the time of the repair or retrofit would have been an excellent means to provide quality control of the installation of FRP and it would have helped to quantify the degradation of the bond during service. Additionally it would be beneficial to have an object of known size that appears distinctly such as a hot or cold coin to reference for size.

2.2.5 Summary of Field Evaluations of Durability

A fair amount of effort has been put forth in the quality assurance of materials and confirmation of design guidelines as is quality control directly following FRP repairs. These values, when found to be satisfactory, are often discarded or not acknowledged in the future. Both the Macedonia and the Pacific Northwest studies were guilty of this practice. By pass/fail interpretation there is a loss in any understanding of the speed or mechanism in which the degradation develops in FRP composites. These initial or

baseline values can not only be indicative of the quality of repair, but allow for comparisons over time.

In addition, both the Macedonia and Pacific Northwest studies are neither durability studies nor field assessments outside the quality control measures previously mentioned. These studies are presenting bridges and structures that have excellent potential as durability studies, but they fail to provide the baseline values as well as the means in which to conduct future field assessments to compare and analyze the data.

Similar to the Macedonia study, both the New York and Utah studies used load tests to determine the durability of the FRP composite. Though a reasonable measure of structural performance, load tests fail to provide the details about how degradation develops. If for instance, the load carrying capacity of a bridge for a certain amount of strain decreases by 5%, it is difficult to determine the cause of the decrease. The structure may be suffering from cracked concrete, crushing concrete, yielding steel, degradation of material properties due to the egress of moisture, debonding of FRP, or it may be due a more benign cause such as thermal expansion due to a warmer day. To more accurately identify the development of degradation, the presence, location, and severity of damage must be determined through field inspections that are more robust than simple load tests.

The amount of value attained from a durability study depends significantly on the frequency and duration of the study. The Macedonia study fails to recommend any field assessment frequency, but does recommend load tests every 8-10 years. This frequency will likely not provide enough detail to the development of degradation. The

New York and Utah studies have poor durations of study. A comprehensive study of durability of a composite that may last up to 20 or 30 years must last longer than the first 10% of its potential life span.

The study in New York included thermalgraphic imaging which is an effective method of detecting voids, but it must be done in a systematic way. The development and propagation of voids may prove to be an essential piece to the evaluation of durability of FRP composites. It is important to employ effective non-destructive, semi-destructive, and destructive testing and inspection techniques during field evaluations to try and quantify the durability or performance of FRP composites

Below are some evaluation and testing techniques available to determine the bond quality, strength, and material properties of FRP. By comparison with baseline values these techniques and methods can quantify the degradation or durability of an FRP application.

2.3 Nondestructive Evaluation Methods

In efforts to detect adverse effects of deterioration in the FRP composite, nondestructive evaluation, inspection, and testing methods and techniques have been utilized. Each evaluation, inspection, and testing method or technique has advantages and disadvantages pertaining to the ease and effectiveness of identifying damage. The objectives of these methods and techniques are well defined by Rytter et al.'s (1993) "four levels of damage identification in increasing order of difficulty to achieve: (1) Recognizing the presence of damage, (2) determining the location of the damage, (3)

determining the severity of the damage, and (4) determining the remaining service life of the structure.”

2.3.1 Acoustic sounding

Clarke (2002) describes acoustic sounding “There are only limited methods for testing the FRP after installation. Tapping the structure gently with a light hammer or coin is a simple, established method and relies on a change in sound when different areas of bond quality are tapped.” ASTM D4580-03(Reapproved 2007), Standard Practice for Measuring Delaminations in Concrete Bridge Decks by Sounding, outlines the techniques and procedures for tap tests that can be used for FRP applications. In addition, this standard outlines plotting (documentation of the results) which is a valuable component to long-term durability studies. Chain dragging is also a sounding technique described in the standard that can be useful for evaluating the bond quality of FRP systems. Tap tests and sliding the metal head of a hammer over the FRP were practiced and described in the case study, Chapter 3.

Acoustic sounding is a very effective method of finding voids or areas with bond defects. Expertise in conducting these tests can be developed in a relatively short amount of time given the person conducting the test has the ability to hear the differences in audible responses resulting from the tapping or sliding metal. The drawbacks to this method are accessibility and speed. It may be difficult to tap in tight spaces and it can be cumbersome to thoroughly tap all surfaces for inspection. A balance must be found with the pattern in which to tap. Too many taps per given area takes too much time, while too few taps could result in missing areas of voids or defects.

2.3.2 Thermalgraphic imaging

ASTM D4788-03 (Reapproved in 2007), Detecting Delaminations in Bridge Decks Using Infrared Thermography, is intended for asphalt or concrete overlays but can also be applied to concrete structures with FRP applications. Similar to acoustic sounding, documentation of delamination or voids is critical for long-term durability studies.

An extensive study of the thermalgraphic imaging technique was conducted by Ghosh et al. (2006). Thermalgraphic imaging is a somewhat popular method, and was used in the following studies among others: Miceli (2002), Hu et al. (2002), Levar (2003), Starnes et al. (2003), Hag-Elsafi et al. (2004), Halabe et al. (2007), and Ghosh et al. (2011). The Hag-Elsafi et al. (2004) study was presented above in section 2.2.3.

Thermalgraphic imaging can be a very time-efficient method to detecting voids, but the process requires certain conditions to be effective in identifying voids. Temperature differentials that exist within a small depth, approximately 1 cm, of the inspection surface are clearly identified with this method. Voids or pockets of air do not conduct heat as quickly as solid materials and therefore appear to be hot or cold pockets in the thermal images. With conditions that are less than ideal, thermalgraphic imaging can produce false-positives or areas that appear to be voids but are not, and false-negatives or fail to identify a void that is present. Because of the frequent occurrences of false-positives and false-negatives using solar radiation as a heat source, testing conditions need to be more controlled and consistent or thermalgraphic imaging would be most efficient when used in tandem with an additional method such as acoustic sounding.

2.4 Tests

2.4.1 Pull-off tests

It is essential that the CFRP is well-bonded to the concrete substrate to transfer stresses. A common evaluation of the bond strength is the pull-off test also called the direct tension pull-off test. A pull-off tester is attached to a puck which is adhered with a fast-setting epoxy to the surface of CFRP. Before the puck is adhered, a core drill is used to establish an isolated area of known area to test. The pull-off test is concluded when a failure of bond occurs at some interface between the surface of the puck and some location within the substrate. The pull-off tester outputs the force or stress applied to the puck and the maximum reading is considered the bond strength. The tensile strength of concrete is approximately $1/7^{\text{th}}$ to $1/10^{\text{th}}$ the compressive strength and therefore typically limits the pull-off test. Any other failure interface other than internal in the substrate is considered a premature failure and is undesirable.

In 1999, the U.S. Army Corps of Engineers published “An Evaluation of Equipment and Procedures for Tensile Bond Testing of Concrete Repairs” that compared pull-off testers and the testing procedures. This study focused on concrete overlays rather than FRP repaired materials and thus is most relevant in the comparison of pull-off testing equipment.

International Concrete Repair Institute (ICRI) published Technical Guideline No. 210.3-2004 in 2004 “Guide to Using In-Situ Tensile Pull-Off Tests to Evaluate Bond of Concrete Surface Materials” followed by No. 210.4-09 “Guide for Nondestructive

Evaluation Methods for Condition Assessment, Repair, and Performance Monitoring of Concrete Structures” in 2009. Technical Guideline No. 0.3739 provides testing procedures and guidelines to testing time and frequency and evaluation of tests results. This guideline is useful in regard to evaluating the bond strength directly following the repair; it does not however address durability. Technical Guideline No. 210.4-09 provides guidance on the decision of which nondestructive tests to choose, one of which is pull-off tests, but does not provide procedural instruction.

ASTM D4541-02 “Standard Test Method for Pull Off Strength of Coatings Using Portable Adhesion Testers,” was the standard followed during the 2003 pull-off test conducted on the Castlewood Canyon Bridge by CTC-Geotek. The standard followed during the case study is ASTM D7522-09, “Standard Test Method for Pull-Off Strength for FRP Bonded to Concrete Substrate.”

Pull-off tests are effective at quantifying the bond strength of FRP composite and can be conducted in the field fairly quickly. The results to pull-off tests can drastically vary for locations within close proximity. This variance in test results obscures the ability to make meaningful comparisons or analyze the data. It is possible that the variance could be reduced by improving the testing procedure. The testing procedure is complicated by the core drilling process which introduces heat, water, and torsional stresses. Torsional stresses will always exist, but could be minimized with proper technique. The heat and torsional stresses affect the bond strength results in ways that are not fully understood. If the heat provides a temperature higher than the glass-transition temperature of the epoxy used to adhere the FRP to the substrate, the

stiffness of the epoxy will decrease likely affecting the bond strength results. The core drilling is often done with a diamond bit which needs to be cooled during drilling. Wet drilling or providing available water to the bit is the best way to cool the diamonds and lubricate the cutting process. The presence of the water complicates the subsequent procedure of adhering the puck to the FRP with epoxy. Even with optimum procedures variance will always exist due to local characteristics of the substrate.

2.4.2 Differential Scanning Calorimetry (DSC)

The quality of the CFRP resulting from the wet lay-up process can vary significantly. Mixture ratios of the epoxy resin, the presence of moisture and the amount of cure during working time of the epoxy, the level of saturation in the CFRP fabric of epoxy, and the temperature during the curing process all affect the future performance of the CFRP composite. DSC is the most commonly used thermal analysis technique and can be used to determine the liquid-glass transition temperature, commonly referred to as “glass transition temperature” (T_g) of the CFRP and filler resins. This is a temperature range in which the material undergoes a change in heat capacity though no phase change occurs. “The glass transition temperature is dependent on the degree of crosslinking. With increasing crosslinking, the glass transition shifts to higher temperatures” (UserCom, 2000). Increasing temperature causes a solid material to transfer from a higher stiffness of a “glass” region to a less stiff “rubber” region. It is important for the glass transition temperature, T_g , to be above any possible temperatures the composite might encounter during its service life. Because of this, low

T_g values or occurrences such as fire or plasticization of the resin can be detrimental to FRP repaired structures.

“The bond between FRP and concrete is essential to transfer loads through the polymer matrix or adhesive. Changes in the mechanical properties of the matrix material at temperatures above T_g have the potential to cause loss of bond at only modestly increased temperatures, resulting in a loss of interaction between FRP and concrete” (Bisby et al., 2005).

The glass transition temperature of a CFRP composite can be improved or increased if the curing process takes place in an environment of higher temperatures. T_g of a polymer pushes higher the more curing it experiences. “As a general rule, an increase in temperature will cause a shorter gel time, as the cure process is exothermic and the cure rate increases as a function of temperature” (Ozokwelu, 1990). The thermosetting epoxy resin dictates the glass transition temperature; the carbon fibers of the composite do not undergo changes in heat capacity in the temperature ranges that the epoxy resin does and, therefore do not contribute to the analysis of DSC. “In general, the glass transition temperature is independent of the filler content. Only with active fillers can relatively small changes in T_g be observed” (UserCom, 2000). During the wet lay-up process, ambient temperatures do not provide the elevated temperatures during cure that are present during the manufacturing of FRP materials such as pultruded bars.

Typical results are presented in plots of heat flow or energy versus temperature. There are different physical phenomena that add complexity that result in visual characteristics in the plot. Information for users of Mettler Toledo thermal analysis systems’ Interpreting DSC Curves (2000) outlines 8 different artifacts or “effects not

caused by the sample under investigation” that can “lead to a possible misinterpretation of results.” These artifacts are irreversible and are created by such things as contact between the sample and pan, inconsistent power source, and change in room temperature during the testing. It is also possible that erratic behavior is due to something related specifically to the specimen such as evaporation of moisture or an enthalpic relaxation peak due to aging. Ideally, the plot of heat flow versus temperature would have a baseline, a near-horizontal smooth line, then a smooth diagonal line with a constant negative slope followed by a return to baseline, another smooth, near-horizontal line.

DSC can provide the T_g which can be indicative of the quality of construction. It is not helpful to test a large sample size because the glass transition temperature is a material property that is not thought of as a random variable. In a stable environment, without the presence of extreme temperatures or heat, the T_g will likely only significantly change with the egress of moisture or water. Available water will act like a plasticizer to the resin, pushing the T_g lower. Obtaining samples on-site, transporting them to a laboratory, and testing the sample without the moisture content changing is very difficult. Ideally, the sample would have the same conditions during testing that it had while in service.

Chapter 3: Case Study

3.1 The Castlewood Canyon Bridge

One of the first reinforced concrete arch bridges retrofitted with FRP, the Castlewood Canyon Bridge is located approximately 6.4 km (4 mi) south of Franktown, Colorado on State Highway 83.



Figure 3.1. Castlewood Canyon Bridge location indicated by the red star (mapquest.com, 2011)



Figure 3.2. Castlewood Canyon Bridge (Mohseni, CDOT)

The Castlewood Canyon Bridge was originally built in 1946 and underwent a major renovation in 2003. The bridge deck and spandrel columns were replaced with precast reinforced concrete members and the existing arches were repaired with CFRP. The identical arches that span approximately 70.1 m (230 ft) in the north-south direction over Cherry Creek were strengthened in shear, flexure, and axially using CFRP. The arch repair also consisted of reinforcing the bases of the arches and wrapping the struts between the arches using a wet-layup application of CFRP fabric.

The arches and their repair comprise the area of focus for this case study. At the time of the renovation, in collaboration with the Research Branch of the Colorado Department of Transportation (CDOT), the University of Colorado, Boulder produced a report titled "Evaluation of the FRP-Retrofitted Arches in the Castlewood Canyon Bridge" (Fafach et al., 2005) that included documentation of the arch repair process and results from laboratory durability studies, structural modeling and testing, and

instrumentation of the repaired structure. Due to this research effort, significantly more information and details were documented and made available for future study than similar repair/retrofitting/reconstruction projects.

Photographs of the bridge prior to and following the 2003 repair can be seen below in Figures 3.3 and 3.4.



Figure 3.3. Castlewood Canyon Bridge prior to the 2003 repair (Mohseni, CDOT)

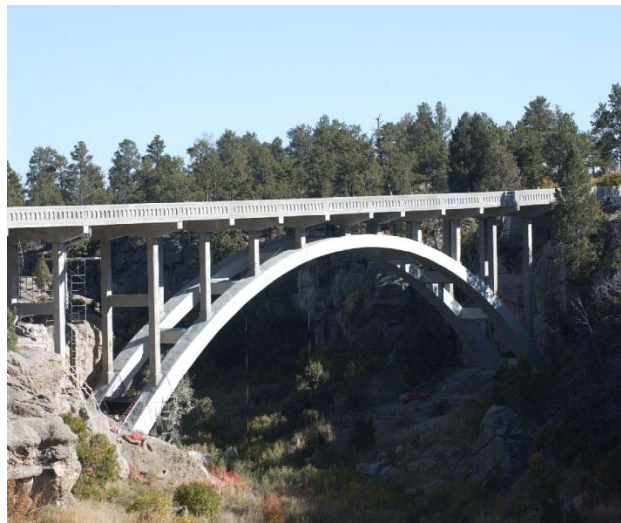


Figure 3.4. Castlewood Canyon Bridge after the 2003 repair (Mohseni, CDOT)

For purposes of this case study, sections of arch between spandrel columns are referred to as “bays” and their numbering begins at 1 in the first bay between the

ground and the 1st spandrel column, ending at 6 which is the middle section at the crest of the arch. North and south are used to denote the two halves of each arch, and the two arches are indicated as west and east, referring to their orientation relative to each other. As an example, the 2SE bay refers to the second bay (between the 1st and 2nd columns) of the east arch on the south end. The majority of the field evaluation in 2011 was conducted on the extrados of the east arch. Below is a plan view of the arches, struts and columns.

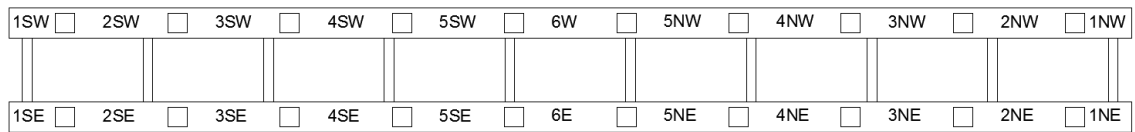


Figure 3.5. Plan view of the arches, struts, and column pedestals showing the bay labeling scheme

3.2 Renovation in 2003

3.2.1 Replacement of Spandrel Columns, Pier Caps, and Bridge Deck

The renovation began with repairing the base of the arches with Leadline™ CFRP rods and the arches and struts with CFRP fabric using the wet lay-up process. The spandrel columns, pier caps, and bridge deck were replaced between Phases 2 and 3 of the CFRP wet lay-up application on the arches and struts explained below. The bridge deck was widened by about 2.44 m (8 ft) to 13.11 m (43 ft) wide and was systematically replaced with precast reinforced concrete members to prevent unsymmetrical loads on the arches during the renovation, seen below.



Figure 3.6. Systematically replacing the bridge deck (Mohseni, CDOT)

Figure 3.7 is a photograph of spandrel columns being replaced with precast reinforced concrete members on new pedestals adjacent to the original columns.



Figure 3.7. Placing the new spandrel columns adjacent to the existing columns (Mohseni, CDOT)

3.2.2 Repair of Arches and Struts

Prior to repair the concrete arches had severe spalling due to the corrosion of the internal steel reinforcement as seen in the photographs in Figures 3.8 and 3.9.



Figures 3.8 and 3.9. Concrete spalling on arch section prior to repair (Mohseni, CDOT)

Loose concrete, typically no more than the few inches of concrete cover, was removed with 6.8 kg (15 lb.) jack hammers and the exposed steel reinforcement was sandblasted free of rust. Seen below, the cross-section was restored with shotcrete which included a corrosion inhibitor, Sika FerroGard 903, to prevent further corrosion of the steel reinforcement.



Figures 3.10 and 3.11. Removal of loose concrete using 6.8 kg (15 lbs.) jackhammer and restoring the cross section with shotcrete (Mohseni, CDOT)

The cross-section of the arches tapers in thickness from 1.78 m (70 in) at the base to 1.02 m (40 in) at the peak of the arch, while the width remains constant at 1.93 m (76 in) wide. Once the cross-sections of the arches were restored, FRP was adhered in three phases. Phase 1 consisted of installing longitudinal and transverse CFRP between the arch base and the first spandrel column. More longitudinal CFRP was used on the extrados than the intrados in this area to resist large negative moments generated from a concentrated truck load located at the second spandrel column. The arches were wrapped transversely confining the arches to provide axial and shear strengthening. The transverse wraps alternated between wrapping entirely around the cross-section and wraps that only covered the sides and extrados of the arch. This alternating pattern created intentional areas without FRP on the intrados of the arch that allowed the arches the ability to drain and/or remove humidity or moisture. During Phase 2, longitudinal CFRP wraps were distributed evenly between the extrados and intrados of the remaining arch followed by transverse wraps with the same alternating pattern previously discussed. The transverse wraps were installed on the arches except where the existing columns were and where the replacement columns were going to be located. In Phase 3, these areas were wrapped after the new columns were installed and the old columns were removed; the struts were also wrapped transversely with the alternating pattern used on the arches concluding the CFRP application.

Below, Figures 3.12 and 3.13 show photographs of the wet-layup process during Phase 1, and the longitudinal and transverse pattern of CFRP.



Figures 3.12 and 3.13. Fyfe’s Tyfo® S Epoxy resin (likely with glass fibers as a filler) being applied to the extrados of an arch and installation of saturated unidirectional CFRP fabric, Tyfo® SCH-41 (Mohseni, CDOT)



Figure 3.14. Longitudinal and transverse CFRP wraps at the base of an arch (Mohseni, CDOT)

The arches and struts were then painted with an exterior acrylic paint to prevent and/or reduce degradation to the resin caused by moisture and UV and to restore the original appearance matching the concrete color.

3.2.3 Initial Values and Quality Control of the Renovation in 2003

As a measure of quality assurance, the contractor of the renovation, Restruction Corporation, was responsible to “obtain suitable documentation from the manufacturer showing results from an independent agency that all materials used in this system meet or exceed the requirements” (CDOT’s construction specifications (Revision of Section 602)). The initial values are critical for the evaluation of durability, and the quality control process should provide the means to collect those values. The following are some of the codes and reference standards used to define the requirements in CDOT’s construction specifications: ACI 440R-96, ACI 318-99, ACI 515R, ACI 546R-96, ASTM D3039, ASTM D4541, ICRI Guideline No. 310.1R-2008, ICRI Guideline No. 310.2-1997, and ICRI Guideline No. 320.2R-2009. CDOT’s policy is to store boxes of records of past projects for seven years after the project is completed. Fortunately, even though the case study occurred eight years after the completion of the repair, CDOT still had two boxes of files that were available to search for information in regard to the repair, initial or baseline values, and quality control.

3.2.3.1 Tensile Properties of CFRP

From CDOT’s construction specifications (Revision of Section 602), the number of layers of CFRP necessary was calculated by Fyfe and was to meet the following performance criteria:

- Minimum ultimate rupture strain = 0.006 cm/cm (0.006 inch/inch)

- Resist a force of no less than 320.9 KN per linear meter (22 KIPS per linear ft.), this strength shall be determined at a strain no greater than a usable strain of 0.0043 cm/cm (0.0043 inch/inch).
- The ultimate tensile strength shall be the mean tensile strength of a sample of test specimens (a minimum of 20 replicate test specimens) minus three times the standard deviation of the test results.
- The ultimate rupture strain shall be the mean rupture strain of a sample of test specimens (a minimum of 20 replicate test specimens) minus three times the standard deviation.

Restruction was to obtain “suitable documentation” from Fyfe showing results from an independent agency that all materials used in this system met or exceeded these requirements and Restruction was to submit this documentation a minimum of two weeks prior to start of work. Fyfe published a guarantee of the mechanical tensile properties but, the “suitable documentation” was not recovered but was assumed to exist due to the completion of the project.

Restruction was also required to provide two 30.5 cm x 30.5 cm (12” x 12”) sample panels for every 92.9 m² (1000 ft²) of FRP installed to be tested by an independent testing laboratory in accordance with ASTM D3039. The independent testing laboratory was to use one of the two panels to conduct tensile tests and prepare a summary report of all test results. Two panels were initially prepared with one panel held in reserve in case test results on the first panel did not meet specified performance criteria. No documentation of these tests was recovered.

Tensile tests were not conducted in the 2003 study conducted by CU, but values provided by the manufacturer of material properties were included in the CDOT report. These values are used as the initial values for tensile strength and are tabulated in section 3.5.1.

3.2.3.2 Bond Strength of CFRP

The contractor was to provide a qualified representative on-site to ensure the proper installation of the CFRP. The representative was required to inspect each completed phase of the installation and advise the project engineer regarding repairs and replacements. No documentation of advice or notes was found in regard to this process.

The contractor was required to conduct a minimum of one direct pull-off test per 46.45 m² (500 ft²) of surface of installed FRP to ensure the required minimum tensile strength of 1.38 MPa (200 psi) was satisfied. No documentation of these tests was recovered.

In addition, the contractor accompanied by the engineer and manufacturer's representative, was required to examine all surfaces 24 hours after application of FRP sheets and initial resin cure to check for voids, delaminations and air bubbles. The inspection was accomplished by visual observation and acoustic tapping tests to locate voids or defects. Areas of voids or delaminations can be detected due to the different sound emitted when tapped or when a solid object is slid over the area. Minor areas of voids of less than 38.7 cm² (6 in²) were injected with resin to fill the void and provide a bond between the FRP and the substrate. Voids larger than 38.7 cm² (6 in²) were

repaired by removing and re-applying the required number of layers of CFRP. A void that had been injected with resin directly following the CFRP application can be seen below in Figure 3.15. There was no documentation of this procedure or any information regarding the areas repaired or filled with resin, but it is assumed that this process was satisfactory.



Figure 3.15. Void injected with resin during 2003 renovation (Mohseni, CDOT)

Restruction was also required to utilize an independent testing laboratory, CTC-Geotek, Inc., to perform a minimum of two random field pull-off tests (ASTM 4541) for each day of FRP application. The pull-off tests were intended to ensure the minimum tensile strength of the substrate of 1.38 MPa (200 psi) was satisfied.

A total of 42 pull-off tests were conducted over 5 days, June 10, 13, 30 and July 9 and 17 in 2003. From Field Observation Reports submitted by CTC-Geotek the following procedures were practiced:

- The pull-off test areas were prepared by core drilling through the composite material and approximately 1 cm (3/8") into existing concrete.
- A 5.7 cm (2 1/4") diameter core barrel was used in conjunction with a Hilti

High Speed core rig

- 5.1 cm (2") diameter pucks were placed using Devcon 10.34 MPa (1500 psi) fast-set epoxy

Tests were performed on both sides and on the extrados of the arches in the following bays: 1SE, 1SW, 1NW, 4NE, 4NW, 5SE, 5SW, 5NE, 5NW, 6E, 6W. The pull-off test locations can be seen below in Figure 3.16.

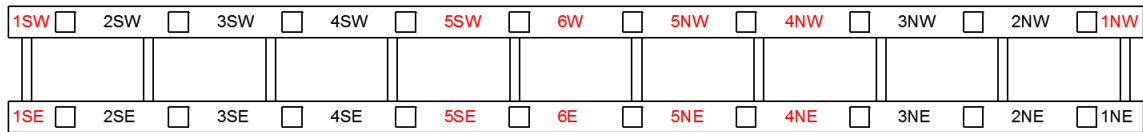


Figure 3.16. Pull-off test locations from 2003 denoted in red

A complete summary of the pull-off test results can be found in Appendix B. CTC-Geotek described the failure modes in a field observation report. The failure modes were converted to be consistent with the failure modes described in ASTM D7522, which is a standard specifically for FRP bonded to concrete substrate. This standard published in July 2009, was not available at the time of the tests conducted in 2003. Failure modes defined in ASTM D7522 are tabulated below.

Table 3.1. ASTM D7522 Failure Modes

Failure Mode	Description
A	Bonding adhesive failure at loading fixture
B	Cohesive failure in FRP laminate
C	Adhesive failure at FRP/adhesive interface
D	Cohesive failure adhesive
E	Adhesive failure at FRP/concrete interface
F	Mixed Mode E and Mode G
G	Cohesive failure in concrete substrate

Pull-off tests with failure modes other than Mode G are considered to be premature failures and are not desirable. Only one test from 2003 was not satisfactory with a pull-off strength of 1.32 MPa (191 psi), but was due to failure Mode A, and therefore was not of concern. Quantities of the different failure modes are tabulated in Table X below.

Table 3.2. Failure Modes of the pull-off tests conducted in 2003

42 Tests	Failure Modes of 2003 Pull-off tests							
	A	B	C	D	E	F	G	NA
Quantity	9	0	0	0	2	3	25	3
Percentage	21.4	0	0	0	4.8	7.1	59.5	7.1

After having a number of pull-off tests with a failure mode A, the pull-off technique was altered to prevent the premature failure of subsequent tests. The tests with failure modes E and F failed at strength values higher than the minimum 1.38 MPa (200 psi) and, therefore it can be deduced that the tensile strength of the substrate also exceeded 1.38 MPa (200 psi). Further discussion of the results and subsequent pull-off tests resumes in section 3.4.4.

3.3 Biennial Bridge Inspections

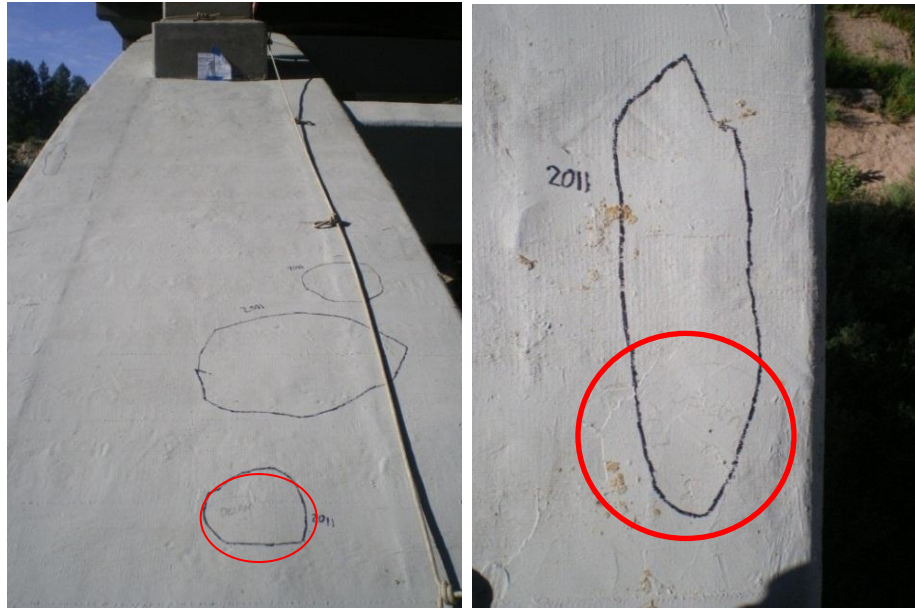
Biennial bridge inspections were conducted on the Castlewood Canyon Bridge following the renovation in 2005, 2007, and 2009. The 2011 bridge inspection had not yet occurred at the time of the field assessment in July 2011. The conditions of the CFRP material and its bond were evaluated as a component of these bridge inspections. These evaluations consisted of visual inspections and acoustic tapping tests of areas easily

accessible which included the extrados and bases of the arches. The boundary of defects in the CFRP were outlined and dated with a “permanent” marker.

In discussing defects or voids in the CFRP composite system, it is necessary to further differentiate between the type of defect and the time of occurrence. The term “void” will be used to denote an area lacking a bond at some interface between the surface of the CFRP and the substrate, but with no distinction of when it developed. The term “unbonded” will refer to areas in which the FRP failed to bond to the substrate at the time of repair. The term “debonded” will be used to denote that at some point following the repair the FRP lost the bond to the substrate that it once had, and “delamination” will refer to a loss of bond between layers of CFRP. Voids found during the bridge inspections, which were denoted using familiar terminology to bridge inspectors as “DELAM”, should be considered as voids and not delaminations. Bond loss between reinforcing steel and the concrete cover is often referred to as a “delamination” by bridge inspectors. Cracks and other imperfections in the CFRP composite will be referred to as defects.

Assuming the tap tests performed directly after the repair were thorough and the FRP was bonded to the substrate at all locations following the repair procedure, any voids found during the bridge inspections were created during service and such debonded areas should be monitored to detect any additional damage that may occur. Debonded areas may increase in quantity or size over time and therefore careful documentation is necessary to evaluate the FRP system accurately.

Markings made with a “permanent” marker on the bridge from the 2007 bridge inspection were barely visible at the time of the 2011 field assessment. Depending on the exposure from moisture and sun, markings on the bridge can exist for only a relatively short time with respect to the life span of the bridge. Below are three photographs of the areas identified from June 2007, two of which were barely visible at the time of the July 2011 visit. There were no markings found on the east arch from the inspections in 2005 and 2009. In addition to the three voids, three cracks in the CFRP were also identified in 2007, one of which can be seen below.



Figures 3.17 and 3.18. Outlined in permanent marker are identified areas of debonding between the FRP and the substrate developed in the structure between inspections in 2007 and 2011. Faintly denoted in the bottom of the photographs (enclosed in red circles) are previously found voids identified with “DELAM 07” and lines distinguishing the boundaries of the voids.



Figure 3.19. Enclosed in permanent marker are identified areas of debonded areas between the FRP and the substrate from 2011 and June, 2007. Notice in this more protected bay of the structure the markings from 2007 are more clearly visible.



Figure 3.20. Crack identified in 2007

It is possible that additional markings on the bridge have become too faded to be recognized. The only other documentation of such markings are brief mentions in bridge inspection reports as “some areas of delams.” This makes quantification of number and size of voids difficult to track over time. In addition, the development of debonded areas may appear more extensive under more meticulous inspection.

3.4 Field Assessment of the Castlewood Canyon Bridge

3.4.1 Planning Tests and Locations

Planning for a field assessment to evaluate the durability of the CFRP application on the bridge began in the fall of 2010. Following extensive literature review, evaluation techniques suitable for the Castlewood Canyon Bridge project were chosen to evaluate the durability of the FRP system. Pull-off tests, tensile tests, and differential scanning calorimetry (DSC) were chosen as the primary methods to evaluate the durability of the FRP application. The pull-off tests indicate values of bond strength which is essential to the performance of FRP composites. Tensile tests provide mechanical properties of the composite material. DSC tests evaluate the glass transition temperature of the composite which can significantly vary depending on the wet lay-up process and the exposure to moisture. Visual inspection, acoustic tapping tests, and thermal imaging were selected as identification methods to identify areas of voids and visible defects.

Two general locations, the crest and base of the arches, were locations of interest prior to the field assessment. The two locations have different exposures and stresses that could potentially affect the durability of the FRP application. The crest of the arch has less exposure than the base of the arch to moisture from precipitation such as driving rains and drifting snow due to the protection of the overhanging deck. However, because the crest of the arch is located closer to the bridge deck it is also more susceptible to moisture draining from the deck as well as deicing agents. The crest of the arch is also more protected from the sun and consequentially experiences lower

thermal stresses than the base of the arch. As a typical arch structure, the base of the arch, in general, has larger stresses due to the self-weight of the arch as well as those generated from service loads. The differences between these two locations provide a variety of conditions that are known to have an impact on the durability of FRP composites.

In addition to conducting the tests described above at these two different locations, the effect of the two different substrates - concrete and shotcrete - on the bond and material properties was also an area of interest. However, it was not possible to identify whether the substrate was concrete or shotcrete at a particular location because the areas where shotcrete was applied during the repair in 2003 were not documented other than in coincidental photographs documenting the progress of the project. Therefore, the effect of the different substrates was not determined in this assessment.

Conduct of the identification and testing methods was planned for the extrados of the arch for two reasons. The extradoses of the arches were easily accessed and navigated. Secondly, from the modeling in the CU study, this is an area that could potentially experience high stresses due to concentrated truck loads over the second spandrel column. Due to limited time and safety equipment the east arch was arbitrarily chosen as the primary arch of focus for the field assessment.

Due to conditions at the bridge site, the north end of the arches was chosen for access and as the location to conduct pull-off tests at the base of the arch. Particular

locations to conduct pull-off tests were established in areas where there were no voids found using the thermal imaging infrared camera or tap tests.

Different techniques for pull-off tests were explored in the laboratory to ensure testing procedures accurately represented bridge conditions. Experiments with wet core drilling, dry core drilling, cleaning, sanding, epoxying, and cure times helped improve the pull-off test methods used in the field. Dry drilling caused too much heat and presumably exceeded the glass transition temperature of the epoxy between the FRP and the substrate and caused the FRP bond to prematurely fail. Drilling after the pucks were adhered to the FRP benefitted the starting of the coring, but presented difficulties due to the heat generated from friction whether the core drilling was wet or dry. The core drilling was more successful using a jig that provided the guidance to start the coring rather than the adhered puck. Wet core drilling introduced moisture and created problems in the adhesion of the pucks to the FRP. Drying and cleaning the adhesion surface with compressed air and alcohol provided the best method for adhesion after wet core drilling. Sanding the pucks with 40 grit sandpaper and a similar cleaning technique provided the preparation for sufficient bonds. Thorough mixing of the two-part epoxy and a minimum cure time of 1 hour were also critical to a successful pull-off test.

Tensile and DSC tests require equipment in the laboratory; therefore samples had to be collected from the bridge to be brought back to the lab for testing. Specimen sizes of CFRP strips approximately 2.5 cm (1") wide and 20.3 cm (8") long were required for the tensile test while samples for the DSC tests are 15 mg of finely ground particles

or powder. The strips were planned to be collected from the outside corner of the arches in the locations of interest with the use of an abrasive cut-off wheel mounted on a right angle grinder and masonry chisel, and the DSC samples could easily be provided from material from the other tests or samples collected.

Experiments in the laboratory prior to the site visit with the infrared camera proved to be beneficial in learning the capabilities and ranges of thermal detection of the camera. Information in regard to surfaces could be received when a temperature differential existed. Because of the delicate nature of the information held in the transient state, it was anticipated that using the camera at different times of day would have significant benefits and drawbacks that would be difficult to predict. It was determined that it would be beneficial to have a preliminary site visit to establish the most effective thermal camera techniques.

A preliminary site visit would also provide an opportunity to establish transportation, parking, arch access, and safety procedures, as well as general familiarity with the project. Necessary equipment to conduct the field assessment included the following: gas-powered generator, air-compressor, hoses, extension cords, drill, grinder, ice, safety equipment, repair CFRP materials, and paint. Planning for the setup of this necessary equipment could also be accomplished by a preliminary site visit.

3.4.2 Preliminary Site Visit

Prior to the site visit, a Special Use Permit was acquired from the Colorado Department of Transportation (CDOT) to inform the necessary parties of the planned activities and to outline procedures and liability. On the 6th of July 2011, the field

assessment of the durability of the FRP repair began with an orientation visit to the bridge. CDOT personnel present at the preliminary site visit included Thomas Moss, a bridge inspector for CDOT, and CDOT Research Staff, David Weld. Mr. Weld provided high-visibility safety vests, parking recommendations, assistance in maintaining proper procedure for roadside activity, and supervision. The north side of the bridge was used for parking and access to the arches. Parking off the shoulder was recommended to eliminate the need for lane-closures.

Mr. Weld was present for the duration of the field assessment as per CDOT policy. Mr. Moss provided guidance to the access of the arches, safety equipment (e.g. safety harnesses, lanyards, and safety ropes), and installation of the safety apparatus on the eastern arch. Mr. Moss demonstrated the proper technique to use the safety equipment. In addition Mr. Moss recounted previous bridge inspections and assisted in locating the previously identified areas of flaws in the FRP repair.

Once the safety rope system was installed on the east arch, a thermal imaging infrared camera, FLIR ThermoCAM™ E4, coupled with the use of a tap test were used to identify areas of voids between the CFRP and the substrate (either concrete or shotcrete) of the arch. Heating, cooling, and the effects of solar radiation on the surface of the arches were also explored in order to optimize the use of the thermal camera in detecting voids. Both thermal imaging and tap tests were used to confirm the existence of voids while the acoustic tapping test was more precise in determining the size and shape of the voids.

The thermal camera was used to identify areas where there was a significant temperature differential. In theory, the concrete or substrate acts as a “thermal sink” pulling heat applied to the surface through the CFRP in areas that are well bonded. Voids between the CFRP and the substrate would not allow the heat to conduct as quickly resulting in a “hot pocket” in the void. Cooling the surface would also work in a similar manner. Multiple external sources of heat and cold were considered prior to the site visit: liquid nitrogen, liquid carbon dioxide, heat blankets, electric iron, heat gun etc. For various reasons these candidates were deemed unfit for the project. Liquid nitrogen and liquid carbon dioxide would provide temperatures of 78 K (-319° F) and 195 K (-109 °F) respectively. Because the coefficient of thermal expansion of CFRP and concrete differ of up to an order of magnitude, externally applying extreme temperatures would introduce thermal stresses possibly compromising the bond between the two materials. Therefore, it was reasoned that any heating or cooling to create a temperature differential should be limited to a moderate change relative to the ambient temperature. The electric iron and heat gun would both require electricity, and would not have significant advantages compared to a handheld propane heater. The use of heat blankets would have provided a more controllable uniformly heated area, but blankets large enough to justify their use would have been too heavy and cumbersome to handle in traversing the arches.

A handheld propane heater was used to supply an external heat source. Initially, the surface of the CFRP registered a constant temperature in the thermal camera due to the heating, followed by a transient state in which the substrate would pull the applied

heat at well bonded areas but not in areas of voids. This method proved to be fairly time intensive including applying the heat and waiting for the transient state to occur. A 929 cm² (1 ft²) section required approximately 3 minutes and the area of the extrados of only one arch exceeded 148.6 m² (1600 ft²). In addition, it was difficult to apply the heat uniformly, resulting in thermal images containing transient temperature differentials due to the application of the heat not necessarily due to the area of voids.

Following the same philosophy as the externally applied heat an alternative technique of externally applying ice water to create a temperature differential was also tested. Using this technique the voids appear to the thermal camera as pockets of cold regions because the substrate conducts heat back to the CFRP in areas that are well bonded. This method was not effective either. Applying the ice water was easier than applying heat when considering large areas, but the transient state was delayed longer until the water on the surface was totally removed. In addition, the uniform contact time and contact area of the ice water to the surface of the arch was difficult to control causing temperature differentials during the transient state that were due to the external application rather than areas of voids.

After trying the propane heater and ice water during the preliminary site visit, it was determined that solar radiation and no other externally applied sources of heat or cold other than that of the sun would be used for the final assessment. The effectiveness of using solar radiation proved to be highly sensitive to the intensity and duration of the exposure to sun or lack thereof. Thermal images from areas of the arch

that had been shaded from the sun for long periods of time were more effective at locating areas of voids than areas that were transitioning in or out of direct sunlight.

Detection of areas of voids was much quicker with the thermal camera than the tap test technique, but the tap test technique was unmistakable in detecting voids. Depending on the recent thermal history, the thermal camera would produce images that would suggest areas of voids that may or may not actually represent areas of voids. The tap test not only was used to find areas of voids and confirm areas of voids found by the infrared camera, but also to identify the size and shapes of the voids.

The preliminary site visit provided the following conclusions:

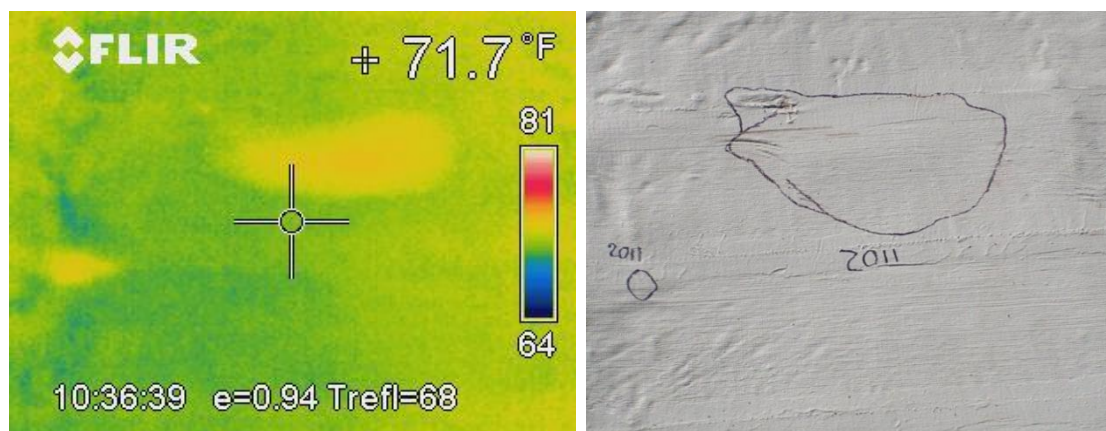
- Parking and access would be at the north end of the arches
- Thomas Moss would set-up a similar safety system extending the entire length of the arch for the field assessment starting on July 11th 2011
- The extradoses and east arch would be accessible and the primary focus of the field assessment
- Quantity, size, and shape of voids would be detected by the coupled use of the thermal camera and acoustic tapping tests
- The thermal camera would rely solely on solar radiation for void detection
- The bridge deck replaced in 2003 was continuous and waterproof with no expansion joints or areas of leakage. The bridge deck appeared to be protecting the arches from any exposure to deicing agents

3.4.3 Void Detection

The week-long field assessment of the durability of CFRP began with detecting voids on July 11, 2011. It was important to detect any areas of voids not only to evaluate the condition of the CFRP bond to the substrate globally but also in order to avoid these areas when conducting pull-off tests.

Thermal imaging and acoustic tapping techniques established from the preliminary site visit were employed to discover the existing voids on the extrados of the entire east arch as well as the 1st bay on the north end of the west arch. In areas where the solar radiation was not ideal, acoustic tapping tests were relied upon to detect voids. In most areas, the thermal camera was more time efficient in detecting voids, but the acoustic tapping test method was more thorough in detecting voids.

A typical thermal image of voids, shown below in Figure 3.21, provided the temperature of the location of the cross hairs in the upper right hand corner of the image, a color-coded temperature scale on the right side of the image, and the time, e (emissivity), and Trefl (the reflected ambient temperature) at the bottom of the figure.



Figures 3.21 and 3.22. Photograph and thermal image from an infrared camera of two voids, (appearing yellow), found in 2011 on the 1st bay on the north side of the east arch

The images above are of two voids found in the 1st bay on the north end of the east arch. The area of the larger void was one of two areas eventually removed from the arch and is referred to as the “smaller” patch removed from the arch. Note the horizontal or transverse cracks enclosed in the red oval near the top of the void in Figure 3.23.

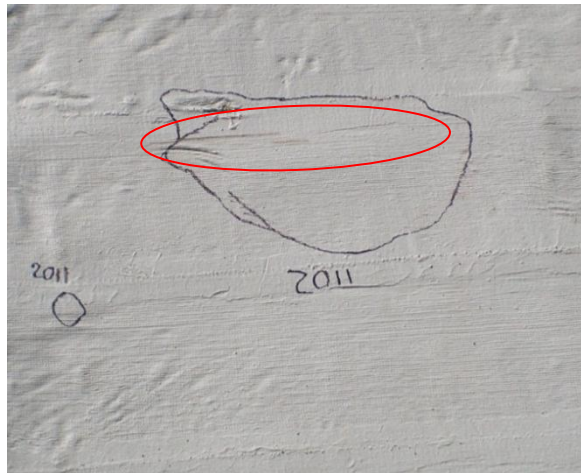


Figure 3.23. Two identified voids during the 2011 inspection, visible cracks in CFRP

All three voids identified during the biennial inspection in 2007 had grown in size and all voids found in the 2011 field assessment that were not previously identified presumably developed in the time between the 2007 bridge inspection and the 2011 field assessment. It was not possible to determine whether the crack identified in 2007 had grown in size; the physical markings on the bridge only indicated the crack existed at the time of the 2007 bridge inspection. In terms of documentation, in addition to the physical markings left on the bridge from both the 2007 bridge inspection and 2011 field assessment, locations and sizes of voids found on the extrados of the east arch are tabulated in Appendix A. There were 28 voids, 3 cracks, and 1 rust spot found during the 2011 field assessment. The voids ranged in area from less than 26 cm² (4 in²) to 9876

cm² (1530 in²) averaging approximately 580 cm² (90.3 in²). Photographs of the bays and the identified areas on the arches can be found in Appendix A as well as thermal images of voids.

3.4.4 Pull-Off Tests

Multiple sources for pull-off test recommendations or standards have been published including the International Concrete Repair Institute (ICRI) Guideline No. 210.3-2004, the Army Corps of Engineers Technical Report REMR-CS-61 (1999), ACI 503R (1993), and ASTM D7522 (2009). Unfortunately some of these reports can be inconsistent. For instance, the Army Corps of Engineers states in their technical report “The important issue associated with pull-off tests is the depth of the core drilling into the existing concrete” adding, “ignoring the effect of drilling depth may be one of the main causes of difficulties in reproducing and comparing test results.” Unfortunately, the other three sources have differing recommendations in regard to the core drilling depth into the substrate. ICRI recommends core drilling a minimum depth of 25 mm (1”) into the existing substrate, while ASTM D7522 requires core drilling between 6 mm (0.25”) and 12 mm (0.5”) into the substrate. ACI 503R recommends “core drill through the coating and down barely into the subsurface.”

Previous pull-off tests described above in section 3.2.3.2 were conducted by CTC-Geotek directly following the repair in 2003 and for the sake of comparing test results, the testing procedure used by CTC-Geotek was replicated as closely as possible. The testing procedure was also intended to be consistent with the majority of the guidelines

and recommendations made by the sources above where possible. While each of these guidelines is respected, the default testing technique was that of ASTM D7522.

As previously discussed, it is essential that the CFRP is well bonded to the arches in order to transfer stresses. To test the bond strength a pull-off tester, Proceq Dyna Z 16, was attached to a 50 mm (2") diameter aluminum puck which was adhered with a 5-minute, 2500 psi, two-part epoxy, Devcon S-210, to the surface of CFRP. The pull-off tester output the force applied to the puck via digital manometer. The digital manometer was also capable of outputting the stress that was applied by the puck to the bond, based on the area of the 50 mm (2") diameter puck.

Three separate sets of nine pull-off tests were performed during the field assessment in 2011. The first set of nine were located on the extrados of the base of the east arch at the north end, the second set was located on the extrados of the base of the west arch at the north end, and the final set was located on the extrados of the center or crest of the east arch. These locations are depicted in red lettering in Figure 3.24 below.

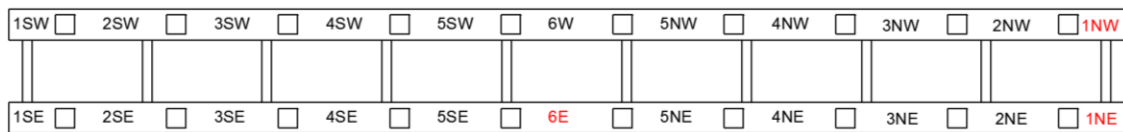


Figure 3.24. Pull-off test locations highlighted in red

A 5.7 cm (2 ¼") outside diameter Husqvarna diamond coring bit was used in a Type DM-225 Husqvarna core drill. This drill is intended for wet-drilling and has an attachment for a typical garden hose. Due to the remote location of the Castlewood Canyon Bridge, a pressurized water source was not available. If the core drilling was

completed dry without the use of externally applied water, damage to the bit as well as damage to the core would have been caused by excessive heat. Therefore, ice cubes were placed inside the 36.8 cm (14 ½”) cylindrical shaft of the 5.7 cm (2 ¼”) outside diameter coring barrel to provide available water for drilling as well as cooling for both the bit and core.

A 2.5 cm x 14 cm x 91.4 cm (1” X 5 ½” X 36”) wood board with a 5.7 cm (2 ¼”) diameter hole was used as a jig to start the holes, as there was no center drill arbor as there are with hole saws. Starting a core hole is the most difficult part of the process and was made much easier by the use of a jig, seen in Figure 3.26. In addition to being dangerous, coring without the use of a jig or center drill arbor could result in damage to the surface due to the coring bit unintentionally translating laterally, seen in Figure 3.25.



Figure 3.25. Damage caused by core bit without the use of the jig

Many core drills are bolted to the surface in which they are to core for these reasons. Below is a photograph of a core hole being started using the jig described above.



Figure 3.26. Starting a core hole using a wooden jig

Once the core hole was established using the jig, the jig was removed and the remainder of the coring process was completed. The core depth of 1 cm (3/8") into the substrate was consistent with that of previous pull-off tests conducted by CTC-Geotek.

Adding torsional stresses to the circular area of CFRP and substrate inside the cored circle was inevitable due to the drilling process. These stresses were minimized by using a less aggressive drill bit with diamonds instead of a coring bit which has more aggressive carbide teeth for instance. Wet drilling by use of the ice also reduced stresses by adding water which created a slurry that removed displaced debris while using the finer particles to aid the diamonds in the cutting process. In one instance out of the 27 cored locations, the stresses induced by the drilling were enough to fail the cored section at the interface between the CFRP and the substrate. Figures 3.27 and 3.28 illustrate this occurrence.



Figures 3.27 and 3.28. The core drilling location that failed due to torsional stresses during the core drilling process, bay 1NW

In anticipation of applying a two-part epoxy to adhere pull-off pucks, remaining moisture and standing water was removed from the cored areas using compressed air and nozzle seen below in Figure 3.29.



Figure 3.29. Removing water and debris from core cuts

The pull-off tests were intended to test the adhesion or bond between the FRP and substrate; therefore the acrylic paint layer was removed using a right angle grinder and masonry grinding disc to eliminate any premature failure of bond that may occur at the paint/CFRP interface. Additionally, this procedure also created a rougher surface

increasing the surface area, improving the likelihood of strong bond between the puck and the CFRP. However, stresses from friction and heat from both the drilling and the grinding procedures could have influenced the results of the pull-off tests. This process is represented in Figure 3.30 below.



Figure 3.30. Removing the acrylic paint later before adhering the aluminum pucks

The areas with paint removed were then cleaned of debris and dust in preparation for the adhesion of the 2" diameter, 1" thick aluminum pucks. Compressed air and nozzle were used once again with the additional use of 70% isopropyl alcohol as a quickly evaporating cleaning agent. The prepared surfaces are in figures below.



Figures 3.31 and 3.32. Prepared areas for the adhesion of aluminum pucks for pull-off tests and a close-up of a prepared surface

The aluminum pucks were also prepared prior to adhering them to the CFRP. Each puck was sanded with 40 grit sandpaper, cleaned with 70% isopropyl alcohol, and then blow-dried using the compressed air and nozzle. Figures 3.33 and 3.34 are photographs contrasting aluminum pucks before and after sanding with 40 grit sandpaper and pucks being thoroughly cleaned.



Figures 3.33 and 3.34. Aluminum pucks before and after sanding with 40 grit sandpaper and preparing the aluminum pucks way up high on the arch

Once both the aluminum pucks and CFRP surfaces were prepared and cleaned, the pucks were adhered to the CFRP at the cored locations with epoxy. This rapid setting epoxy achieved full strength in one hour, making it ideal for field work. The aluminum pucks were allowed approximately 3 hours before the pull-off tests commenced.

The pull-off tests were conducted in the same chronological order as the pucks were adhered. In the center of the aluminum pucks a threaded hole allowed for a spherical headed bolt to be threaded hand-tight into the puck. The pull-off tester was then moved into place to engage the spherical head of the bolt threaded into the puck. The pull-off tester was then leveled parallel with the testing surface and the digital manometer was zeroed and the pull-off test started. Smooth continuous rotations of a

hand-crank applied an upward force on the puck until failure. Figures below show adhered pucks, the spherical headed bolt threaded into a puck, the pull-off tester being placed, the pull-off test with a reading from the digital manometer, and removing the puck following the test from the pull-off tester.



Figure 3.35. Adhered aluminum pucks for pull-off tests



Figures 3.36 and 3.37. Spherical headed bolt threaded into puck and placing the pull-off tester to engage the spherical headed bolt



Figures 3.38 and 3.39. Conducting a pull-off test with the digital manometer reading and removing the tested puck from the pull-off tester

The maximum stress applied and failure modes of the tests were recorded in accordance with ASTM D7522. The results of the pull-off tests can be found with the results from CTC-Geotek tests in tables in Appendix B. Failure modes A, B, E, F, and G as defined above in Table 3.1 occurred during the testing. Representative photographs of these different failure modes are shown below.



Figure 3.40 and 3.41. Failure Mode A: bonding adhesive failure at loading fixture (on left), Failure Mode E: Adhesive failure at CFRP/substrate adhesive interface (on right)



Figures 3.42 and 3.43. Failure Modes B and F: cohesive failure in FRP laminate, and mixed cohesive failure in substrate and adhesive failure at the adhesive/substrate interface, respectively (on left), Failure Mode G: cohesive failure in concrete substrate (on right)

Two pull-off tests were not able to be recorded due to technical difficulties. One of the tests failed during the preparation process of core drilling and the other test had a puck with faulty threads that would not allow for the spherical headed bolt to be engaged. These tests are represented as not available, NA, in the tables and plots. A summary of the failure modes for the 27 pull-off tests from 2011 and the 42 pull-off tests from 2003 are below in Table 3.3 and Figure 3.44.

Table 3.3. Summary of Failure Modes for the Pull-off Tests

42 Tests	Failure Modes of 2003 Pull-off tests							
	A	B	C	D	E	F	G	NA
Quantity	9	0	0	0	2	3	25	3
Percentage	21.4	0.0	0.0	0.0	4.8	7.1	59.5	7.1
27 Tests	Failure Modes of 2011 Pull-off tests							
	A	B	C	D	E	F	G	NA
Quantity	2	2	0	0	7	8	8	2
Percentage	7.4	7.4	0.0	0.0	25.9	29.6	29.6	7.4

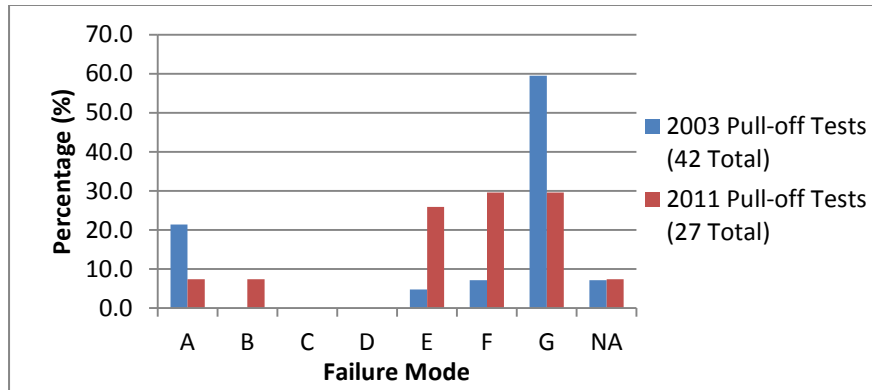


Figure 3.44. Failure Modes of Pull-off Tests from 2003 and 2011

The number of failure modes E, F, and G are roughly equal in number with only approximately 7% of the specimens failing in each of the A, B, and NA failure modes for the tests conducted in 2011. From Figure 3.44 it is apparent that the high percentage of failure mode G from 2003, significantly decreased to the evenly distributed modes E, F, and G of the 2011 test results. Mode B was a failure mode that did not occur in 2003, but did in 2011 twice out of 27 tests. An increase in percentage of failure modes B, E, and F indicates that other interfaces other than within the substrate are weaker and controlling. Failure Mode B is, according to ASTM D7522, “an indication of poor through-thickness properties of the FRP. Such failures may be due to incomplete wet-out of the fibers or plies comprising the laminate. Such failures may also result from environmental degradation of the FRP material itself.” The term “wet-out” is referring to the quality of the CFRP composite material and whether the fibers were fully saturated in epoxy during the wet lay-up process. Failure Mode E is an indication of poor adhesion properties and Failure Mode F is a commonly observed mixed failure mode that is believed to initially fail in the cohesion in the substrate, followed by propagation to the adhesive interface.

Different substrates at the location of the pull-off tests of 2003 and 2011 could have influenced both the failure mode and results of the pull-off tests. It is reasonable to consider that the tensile strength of concrete could have improved marginally since 2003 due to continued curing especially if the substrate was shotcrete rather than the original concrete. However, even in the case of shotcrete as the substrate this improvement or increase in strength would be fairly marginal. Comparing bond strengths of the 2003 and 2011 tests of only failure mode G tests would be a reasonable evaluation of this possible strength gain of the substrate if the testing processes and substrates were identical or had very little variation. Below is a table with strengths of failure mode G for comparison.

Table 3.4. Pull-off Test Results of Failure Mode G Tests

	Average		Maximum		Minimum		Sample Size
	MPa	psi	MPa	psi	MPa	psi	
2003	2.92	423	4.12	597	1.50	217	25
2011	2.07	300	3.81	553	0.13	19	8

According to the values in Table 3.4, the tensile strength of the substrate decreased or became weaker over time. Average, maximum, and minimum strength values all decreased from 2003 to 2011. The minimum test value of 2011 may have been so low due to imperfections during the core drilling process that completely failed one specimen with a failure mode E. The two low values could have also been due to areas of poorly mixed concrete. The failure interface appeared relatively homogeneous with little to no aggregate and had a solid gray color seen in Figures B22 and B25 in Appendix B. The average value of the 2011 tests was significantly influenced by the one low value

because of the small sample size. The tensile strength of the substrate decreased from 2003 to 2011. Local phenomenon or testing procedures may be responsible for some or all of this difference in strength.

Of the 27 pull-off tests conducted in 2011, nine tests, two of which were failure mode G, failed to meet the 200 psi minimum requirement of CDOT's construction specifications (Revision of Section 602) compared to only one of the 42 tests conducted in 2003. Six of the nine tests that had strengths less than 200 psi had failure mode E. This failure mode is a failure at the interface between the CFRP and the substrate. As seen in Figure 3.12, a relatively thick layer of resin was used to smooth the surface of the substrate at the time of the CFRP repair.

The thick "filler" resin varied in thickness and in color and was more prevalent at the base of the arches in bays 1NE and 1NW. The pull-off tests with low values all appeared to have very similar failure modes and strengths as well as appearance of the failure plane. Of the nine inadequate bond strengths, two existed in bay 6E with failure mode G. The pull-off test from bay 6E compared to bays 1NE and 1NW averaged higher strengths (2.14 MPa vs. 1.80 MPa) and had a larger percentage of the ideal failure mode G (77.8% vs. 6.3%). Below are two figures displaying the distribution of pull-off strengths and probability density functions based on a normal distribution of pull-off strengths.

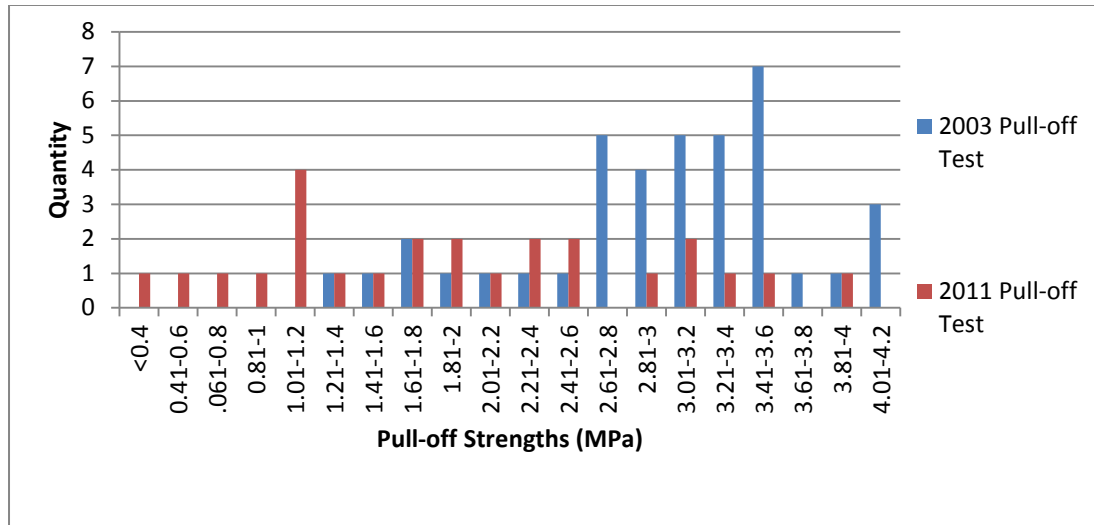


Figure 3.45. Histogram of Pull-off Test Strength

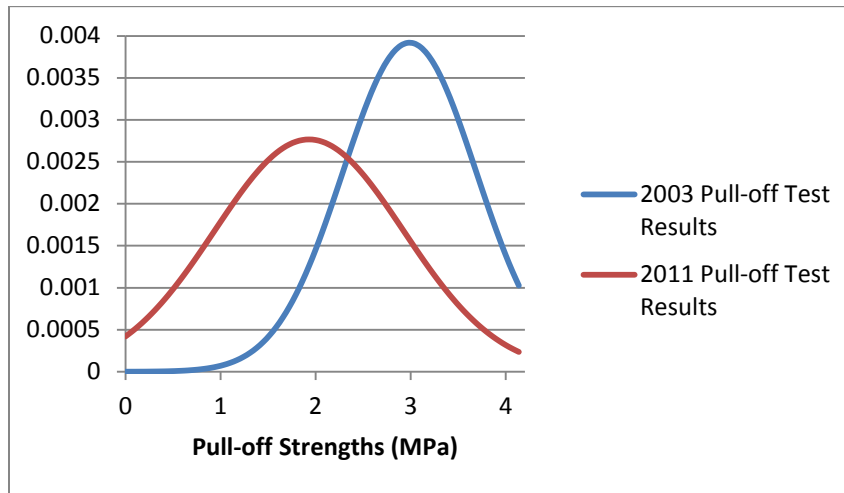


Figure 3.46. PDF of Pull-off test results

The lower, wider, curve of the 2011 PDF in Figure 3.46 gives evidence that the standard deviation increased from 2003 to 2011. In addition from 2003 to 2011 the mean lowered, shifting to the left. If the influence of the testing procedure could be disregarded, the larger variance of the 2011 results would likely represent the varying conditions in which the CFRP was exposed. The decrease in the mean from 2.98 to 1.93 from 2003 to 2011 gives indication of an overall decrease in the bond strength of the

CFRP to the concrete. This indicates a possible durability concern for long-term applications.

The detection of voids, void sizes, and the bond strength evaluation provide several different types of evidence that consistently showed there are some issues in regard to the durability of the CFRP. The increase in number of voids, increase in size of existing voids, change in distribution of failure modes, decrease in average bond strength with more inadequate strength values, and increase in variance of bond strengths all indicate deterioration of the bond between the CFRP composite and the concrete arch. It would be prudent to monitor the durability and performance of the bond closely and consistently to try and accurately quantify the development of the degradation.

3.4.5 Collecting Specimens for Laboratory Testing

The original plan was to remove strips of CFRP from the exterior corner of the extrados of the arch to provide the specimens for the tensile testing and DSC testing in the laboratory. After detecting voids on the extrados of the east arch, it was determined that it would be beneficial to remove two large voids found rather than remove strips of FRP that were intact. Three reasons contributed to this decision. Intact or well-bonded CFRP would not have to be removed from the arch for the laboratory testing. This would preserve the strength the CFRP was providing to the bridge and it would significantly reduce the necessary efforts of trying to remove intact CFRP by chipping or cutting concrete and avoiding causing damage to the CFRP. Secondly, inspection of the substrate would be possible by the removal of larger areas of CFRP. Lastly, repairing

areas of voids would improve the performance of the CFRP retrofit by allowing stresses to be transferred from the substrate to the CFRP via the bond which it lacked at the time of removal. Below in Figure 3.47 is a plan view drawn to scale of the locations of the patches removed.

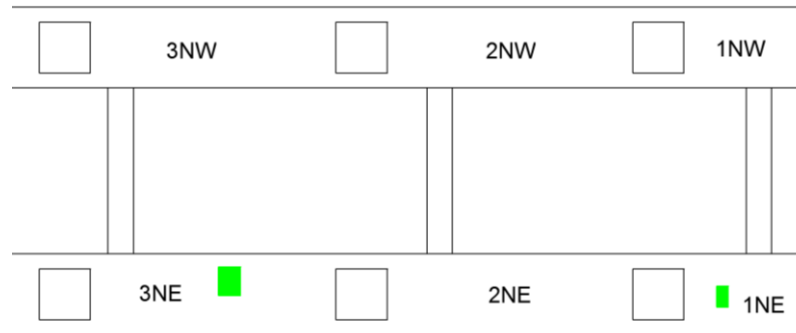


Figure 3.47. Areas removed are highlighted in green

The smaller of the two voids, approximately 28 cm x 51 cm (11" x 20") in size, was removed from the extrados of the 1st bay on the north end of the east arch. This void had a previously identified crack running in the transverse direction on the arch. A right angle-grinder mounted with 11.4 cm (4 ½") masonry cutting wheel was used to cut through the CFRP layer in a rectangular shape enclosing the area of the void. Once the CFRP was removed, it was reasoned that this area of CFRP was at one time bonded to the substrate, because the crack previously seen in the surface of the CFRP was also present in the substrate. It was likely that the concrete cracked due to service loads or shrinkage. Or it is possible the crack was present before the CFRP was applied and the crack opened more causing the CFRP to crack. According to CDOT's construction specifications, cracks in the substrate larger than 1.5 mm (0.06 in) in width were to be pressure injected with epoxy resin prior to the application of the CFRP. When the

concrete cracked or the crack widened due to internal tension, the same strain was imposed on the CFRP to cause cracking there as well. A local bond would have been necessary to impose the same strain to the CFRP. Once the CFRP became cracked, water and moisture was able to penetrate the CFRP layer and subsequent freeze/thaw cycles not only opened the crack more, but debonding of the CFRP from the substrate also occurred. The debonded area increased over time due to freeze/thaw cycles and temperature fluctuations. The unidirectional CFRP fabric was more susceptible to cracks in the transverse direction because the carbon fibers were aligned in this same direction and no, or very few, fibers had to rupture. The ultimate tensile strength 90 degrees to the primary fibers of Tyfo® SCH-41, according to Fyfe, is approximately 4.6% of the ultimate tensile strength in the direction of the primary fibers.

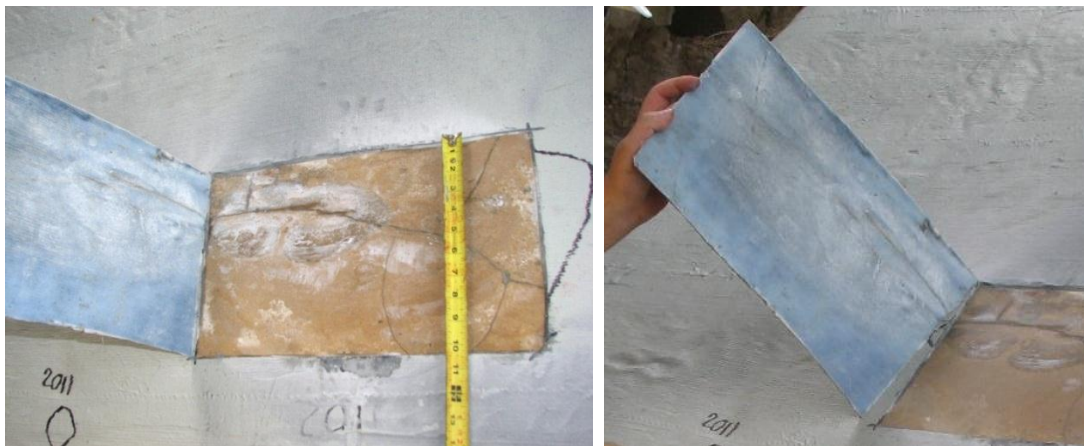
Upon cutting the lower edge of the CFRP rectangle, water exited the cut at the bottom of the void revealing standing water at the interface between the CFRP and substrate. Photographs of the void and the removal of the CFRP layer are shown in Figures 3.48 – 3.52 below.



Figures 3.48 and 3.49. Void in CFRP with transverse crack identified with red arrows and Cutting the perimeter of the void in the CFRP



Figure 3.50. Water exiting the void area directly after the lower cut through the CFRP was completed

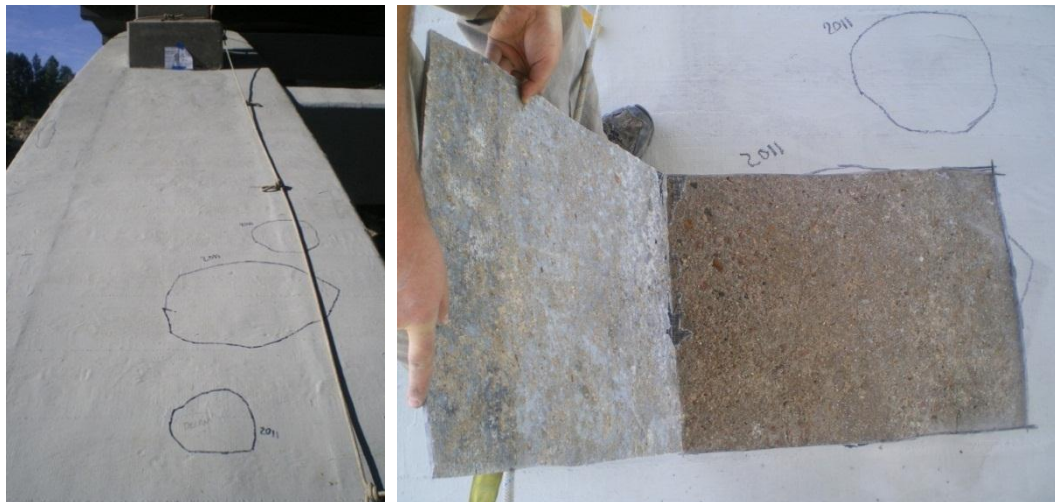


Figures 3.51 and 3.52. Cracks in the substrate were transmitted through the CFRP and notice the smooth texture and blue and white color of the underside of the CFRP

It is worth noting the condition of the underside of the CFRP panel removed. It is blue and white in color and smooth in texture. This smooth texture is the underside of a thick layer of resin referred to as a “filler resin” used to smooth the rough surface of the substrate. There are no pieces of the substrate adhered to the CFRP panel, which when compared to the other area removed would strengthen an argument that this area was

never well bonded to the substrate. The transmitted crack and the smooth surface provide contradictory indications as to the quality of bond over time. The transmitted crack indicates a strong bond existed at one time and the smooth textured underside of the CFRP indicates that this area may have never been well bonded.

The second void was removed from the 3rd bay on the north end of the east arch. A rectangular section of the CFRP was removed with the same procedure previously described. Photographs of the area of the void and the removal of the CFRP rectangle are in Figures 3.53 and 3.54 below. There was no standing water or evident moisture in this larger void area, but there was significant pieces of the substrate adhered to the underside of the CFRP patch removed.



Figures 3.53 and 3.54. Voids found in the 3rd bay on the north end of the east arch and removal of the CFRP of the largest void

Both sections of CFRP removed from the arch were taken to the laboratories at CSU for tensile tests and differential scanning calorimetry tests. These tests and their results are discussed in Section 3.5.

3.4.6 CFRP Repair

Due to the pull-off tests, a total of 27 – 57.15 mm (2 ¼”) diameter holes of varying depths, depending on the failure mode, were created on the arch. These areas were filled with epoxy to restore the profile of the arch. Initially, the same epoxy used to adhere the aluminum pucks to the CFRP was used to fill the holes created from the pull-off tests. Due to the inclined angle, this epoxy, which is less viscous before curing, would slump and run down slope on the locations near the base of the arches. This was undesirable and a more viscous epoxy, 3000 psi Loctite epoxy gel, was used to fill the holes created from the pull-off tests. These filled holes of varying depths can be seen below.



Figure 3.55. Epoxy filled holes following the pull-off tests

Once the holes were filled with epoxy, the 3 areas of pull-off tests and the 2 areas of removed CFRP (debonded regions) were prepared for a repair process. First these areas were washed using a non-toxic, biodegradable, soap and water, then they were cleaned with 70% Isopropyl alcohol to remove any remaining soap film. CFRP patches must overlap a minimum of 6”; therefore primer was applied to the affected

areas of the arches plus a minimum of 6" in each direction. The primer used for the repair was a two part epoxy made by HJ3, STRONGHOLD Primer Epoxy (STR-BW-200A). The mix ratio was 2 parts of the PC-200 Primer Resin, Part "A", to 1 part of the PC-200 Primer Hardener, Part "B". Once the two-part epoxy was well mixed, the primer was distributed to the repair areas using 9" rollers as seen in the photograph below.



Figure 3.56. Applying a primer coat to the areas for repair

Following the recommendation of HJ3, the primer was allowed to cure for 24 hours before the repair process was continued. The CFRP material, comparable to that of the CFRP fabric used during the 2003 repair, was also provided by HJ3. HJ3 provided both CF-516 Uniaxial Carbon Fabric and CF-528 Biaxial Carbon Fabric for the repair. Below is a table with material properties of the existing material made by Fyfe and the comparable repair material made by HJ3.

Table 3.5. Material Properties of the Existing and Repair Materials

Material Properties of Uniaxial Carbon Fabric						
Date of Information	Manufacturer	Product	Tensile Strength MPa (ksi)		Modulus of Elasticity GPa (ksi)	
			Typical Values	Design Values	Typical Values	Design Values
2003 (CDOT Report*)	Fyfe	Tyfo® SCH-41	876 (127)	745 (108)	72.4 (10500)	61.5 (8900)
2011	HJ3	CF-516	1034 (150)	818 (119)	85.4 (12380)	71.9 (10433)

The CFRP fabric was saturated by applying a well-mixed two part epoxy, two parts of HJ3 SRS-400-A Resin and one part HJ3 SRS-400-B Hardener, to both sides of the fabric. The two part epoxy was also applied to the repair areas identical to that of the primer. The saturated fabric was then placed on the arch and the use of hand pressure and rollers eliminated air bubbles and pockets between the fabric and the substrate. Unidirectional CFRP fabric was used to repair the area where the patches were removed. Proper alignment of the fiber direction in the transverse direction was necessary to repair the transverse wraps. The pull-off tests were conducted closer to the edge of the arches damaging both transverse and longitudinal sections. Therefore, biaxial patches were used to repair these areas. This process is represented in the photographs below.



Figures 3.57 and 3.58. Allocating fabric for repair and applying the second layer of CFRP to the area of pull-off tests on the east arch



Figures 3.59 and 3.60. The repaired sections on the north end of the arches

Following the CFRP repair, 24 hours was allowed for curing before the areas were painted.

3.5 Laboratory Tests at Colorado State University

3.5.1 Tensile Tests

The two rectangular pieces of CFRP that were removed from the Castlewood Canyon Bridge were taken back to Colorado State University for testing. The pieces removed, approximately 55.9 cm x 71.1 cm (22" x 28") and 27.9 cm x 50.8 cm (11" x 20"), were cut using a band saw into strips 2.5 cm (1") wide by 21.6 cm (8.5") long. The cuts were made to isolate areas of CFRP that were only one layer thick, and the 21.6 cm (8.5") direction was required to be parallel with the direction of the fibers. Twelve samples from each area were tested at the Foothills campus of CSU at the Engineering Research Center using a United universal testing machine in accordance with ASTM D3039M-08 except the alignment procedures with the strain gauges and tabs were not used. For each test the failure mode, ultimate strength and modulus of elasticity was recorded.

The thickness of the CFRP strips varied significantly due to the rough contour of the adhered side of the CFRP. As previously discussed in sections 3.2.4 and 3.2.5, a thick filler resin was applied to smooth the surface of the substrate prior to adhering the CFRP fabric to the arches. This process can be seen above in section 3.1.1.2 in Figure 3.12. A photograph of the rough texture is below.



Figure 3.61. The rough contour of a tensile test strip of CFRP

The tensile strength and modulus should be dominated by the fibers, and thus the built up addition of filler resin was not considered as the thickness, but rather the manufacturer's data of 1.02 mm (0.04") for the thickness per layer was used to calculate the area of the specimens. This is referred to as "normalizing" the results, instead of using the average of actual dimensions measured. Before the testing began, an extensometer was placed in the mid-section of the specimen and was removed during the testing when the load reached 8896 N (2000 lb.) for most specimens.

Three letter failure codes were used in accordance to ASTM D3039. The first letter signifies failure type, the second identifies failure area, and the third refers to the location of failure. A summary of the codes and their respective failure modes are tabulated in Table 3.6.

Table 3.6. ASTM D3039 Letter Codes for Failure Modes

First Character		Second Character		Third Character	
Failure Type	Code	Failure Area	Code	Failure Location	Code
Angled	A	Inside grip/tab	I	Bottom	B
edge Delamination	D	At grip/tab	A	Top	T
Grip/tab	G	<1W from grip/tab	W	Left	L
Lateral	L	Gage	G	Right	R
Multi-mode	M	Multiple areas	M	Middle	M
long Splitting	S	Various	V	Various	V
eXplosive	X	Unknown	U	Unknown	U
Other	O				

Ideally, the specimens would fail in the area of the extensometer away from the grips. Photographs of the failed tensile test specimens displaying varying combination of failure modes are shown in Figures 3.62 and 3.63. Note the striking difference in appearance of the underside of the CFRP sections removed.

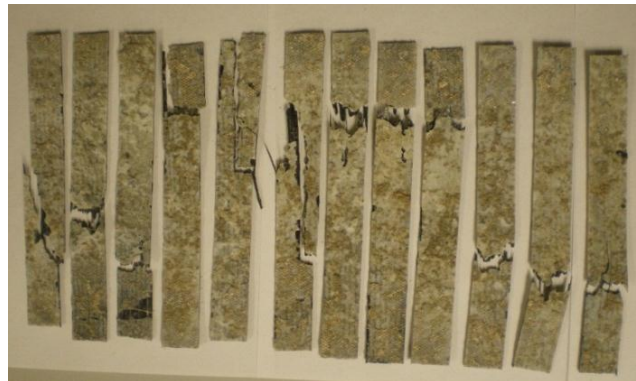


Figure 3.62. Failed tensile test specimens from the large void removed from bay 3NE, note the oatmeal appearance

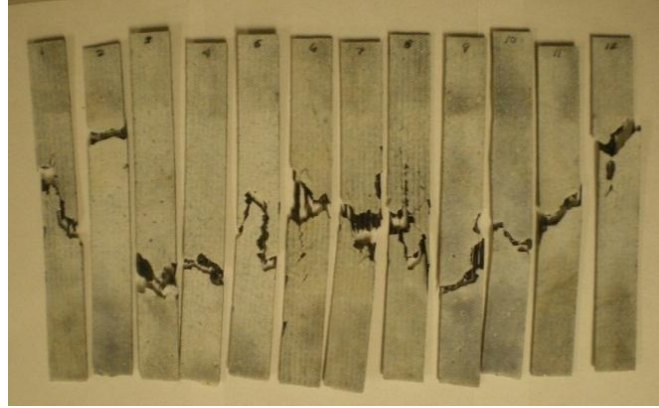


Figure 3.63. Failed tensile test specimens from the small void removed from bay 1NE, note the milky appearance

Test results can be found in Appendix C. The modulus of elasticity was not calculated during three of the 24 tensile tests due to difficulties with the extensometer. Test specimens from bay 3NE had lower ultimate tensile strengths perhaps due to more grip failures or failures closer to the grips. Bar charts in Figures 3.64 and 3.65 display the distribution of values of tensile strength and modulus of elasticity of the tensile tests.

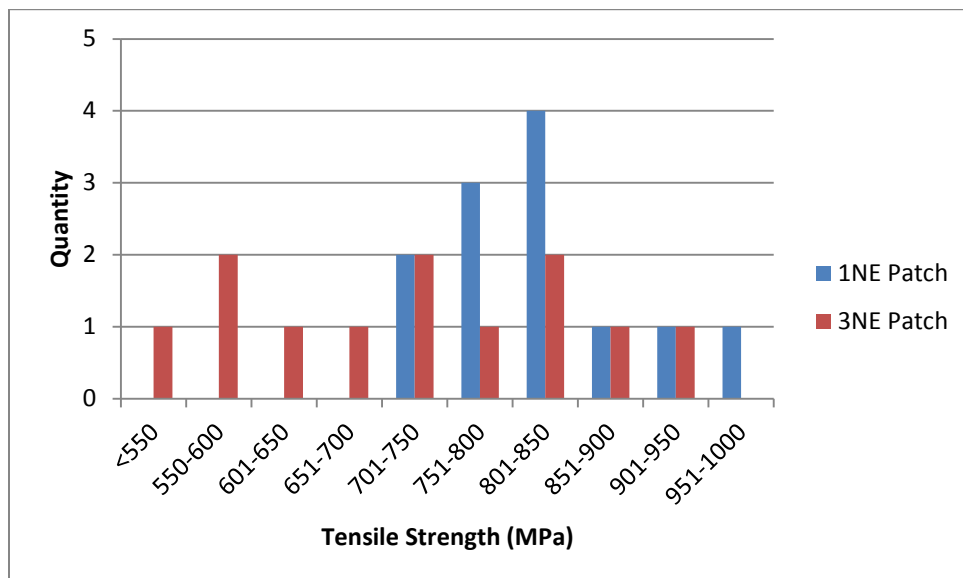


Figure 3.64. Distribution of Tensile Strength Results

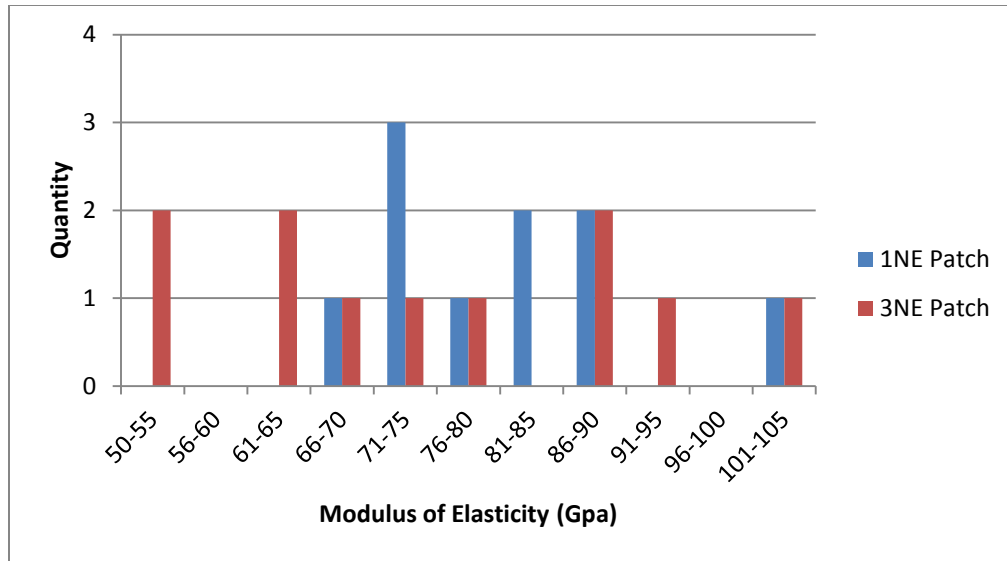


Figure 3.65. Distribution of Modulus of Elasticity Results

Material properties of the CFRP used in 2003 are tabulated below for comparison purposes. These values are considered the initial values before any degradation has occurred.

Table 3.7. Material Properties of 2003 CFRP

Material Properties of Uniaxial Carbon Fabric						
Date of Information	Manufacturer	Product	Tensile Strength MPa (ksi)		Modulus of Elasticity GPa (ksi)	
			Typical Values	Design Values	Typical Values	Design Values
2003	Fyfe	Tyfo® SCH-41	876 (127)	745 (108)	72.4 (10500)	61.5 (8900)

A graphical representation of the test values relative to the manufacturer’s values reported in the CDOT report are the probability density functions shown in Figures 3.66-3.69. The typical values and design values given by the manufacturer are represented as dashed lines in the plots below. The design tensile strengths are typically some percentile of a distribution while the modulus of elasticity is usually the mean. For

instance, from the CDOT specification, “the ultimate tensile strength shall be the mean tensile strength of a sample of test specimens minus three times the standard deviation.” Statistically, this would correspond to a percentile of 0.14 which is very restrictive. This CDOT specification also required a minimum of 20 specimens to determine material properties. This would require combining the samples from the small and large patch totaling 24 specimens, resulting in a usable ultimate tensile strength of 288.2 MPa (41.8 ksi). These values referred to as “CDOT Design Strengths” are in Table 3.8 below and are represented as solid vertical lines in the plots below for each set of samples as well as all the tests combined. A common statistical reference used in other guidelines (Technical Report No. 55, 2000), is the 5th percentile which is also depicted as a solid vertical line in Figure 3.67 below. To determine the 5th percentile, 1.645 times the standard deviation was subtracted from the mean.

The probability density functions assuming normal distributions were generated using the statistics in Table 3.8 below. The vertical axis for the probability density functions is relative to the horizontal axis; the area under the curve equals unity.

Table 3.8. Statistics from the Tensile Samples

	Modulus of Elasticity (GPa)			Ultimate Tensile Strength (MPa)		
	1NE	3NE	Total	1NE	3NE	Total
Mean	81.1	74.0	77.3	820.5	688.2	754.4
Standard Deviation	10.7	16.3	14.1	79.3	186.2	155.4
CDOT Design Tensile Strength				582.5	129.6	288.2
5th Percentile				690.0	381.9	498.8

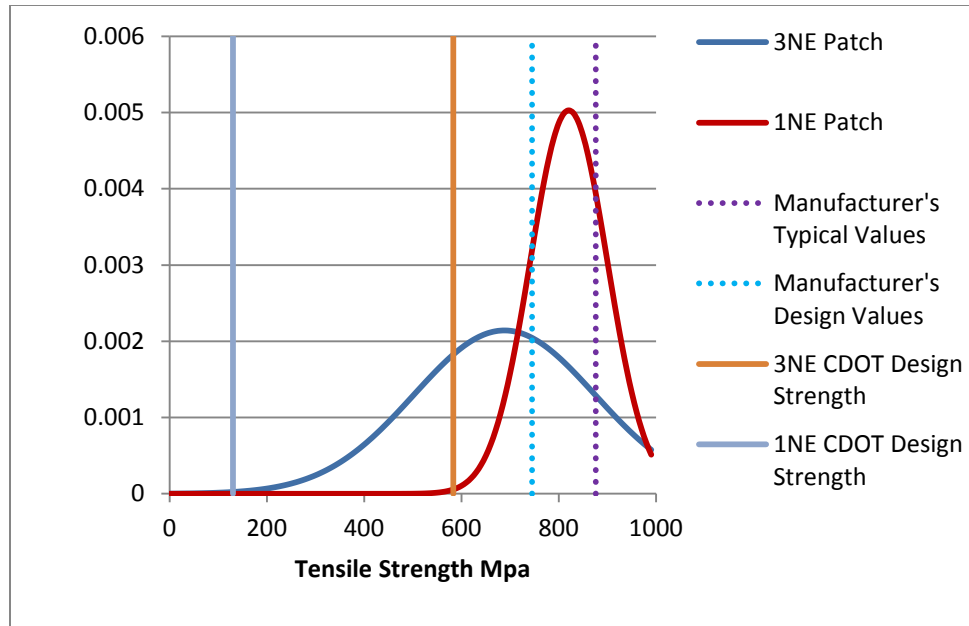


Figure 3.66. Probability Density Function of the Two Samples, Tensile Strengths

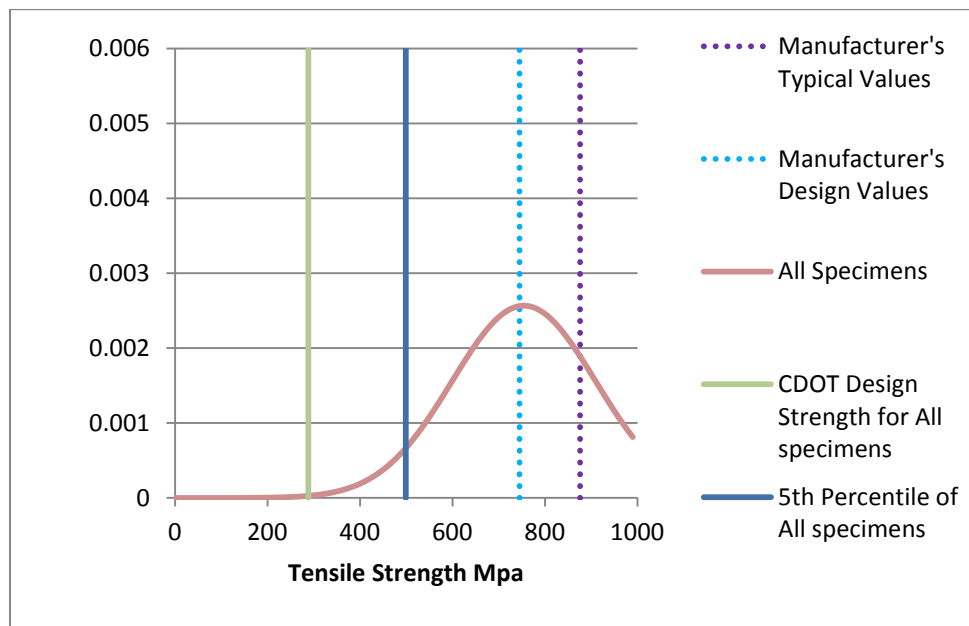


Figure 3.67. Probability Density Function of All Tensile Tests

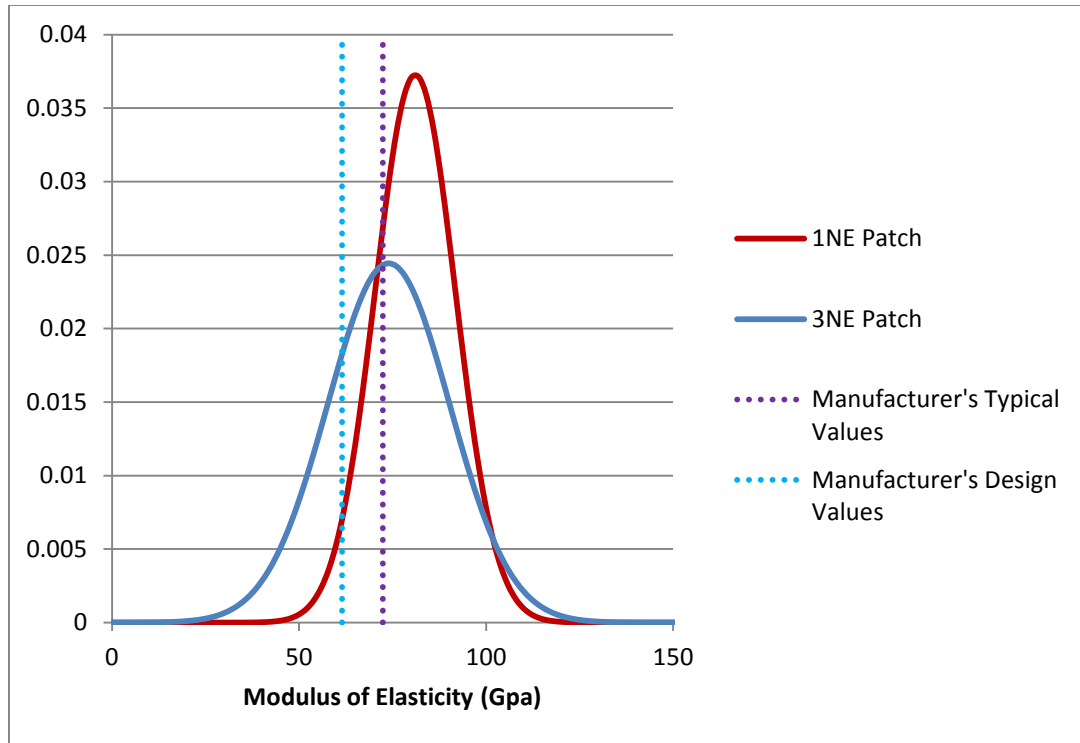


Figure 3.68. Probability Density Function of the two samples, Modulus of Elasticity

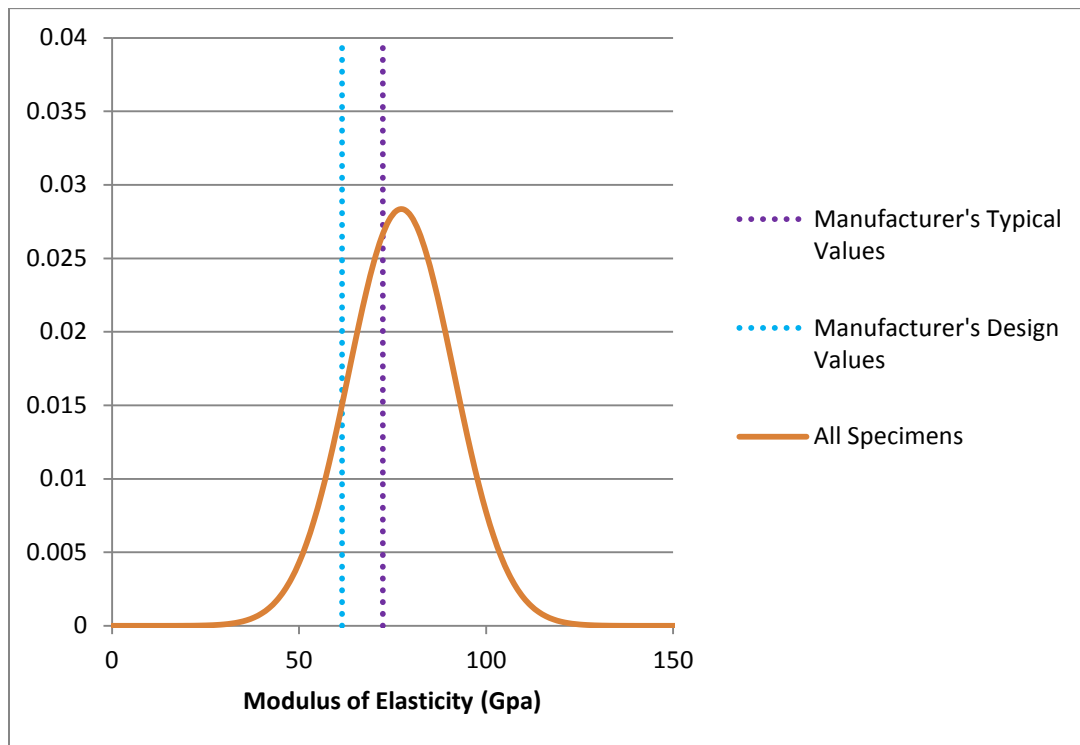


Figure 3.69. Probability Density Function of All Modulus of Elasticity Samples

Looking at the location of CDOT’s design strength and 5th percentile values relative to the probability density function in Figure 3.67 above, there is a very concerning discrepancy between the values of tensile strength provided by the manufacturer, the values generated from the tensile tests and the required values of the stringent CDOT specifications or the more permissive 5th percentile value. The values of modulus of elasticity are fairly representative of the values provided by the manufacturer.

By assuming the stress versus strain response of the CFRP was linear until failure, the rupture strain was found by dividing the ultimate tensile strength by the modulus of elasticity, which was the chord modulus of 0.0043 strain or less. CDOT’s construction specifications (Revision of Section 602) required a minimum rupture strain of 0.006 cm/cm. The rupture strain of the material at the time of repair was identified in the CDOT report as being 0.012 cm/cm for both the typical and design value.

Table 3.9. Tyfo SCH-41 Rupture Strain Values

Date of Information	Rupture Strain	
	Typical Values	Design Values
2003 (CDOT Report)	0.012	0.012
2011 Testing (Revision of Section 602)	0.0098	0.00308

Similar to the tensile strengths, CDOT’s construction specifications (Revision of Section 602) required “the ultimate rupture strain shall be the mean rupture strain of a sample of tests specimens minus three times the standard deviation.” A table of these values is below.

Table 3.10. Rupture Strain Values from the 2011 Tensile Tests

Rupture Strain	
Mean	0.00981
Standard Deviation	0.00224
CDOT Design Rupture Strain	0.00308
5th Percentile	0.00612

The 5th percentile value in the table above would satisfy the minimum rupture strain requirement of CDOT’s construction specifications (Revision of Section 602), but the “CDOT Design rupture strain” calculated per CDOT’s construction specifications (Revision of Section 602) is not adequate. A visual representation of this can be found in the probability density function in the figure below.

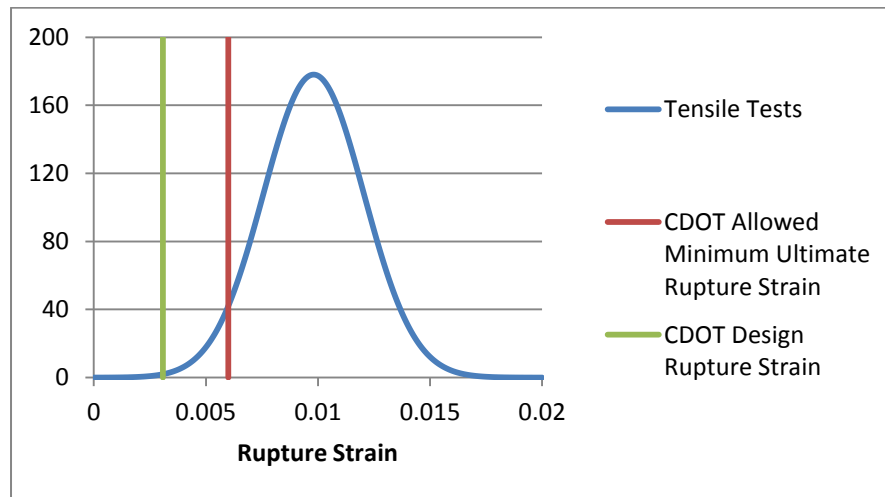


Figure 3.70. Probability Density Function of the Rupture Strain of All Tensile Tests

In summary, the tensile strengths were significantly lower than the values reported by the manufacturer, Fyfe and required by CDOT. It is difficult to determine whether these values are due to poor workmanship during the 2003 repair or degradation. Initial values at the time of repair would help make this differentiation if the samples tested in 2003 were representative of the material on the bridge. No results

from such tension tests were recovered for comparison. The modulus of elasticity values were reasonably close to reported values considering the sample size. The rupture strain, similar to the tensile strength, had values lower than acceptable design values according to CDOT's construction specifications (Revision of Section 602).

3.5.2 Differential Scanning Calorimetry (DSC)

Dr. Radford at the Motorsport Engineering Research Center on the Foothills campus of Colorado State University provided the guidance and equipment to conduct the DSC analysis. After material was allocated for tensile tests from the patches removed from the bays 1NE and 3NE, the remaining material was used for DSC. Samples of CFRP and the filler resin were tested using a Seiko SSC/5200 DSC testing machine. Testing specimens consisted of 15 mg of small particles. Specimens consisting of smaller particles are more desirable because there will be better contact between the specimen and the aluminum pan containing the specimen resulting in better accuracy and fewer resulting artifacts.

The specimens of the CFRP material were prepared in two ways. The first method was by grinding the material and collecting the debris from this process. The advantage of this procedure was that very small particles could be created quickly which resulted in better contact to the aluminum pan. The disadvantage was heat was introduced to the sample which may have exceeded the thermal history of the material causing some post-curing, resulting in T_g higher than the actual T_g during service. The second technique used in preparing specimens of CFRP was mincing or dicing the material into small pieces with the use of a knife. The advantage of this technique was

no additional heat was introduced to the specimen; the disadvantage was the time-intensive preparation and the larger pieces would have less contact with the aluminum pan. This second technique was also used for the preparation of samples of the “filler” resin. Unmeasured specimens can be seen in a photograph in the figure below.

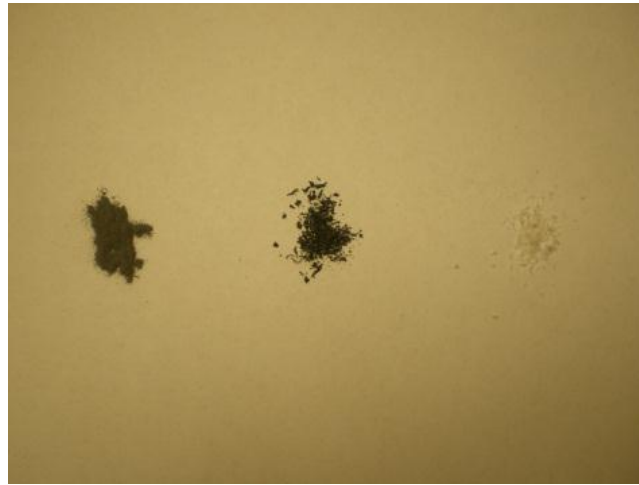
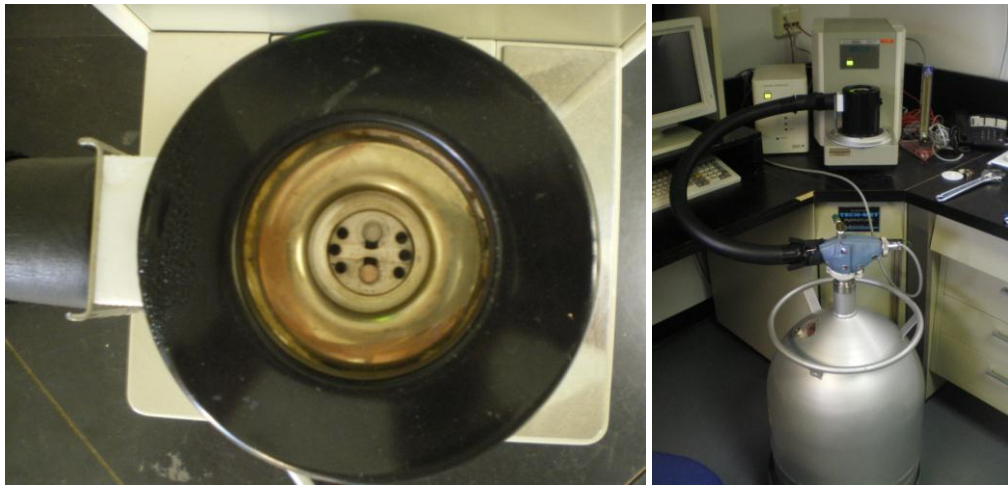


Figure 3.71. Ground CFRP, Diced CFRP, and Diced Filler Resin

A maximum of 15 mg was used for each DSC evaluation. The reactive material was only the resin of the composite and the percentage of resin to fiber was unknown. If the amount of constituents of the composite was known, additional information such as the amount of energy absorbed could be calculated by the hysteresis of the DSC test. The CFRP material likely had a lower percentage of reactive material, resin, than the filler resin and therefore smaller specimen sizes of the filler resin were sufficient in providing ample reactive material. Additionally, available water acts as a plasticizer to the resin and can cause the glass transition temperature to decrease. By the time the specimens were removed from the bridge and then transported to and tested in the lab, the moisture content of the specimens was likely more representative of the relative humidity of the lab environment than their condition during service. Therefore, the

lowering of the glass transition temperature due to higher water content was not detected, but likely existed on-site especially in the case of the section removed from bay 1NE where water drained from the area in which the patch was removed.

Each specimen was placed in an aluminum pan and an aluminum top was crimped in place to the bottom pan to enclose the specimen. The specimen was then inserted into the DSC testing machine, the mass of the specimen was entered into the software and the DSC was started. Liquid Nitrogen was used to cool the specimen to -30°C and the temperature was held until the DSC returned to equilibrium. The derivative of DSC, DDSC, was used to determine the beginning, middle, and end of transient states. The beginning and end of transient states had DDSC values of zero and the middle of the transient state was often considered the maximum absolute value of the DDSC between the zero values.



Figures 3.72 and 3.73. DSC Specimen Chamber and DSC with Liquid Nitrogen

Once the specimen was held at -30°C for approximately 5 minutes, a pre-programmed temperature versus time environment was created in the testing chamber.

Starting at -30°C , the DSC established a baseline and a built-in furnace provided the heat flow to the specimen's chamber. This constant increase in temperature, $10^{\circ}\text{C}/\text{min}$, continued for approximately 15 minutes until a temperature of approximately 130°C was achieved.

The temperature of 130°C was held for approximately one minute to allow the specimen to reach equilibrium in its transition from being endothermic to exothermic. Liquid Nitrogen was then used to cool or drop the temperature of the specimen at a constant rate back to the approximate room temperature of 20°C . During this returning of temperature, the DSC displayed similar behavior as before with an initial baseline, followed by a transient state, returning to a baseline below that of the previous baseline. This transition also represents the glass transition temperature; below is a plot graphically showing the temperature versus time relationship of the specimen chamber during the DSC test.

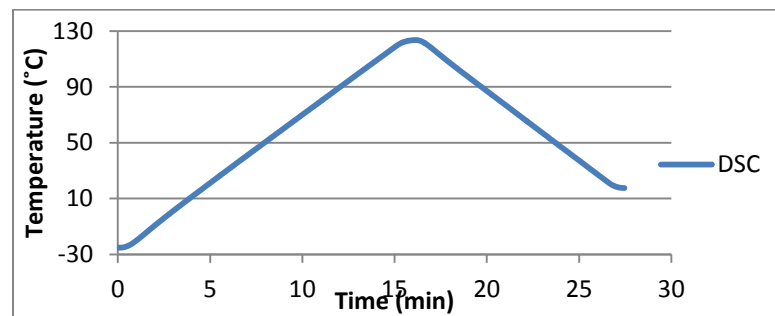


Figure 3.74. Temperature vs. Time of the DSC Analysis for the Ground CFRP1 Specimen

The first specimen tested was of the ground CFRP material. The DSC curve is in the plot below. The glass transition temperatures are two points identified in the plot.

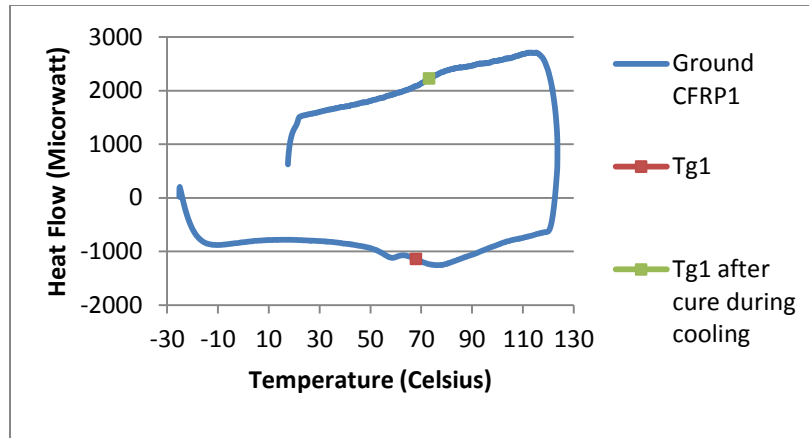


Figure 3.75. Ground CFRP Specimen

During heating the glass transition temperature, T_g , was 67.95°C, while during the cooling process the T_g was 73.19°C. This increase in T_g is due to the curing process caused by the heating up to 130°C. The glass transition temperature of the CFRP composite was expected to be between 60°C and 82°C as quoted by the manufacturer as being the design value and typical test value respectively. The highest temperature of the composites thermal history was probably not much greater than 40°C, which explains the additional curing and the upwards shift in the T_g during the heating process up to 130°C.

The same testing procedure was conducted for a second time on the same specimen because “differences between the first and second heating curves can be very informative” (Mettler Toledo, 2000). Two reasons in particular justified this decision. Firstly, it was of interest to explore the influence the heating process has on the specimen and its glass transition temperature due to post-curing. Secondly, if the erratic behavior disappears it would be considered an artifact and less significant in the first

test as opposed to a descriptor of a material property such as T_g . This specimen was referred to as Ground CFRP1A and its plot is below.

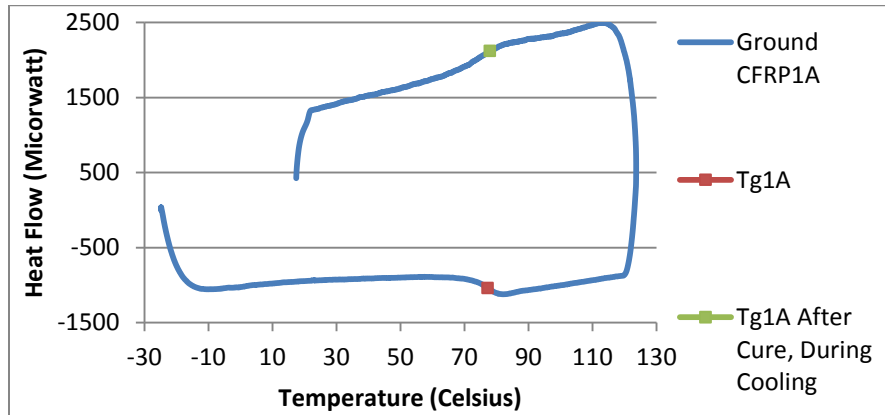


Figure 3.76. Ground CFRP1A

The erratic or irreversible behavior does not exist in the classic behavior of the DSC curve in the plot above. The behavior during heating and cooling are reversible and look identical. Subtracting the Ground CFRP1A curve from the Ground CFRP1 curve would yield an area that represents irreversible behavior.

The two glass transition temperatures were found to be 77.38°C and 78.02°C for the heating and cooling processes respectively. The second time the specimen was heated to 130°C the T_g increased by a much smaller amount due to the post-curing that occurred during the first test. The closer a specimen gets to being fully cured, the smaller the influence additional heat will have on T_g . Additionally, there is a relatively small shift in the T_g that is due to the different processes of heating and cooling that should be considered when comparing the T_g s found during the heating and cooling processes. During the heating the T_g is shifted to the right and during the cooling the T_g is shifted to the left; the glass transition temperature should be taken as the average of

the two values found during the heating and cooling processes if no significant curing occurred during the heating process. A plot of the heat-cool-reheat-cool process is in the figure below.

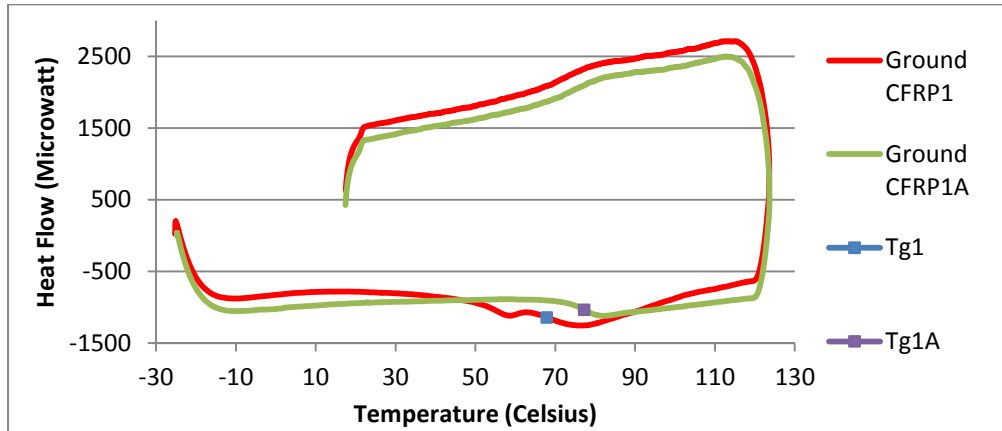


Figure 3.77. Heat-Cool-Reheat-Cool of the Same Specimen

DSC is not usually approached as though the data or results are random variables with corresponding distributions and therefore multiple tests are not usually conducted. However, a second test of ground CFRP was conducted to compare the T_g s and the presence of erratic or irreversible behavior. This specimen was Ground CFRP2 and its plots are below.

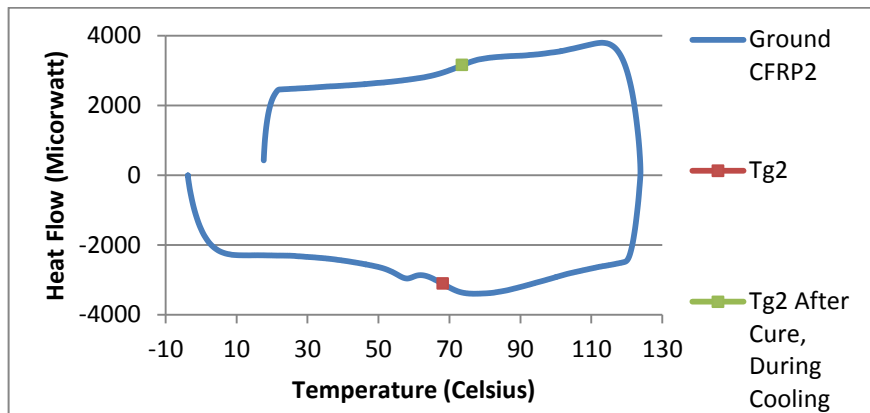


Figure 3.78. Ground CFRP2

The T_g s were very close to that of Ground CFRP1, 68.13°C and 73.56°C respectively, as was the general response and presence of the irreversible behavior. Diced CFRP was also analyzed as opposed to the ground CFRP. The diced CFRP had slightly lower values of T_g , possibly due to the heat added to the ground specimens but the difference was fairly marginal. All three plots are combined in the figure below. To reduce the test time and conserve liquid nitrogen, the start temperature was changed to from -30°C to -10°C for the Ground CFRP2 test.

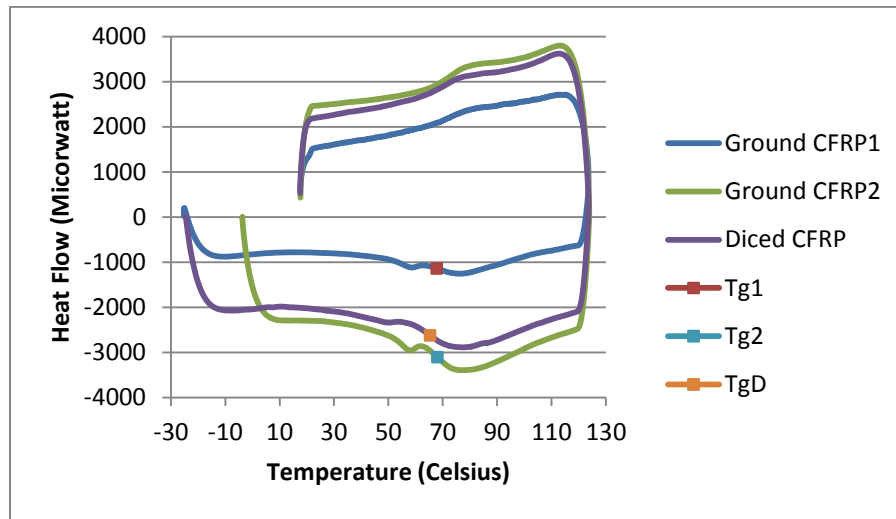


Figure 3.79. Ground and Diced CFRP DSC Results

The vertical shift in the DSC curves is due to the amount of reactive material within each specimen. The percentage of reactive material was likely very similar among the CFRP specimens but the different specimen sizes resulted in this vertical shift.

Two different types of filler resin were used in the DSC analysis. The specimens labeled “Filler Resin1” and “Filler Resin2” were made from the thick white filler resin found on the patch removed from bay 1NE. The specimen labeled “Bonded Filler Resin”

was created from diced filler resin that was more translucent and less thick and white which came from a section of CFRP that was well-bonded to the substrate.

The first filler resin tested was Filler Resin1, which resulted in a DSC curve that had erratic behavior early in the test that was presumed to be irreversible behavior. The plot of all 3 curves is in the figure below.

Due to the erratic behavior near 30°C during heating, it was decided to re-run this analysis with a new specimen, but to heat the specimen up to 40°C then return the specimen to -10°C and restart the DSC test. This would hopefully remove any irreversible behaviors without post-curing the specimen and consequently increasing the T_g . The erratic behavior was not however present in the second sample labeled Filler Resin2. The start temperature was moved back to -30°C for the analysis of Filler Resin2 and Bonded Filler Resin.

The Bonded Filler Resin specimen was prepared similar to the other Filler Resin Specimens, but resulted in significantly different behavior and a higher T_g value. The T_g values are tabulated below in Table 3.11.

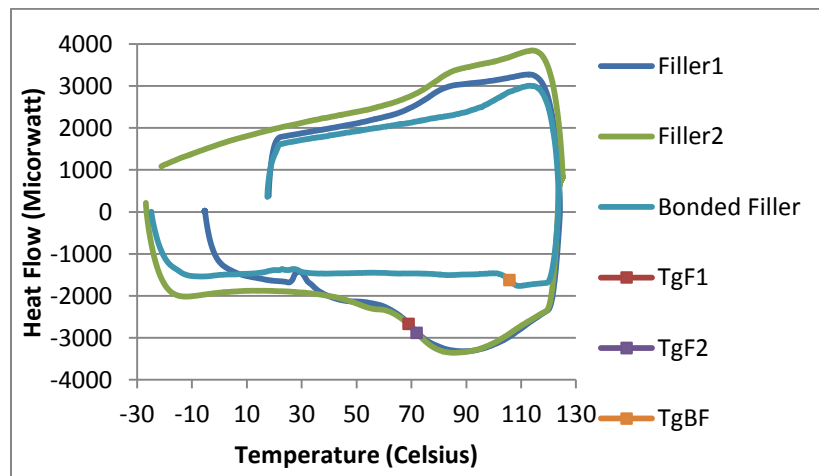


Figure 3.83. Filler Resin DSC Results

Table 3.11. Glass Transition Temperatures of CFRP and Filler Resins

	T_g	T_g , After Cure During Cooling
Ground CFRP1	67.95	73.19
Ground CFRP1A	77.38	78.02
Ground CFRP2	68.13	73.56
Diced CFRP	65.43	72.33
Filler Resin1	69.14	76.51
Filler Resin2	72.08	80.27
Bonded Filler Resin	105.83	96.15

The response of the Bonded Filler Resin is somewhat peculiar. It is possible that the milky white filler resin had higher water content, acting as a plasticizer reducing the T_g of the Filler Resin1 and Filler Resin2 specimens. As previously mentioned, even though there was water in direct contact to the CFRP patch of Filler Resin1 and Filler Resin2, by the time the material was tested, the moisture content was likely the same for all the specimens and very similar to that of the lab environment. All filler resins likely had similar if not the same curing conditions also making the higher T_g of the Bonded Filler Resin somewhat surprising.

All specimens had T_g values over the manufacturer's value of 60°C which is well above any temperatures that the material could reach during service. The results other than the Bonded Filler Resin seemed reasonable and similar materials produced similar results. The T_g values measured at the laboratory were probably higher than the actual values of the material in contact with moisture on the arches of the bridge.

3.6 Summary of Field Assessment and Laboratory Testing

Voids, pull-off tests, physical characteristics of the specimens collected, tensile tests, and DSC all contribute to the evaluation of the durability of the CFRP. All of these findings represent the extrados of the east arch and bay 1NW.

- The number of voids identified increased from 3 to 28 over 8 years of service
- Voids found previously (3) had an average increase in size of approximately 400%
- Filler Resin appeared thick, white, and smooth for some pull-off tests (6 of the 9 that were inadequate strength and failure mode E) and the 1NE patch removed
- Pull-off test failure modes were distributed differently than 2003 results with more failures occurring in the FRP layer Pull-off tests results of 2011 had a lower mean and higher standard deviation than the 2003 results
- 33% (9 of 27) of pull-off tests in 2011 were below the minimum 1.38 MPa (200 psi) compared to 2.4% (1 of 42) in 2003
- Ultimate tensile strengths were significantly lower than manufacturer's data, 745 MPa, 5th percentile was 498.8 MPa
- Rupture strains were significantly lower than CDOT construction specification minimum, but 5th percentile was adequate at 0.00612.
- Modulus of Elasticity values were representative of the manufacturer's data, mean of 77.3 GPa met the manufacturer's design value of 61.5 GPa
- Glass transition temperatures of both the CFRP and Filler Resins exceeded the manufacturer's value of 60°C

- Physical phenomena causing irreversible behavior of DSC was not fully understood

The increase in number and size of voids may be due to poor documentation of the past or there may be definite cause for concern. Initial values of tensile tests, T_g , and bond strengths coupled with thorough void identification could help identify poor workmanship or quality. The pull-off test may have provided more of an insight into testing technique than bond strength. The unsatisfactory results of ultimate tensile strength and rupture strain are due in part to the stringent demands of the CDOT specifications. The modulus of elasticity, 5th percentile of rupture strain, mean of ultimate tensile strength, and glass transition temperatures were all satisfactory. Based on these results there appears to be some deterioration, but a more detailed test program would be needed to thoroughly characterize the deterioration over time. More data points for all tests (initial values and additional points upon every evaluation) would provide more insight into trends, durability thresholds, and performance.

Chapter 4: Developing a Durability Model for FRP

A major issue of concern when it comes to field durability and assessment of structures repaired with externally bonded FRP is the lack of knowledge related to the durability of FRP in field environments. Based on the test results presented in Chapter 3, there does appear to be some degradation in FRP material properties over time, but careful experimental design is needed in order to verify and quantify the extent of the deterioration. The first portion of this chapter discusses the type of research needed to better describe the durability of FRP in field environments, and lays out a specific plan that can be followed to provide the kind of information needed for service life models. Service life models provide estimations of remaining service life depending on available inputs such as material properties, bond strength, loading and exposures.

Another issue of concern is how the FRP applied to existing structures can be effectively inspected and monitored. FRP is often applied to repair bridges, which must be inspected every two years. There is a lack of guidance available to bridge inspectors when it comes to inspecting FRP based repairs. The second part of this chapter is devoted to making suggestions about field assessment, and discussing the type of further research that could be conducted to provide enhanced guidance. For both topics

in this chapter, experience gained through the case study described in chapter 3 is applied to make suggestions and recommendations, but it must be recognized that as discussed in chapter 2 there is very little existing work in these areas, and further work is needed. Thus the ideas presented in this chapter represent recommendations that may merit further revision as more research is conducted in this area.

4.1 Durability of FRP in Field Environments

Returning to a repaired structure after 8 years of service (as was the situation with the case study) does not provide enough data upon which to build a durability model, but it did offer the chance to gain important insights and knowledge as to what is needed in order to do so. The durability of FRP applications is critically dependent on maintaining bond strength and material properties, which can be degraded by certain exposures. Field assessments can quantify the degradation by measuring the bond strength and material properties with respect to exposures and time.

Previously discussed in Chapter 2, Karbhari et al. (2003) stated:

“It is thus critical that steps be taken to collect, on an ongoing basis, data from field implementations. This data is invaluable to the establishment of appropriate durability based design factors, and the opportunity of having new projects from which such data could be derived in a scientific manner should not be wasted.”

It does not appear as though any significant field data has been gathered. To create a durability model, it is necessary to collect data about bond strength and material properties from multiple sites over time and to quantify the exposure conditions. Data collection from multiple structures would allow for a larger sample size

per particular exposure which would improve accuracy and provide comparisons/validation of results.

It is important to maintain accuracy and comparability across sites by having prescriptive frequencies and methods of testing. Furthermore, documentation of the data should be congruent. Based on what was learned from the case study and information available in the literature, a durability testing model is proposed that if followed would provide powerful data for describing the long-term durability of FRP. Anticipating the much need data, determining standards or specifications in which collaborators could abide would better serve future durability studies for comparisons and analysis.

4.1.1 What was learned in the case study?

- **Choose structures that are easily accessed**

The evaluation of the durability of FRP via field assessments should consider the accessibility of the structure to be assessed. Lane closures, necessary equipment, power and water sources, and remote locations may limit the feasibility of conducting the multiple field assessments that may be necessary. Locations less remote with close laboratories or other helpful resources such as nearby weather stations are optimal. Areas in downtown or urban districts may be close in proximity, but difficult to store specimens and lane closures and access could prove to be cumbersome to the project. Multiple field assessments compound costs such as travel time, lane closures, and aerial access equipment and should be considered during the candidacy search.

The case study described in Chapter 3 had the benefit of reasonable access to the extrados of the arches without the need of lane closures or aerial access equipment. However, the location was fairly remote without power or water and access to the intrados and sides of the arches would have been extremely difficult to accommodate. Equipment and materials had to be transported by hand across rugged terrain. Additionally, time constraints and safety equipment limited the access to one of the two arches.

- **Establish frequencies, durations, and sample sizes of field assessments and manufacture needed specimens at the time of repair**

Each collaborated effort would be responsible to submit a report of quantities and values of testing and conditions periodically. The anticipation of the study would not only aid in the allocation of necessary resources (future tests and specimens), but the repaired structures would potentially benefit by not enduring destructive testing when possible. Additionally, continuity could be provided by restricting repair material options and establishing particular ages of the repair in which to conduct the assessments.

A trade-off exists in choosing both the sample size and frequency with which to test the samples. Larger samples provide results with more accuracy than smaller samples and can help to quantify the degree of uncertainty in a model. Similarly, more frequent testing provides more information than less frequent testing. Too small of sample or infrequent testing may render meaningless data, while too large of sample or too many tests may undermine the feasibility of the study. The determination of sample

size and testing frequency will be achieved by the guidance of existing guidelines, specifications, and standards.

The case study in this work was conducted eight years after the repair with minimal assessment conducted every two years via bridge inspection. No future assessments are currently planned. The durability study is already handicapped by missing baseline data, and any degradation that has occurred is identified as being sometime in the last eight years. We had to do destructive testing on site, and repairs (which would be a hassle if you were out doing this all the time).

- **Document voids and defects off-site in a long-term database**

Extensive efforts should be made to quantify the number, size, and location of any areas of voids or defects of the FRP application. Previously found voids in this case study increased in size over time. To understand how defects and voids propagate over time, careful documentation from the time of repair through the life span of the repair is essential. Documentation directly on the structure with “permanent” markers provides a great visual representation of found defects and their propagation, but the markings fade over time and potentially encourage graffiti. The primary documentation must be done offsite in a database that can be maintained and updated ideally for the lifespan of the repair or repaired structure similar to current bridge inspection reports.

Only three voids were identified with faded “permanent” marker directly on the arch as existing voids during the case study. The only other documentation of voids was from the brief mention in the bridge inspection report in addressing the FRP repair as a whole stating “Look good but some areas of delams” found from “sounding” the top

and sides of the arches with no other documentation of quantity, sizes, or locations. The existing voids significantly increased in size and approximately 25 voids were found on only the extrados of the east arch on 2011.

- **Find initial or baseline values as the first data point for durability**

Initial values of bond strength and material properties are not only the first of many data points collected, but are indicative of the quality of the repair. The quality of FRP using a wet lay-up process is highly dependent on the workmanship with which the composite is created and installed and it shouldn't be assumed that the manufacturer's provided values are representative of the product created on-site. Without initial values, once data is collected after some time of service, it is difficult to differentiate between the occurrence of degradation and low starting values due to poor workmanship. It is not enough to assume the manufacturer's data will suffice.

Conducting a field assessment eight years after the repair, identifying the initial values proved to be difficult in some cases. Documentation of tensile test results was never found. It was fortunate that some information was recovered at all because CDOT's policy is to keep records for seven years. It is essential to durability studies for documentation to remain available, updated, and continuous throughout the lifespan of repairs or retrofits.

- **Follow standards and create testing instruction and procedures to eliminate variance and error**

In order to provide the data that is needed for the evaluation of durability, certain tests must be conducted. Choosing the best possible testing methods available, difficulties in acquiring valuable data is still encountered. For instance, pull-off tests are

influenced by the process in which they are conducted, namely the core drilling. It is recommended that the core drilling process is reproducible and consistent. The variation of the recommended depth to which to drill has been previously addressed in Chapter 3 and is an example of the different philosophies that exist with a particular detail of core drilling. No matter the drill depth chosen, if well documented and repeated for each subsequent test it will serve the consistency of the study introducing at most a systematic error that will be present for all specimens in the study. Similarly, if it is too cumbersome to use a core-drilling rig that attaches to the drilling surface to provide a perpendicular axis for the drilling operation, a jig or modified apparatus should be used to ensure no additional stresses are introduced to the specimen due to the off-axis tilting of the core drill.

Differentiating the cause of lower bond strength values becomes difficult considering different test preparation techniques for the two testing times for the Castlewood Canyon Bridge, let alone multiple tests from multiple sites. Therefore, procedures should be carefully outlined and adhered to by participating parties.

- **Test sacrificial areas or stored specimens (voids included) when possible**

No samples or sacrificial areas existed on-site for the case study limiting any tests to areas on the repaired arch. Conducting pull-off tests and acquiring samples to test in the laboratory required causing damage to the bridge that needed to be repaired after testing. Repair could be a significant time sink, particularly if it must be conducted after frequent site assessments. Removing areas of voids or debonded regions allowed for the FRP repair to be improved without removing an area of the repair that was

effectively acting to strengthen the structure. In addition it would have been very difficult to remove an area of bonded FRP from the arches for tensile tests and DSC. It is ideal to use debonded regions because unlike stored specimens, they have all the synergistic effects including those caused by service loads, at least up until the debonding occurred.

- **Use normalized properties for comparisons and identify physical differences of the repair such as thick bond filler or resin areas to correlate with durability**

Tensile tests provide values of material properties that are essential to the performance of FRP composites such as ultimate tensile strength, rupture strain, and modulus of elasticity. These material properties by definition are dependent on the cross-sectional area of the specimen. If the specimens are removed from the bridge, which is a good alternative when large voids are found, the cross-sectional area varies greatly depending on the filler resins or pieces of the substrate adhered to the specimen after removal. The material contributing to the larger cross-sectional area does not add any significant strength but causes the appearance of a lower ultimate tensile strength which is computed as a stress. For this reason it is recommended to use the thickness of the layer provided by the manufacturer and the measured width of the specimen to determine the area in calculating the material properties of interest. This adjustment to the area used in calculation was practiced and described in Chapter 3.

- **Find the level of cure and T_g of the composite**

Differential scanning calorimetry (DSC) can be used as a good measure of the level of cure and glass transition temperature (T_g). If there are different levels of curing between sites, comparisons could be made to understand how it affects the durability

of the individual materials. It is difficult to obtain a specimen on-site, transport the specimen to the lab, and conduct DSC without the water or moisture content of the specimen changing due to the exposure of the environment and container of transport. Initial T_g values can also be indicative of the quality of workmanship in which the FRP was installed. Further understanding of abnormalities present in the results could provide not only clarity of the results, but with further study, phenomena such as enthalpic relaxation peaks could possibly provide quantitative insight into the aging process and remaining life span of the epoxy resin before critical thresholds are reached.

- **Quantify exposures**

In addition to tracking the bond strength and material properties over time, it would be beneficial to document events known to cause degradation in FRP composites such as applications of deicing agents, freeze/thaw cycles, extreme temperatures, equivalent truck loads, and precipitation. The synergistic effects are best understood by data acquired in the field but is still not well understood. With enough data collected, correlations between influencing events and durability could be possible.

The number of freeze/thaw cycles, applications of deicing agents, and precipitation amounts were not quantified for the case study, but would be beneficial in developing a robust durability model.

4.1.2 Mock Example

Motivated by literature in regard to the long-term durability of FRP and based on the experience gained from the field assessment of this study, the following is a

proposal to collect the data needed to build a durability model. A mock example is provided below to illustrate the above recommendations with specific numbers.

Step 1: Identify collaborators based on the following criteria:

- **Eligibility (FRP Strengthening of RC bridges or bridge members)**
- **Timing (Planning phase)**
- **Feasibility (Location, access, amenities)**

Potential collaborators are limited to those associated with reinforced concrete bridges throughout the US that have structurally deficient members and are eligible for FRP repair. The collaboration is further narrowed to those bridges that have yet to be scheduled for repair or retrofitting with FRP, and are still in the preliminary phases of planning. Among these bridges the collaboration is finally reduced to those teams associated with a finite number of bridges that were most ideal when considering location, access, and amenities.

Step 2: Identify Global and Local Scopes of Study

- **Global Scope**
 - **Repair Material (CFRP and epoxy resin) and Construction**
 - **Frequency, Duration, Format Requirements of Assessments and Data Collection**
 - **Minimum Requirements of Sample Size and Testing Procedures**
- **Local Scope**
 - **Applicable Exposure Categories**
 - **Specimen Storage and Sacrificial Areas**

Global Scope

Global scope is overarching and applies to all collaborators participating in the effort. Local scopes are defined and established by each collaborator, but are still in accord with the global scope. Features of the global scope include:

- **Comparable Gross Laminate Material Properties**

CFRP and epoxy resins of comparable gross laminate material properties should be used (for example, ultimate tensile design strength of approximately 745 MPa (108 ksi), design tensile modulus of 61.5 GPa (8900 ksi), and T_g of 60°C (140°F)). Depending on the global size of the study, it might be attractive to consider materials from several manufacturers, but at least two projects with similar exposure should be available for each specific manufacturer to allow for at least some level of validation.

- **Competent Installers and Established Materials**

The construction of the repair should be completed using materials and installers with established histories of competence. The following guidelines, specifications, and standards are available to assist the construction process: National Cooperative Highway Research Program (NCHRP) Report 609 titled “Recommended Construction Specifications and Process Control Manual for Repair and Retrofit of Concrete Structures Using Bonded FRP Composites,” ACI 440 (2008) “Guide for the Design and Construction of Externally Bonded FRP Systems for Strengthening Concrete Structures,” and many publications and conferences provided by International Concrete Repair Institute (ICRI).

- **Biennial Field Assessments**

In addition to the construction of the repair or retrofit, resources also need to be budgeted for the manufacturing, storing, and testing of enough samples to represent the categorized exposures for the life span of the bridge. With a similar frequency as bridge inspections, conducting biennial field assessments would likely satisfy the need for data to identify the development of degradation. It is possible that this frequency is not necessary for the entire life span of the repair, but it is better to error on the side of more frequent testing because if the information is not gathered it will not be possible to retrieve it later.

Addressing sample sizes and number of test specimens, in the absence of available guidelines, there are ASTM standards that can be used for guidance. ASTM D3665 (2007) “Random Sampling of Construction Materials” and ASTM E122 (2009) “Calculating Sample Size to Estimate, With Specified Precisions, the Average for a Characteristic of a Lot or Process” are sources that can aid the decision process of how many specimens/evaluations for which to budget resources.

Local Scope

- **Identify Principle Exposures and Quantify**

Principle exposures will be identified and categorized for each site. Though many exposures occur simultaneously, the principle elements, or principle couples should be identified for future assessments. For instance exposures such as moisture, humidity, and salt water would be likely exposures for a bridge located in Florida, while dry direct sunlight or extreme temperatures would be more fitting for a bridge located in Arizona.

Bridges in Montana or Colorado would be candidates for freeze/thaw cycles, extreme temperatures, and deicing agents. The number of occurrences or amount of exposure with respect to time is important to quantify.

Step 3: Tasks to Conduct During and Directly Following Repair

- **Collect Initial and Baseline Values**
- **Create and sacrificial areas and specimens**
- **Store specimens**

Quality assurance prior to the repair should be completed to establish the required strengths of the FRP material and substrate is satisfied. During the repair, sacrificial areas on-site should be identified and prepared with the same procedure as the repair of the structure for the sole purpose of conducting pull-off tests in the future and collecting aged material for laboratory tests. Abutments or other structural members not in need of strengthening and that could withstand minor destructive testing are best suited for sacrificial areas. In addition to the sacrificial areas, future test specimens shall be created and stored on-site to satisfy testing for the service life of the structure. Similar to the Utah, 2004 study, samples should be kept in locations representative of the different exposures present at the site such as on the ground in a locked cage, on top of the pier cap, and possibly in a nearby laboratory as a control sample. Directly following the repair, quality control tests also provide the initial values of the material properties of the composite and bond strength.

Step 4: Detect Voids and Conduct Tests

- **Acoustic Sounding and Thermographic Imaging**
- **Pull-off Tests, Tensile Test, and DSC**

- **Detect Voids and Conduct Pull-off Tests, Tensile Tests, and DSC**

Each bridge would be subject to multiple field assessments that would include void detection, pull-off tests, tensile tests, and differential scanning calorimetry and should have material aging on-site to accommodate all possible tests. Any specimens that can be retrieved directly from the bridge will be more representative than specimens stored on-site because of the added synergistic effects of service load induced stresses. Areas of voids could be removed and used as specimens for tensile testing and DSC. Areas with similar exposures that are not critical or in need of repair could be used as future locations for pull-off tests.

- **5 Specimens per Test Condition for Pull-off and Tensile Tests**

According to ASTM D7522 (2009), at least 5 specimens per test condition shall be used from a sample during pull-off tests. CDOT's construction specifications (Revision of 602) recommend an independent testing laboratory conducts a minimum of 2 random pull-off tests per day of application directly following the repair. In addition, the contractor is responsible to conduct a minimum of 1 pull-off test per 46.5 m² (500 ft²) of installed FRP to ensure a minimum of 1.38 MPa (200 psi) bond strength. ICRI Technical Guideline No. 210.3-2004 recommends a minimum of 3 pull-off tests per project and a minimum of 3 pull-off test per 465 m² (5000 ft²) of installed FRP.

- **20 Test Specimens to Determine Ultimate Tensile Properties**

In accordance with ASTM D3039, tensile tests would number a minimum of 5 test specimens per test condition. Similar to CDOT's construction specification, Revision of Section 602, a minimum of 20 test specimens are necessary to determine ultimate tensile properties. Therefore, each assessment will have a minimum of 5 subsets consisting of a minimum of 5 specimens each; the additional 5 specimens would be reserves in case some specimens are damaged or the testing equipment malfunctioned. It is more desirable for all 20 specimens to come from the same or similar exposures. These subsets will be samples taken from on-site storage. In the case of large voids found (with dimensions equal to or greater than of 15 cm x 20 cm (6" x 8")) the areas of voids can be removed from the bridge to create a subset for ASTM D3039. Assuming no voids were found during the ten biennial field assessments on the bridge over its entire life span of 20 years, a total of 250 specimens of dimensions 2.5 cm x 20 cm (1" x 8") would need to be stored on-site in various locations representative of its respective categorized exposures. If the FRP fabric was unidirectional, the fiber direction would be required to be in the 20 cm (8") direction. Assuming the fabric was 30 cm (12") wide approximately 10 specimens could be prepared from each 20 cm length of fabric considering lost area to saw kerfs to cut the specimens from the sample. A total length of 5.2 meters (17 ft) of the 30 cm (12") fabric would provide the necessary specimens for tensile tests for the life span of the bridge repair or retrofit. This would be a significant amount of material, but the preparation and on-site storage could be managed.

- **15 mg per Testing Condition for DSC**

DSC specimens could likely be generated from the material collected for tensile tests. Only 15mg of finely ground material is needed per testing condition. Care should be taken in not introducing excessive or additional heat in creating the specimen material by grinding or cutting.

Tabulated below is a table with recommended quantities of specimens for each sample, field assessment or evaluation, and lifespan of the structure.

Table 4.1. Quantities of Samples and Specimens

Anticipated Lifespan of 30 years and 2 year evaluations			
N = number of conditions on location			
	Quantities of Specimens		
	Per sample, (X)	Per Evaluation, (Y)	Per Lifespan, (Z)
Pull-off Tests	$X \geq 5$	$Y = (X \times N)$	$Z = 15 \times Y$
Tensile Test	$X \geq 5$	$20 \leq y \leq (X \times N)$	$Z = 15 \times Y$
DSC	$X = 15 \text{ mg}$	$Y = (X \times N)$	$Z = 15 \times Y$

Assuming two conditions or exposures are of interest, using the above table with service life of 30 years and biennial evaluations, the following tabulated quantities of tests would be required.

Table 4.2 Specific Amounts for Mock Example

	Quantity	Area (m ²)
Pull-off Tests	150	3.4
Tensile Test	300	1.5
	Quantity	Mass (mg)
DSC	30	450

For a reference of FRP area, the Castlewood Canyon Bridge had in excess of 850 m² installed on the arches and struts. The sacrificial areas and specimens required for

the durability study are relatively small additional amounts of repair material. For the Castlewood Canyon Bridge, the testing area required is less than 0.6% of the repair area.

Chapter 5: Summary, Conclusion, and Additional Areas of Research

5.1 Summary

In an attempt to provide much needed field data to evaluate the durability of FRP in service environments, a field assessment of the Castlewood Canyon Bridge was conducted. Detection of voids, pull-off tests, tensile tests, and differential scanning calorimetry all contributed to the assessment of the FRP. Test values were analyzed and compared with manufacturing data and values from tests conducted in 2003. Very little field data of the durability of FRP exists. Most, if not all, of the previous field evaluations of FRP were focused on visual or load tests as a measure of quality control or design validation rather than long-term durability. To understand the development of the degradation of FRP, additional field data is required. Only through the collection of field data over time can the synergistic effects on bond strength and material properties be measured.

Field data was gathered and in evaluating the performance or durability of the FRP system, difficulties were encountered. Lack of thorough documentation of previous test values made it difficult to determine if there was poor workmanship or occurrence

of degradation. If degradation did occur, it is unknown as to how or when it developed. To improve future durability studies and potentially develop a robust durability model, recommendations were made based on literature review and the experience gained from the case study. Recommendations were intended for two entities; the first of which are the parties interested in research and academia and the second are the parties in roles of management such as DOTs.

5.2 Conclusions

After 10 years of FRP applications in the northwest US, Barlow (2005) concluded “The success of these applications is based on sound design, developing of a clean and properly profiled substrate to ensure adhesion and a continuing quality control program that includes on-site inspection, bond strength testing and in situ material property testing.” Barlow (2005) clearly states *what* is necessary for successful applications of FRP. This guidance was followed and the case study provided the “on-site inspection, bond strength testing and in situ material property testing.” By conducting this field evaluation it was discovered that there was a lack of guidance and instruction as to how to conduct durability assessments. In addition to collecting field data, this thesis is a beginning in the development of *how* to provide these necessities, both managerially and technically, while optimizing the impact on the analysis, structure, and future designs.

The results to the case study were limited by the lack of data available from tests conducted at the time of the repair. Locations and values of some pull-off tests, all tensile tests results, and any information in regard to previously found/repaired voids

were omitted from the records still on file with CDOT. When test values were lower than the values provided by the manufacturer it becomes difficult to determine if and when degradation occurred. Furthermore, no documentation was found of the locations of the arch that were repaired with shotcrete. The substrate is not only an integral component of the FRP system; it can influence the durability of the FRP system by the exposure it creates (e.g. carbonation, pore water alkalinity, chloride ions, etc.). Durability studies in the future need to have baseline data and pertinent information in regard to the repair to be able to conduct meaningful analysis of the rare data collected.

Data collected from field assessments can be evaluated by comparisons to design minimums and assumptions, data manufacturer's values, baseline values, and previous values for reference to identify significant changes or trends. Future field assessments must be anticipated at the time of repair to make the data from field assessments most valuable. This anticipation is the necessary management to responsibly advance the process of repairing and strengthening reinforced concrete bridge components.

Although it is difficult to fully assess the durability of the FRP repair in the Castlewood Canyon Bridge without a strong definition of baseline values, the following conclusions were reached.

- The number of voids identified increased from 3 to 28 over 8 years of service
- Voids found previously (3) had an average increase in size of approximately 400%

- Filler Resin appeared thick, white, and smooth for some pull-off tests (6 of the 9 that were inadequate strength and failure mode E) and the 1NE patch removed
- Pull-off test failure modes were distributed differently than 2003 results with more failures occurring in the FRP layer Pull-off tests results of 2011 had a lower mean and higher standard deviation than the 2003 results
- 33% (9 of 27) of pull-off tests in 2011 were below the minimum 1.38 MPa (200 psi) compared to 2.4% (1 of 42) in 2003
- Ultimate tensile strengths of the FRP were significantly lower than manufacturer's data and Rupture strains were significantly lower than specified minimum
- Modulus of Elasticity and glass transition temperatures were representative of the manufacturer's data

Items that are necessary for the evaluation of the durability of FRP, but were not available for this study are:

- Initial values of tensile tests, T_g , and bond strengths coupled with thorough void identification could help identify poor workmanship or quality versus the occurrence of degradation
- More data points for all tests (initial values and additional points upon every evaluation) would provide more insight into trends, durability thresholds, and performance

5.3 Additional Research

The difficulties and limitations encountered in this case study suggest several possible areas for further research. Technical and managerial methods and procedures in the field need to be developed to provide the much needed field data. Coinciding with the collection of field data, methods and models need to be developed to correlate field data with the durability of the FRP and ultimately the performance of the repaired structure.

Currently, there is a difficulty in linking field assessments with structural response. Previously, load tests have been conducted to confirm load carrying capacity or stiffness, but linking how the development of degradation (e.g. reduced FRP properties, larger debonded areas) affects the performance of a structure is still unknown. Furthermore, this may be a difficult task to accomplish considering the unique conditions and geometries that may exist. By implementing the plan presented in Chapter 4, additional field data would be available to develop service life models.

Well-functioning service life models that use quantitative inputs from field assessments need to be developed. Relationships between bond strength and material properties with flexural/shear capacities, as well as the degradation of bond strength and material properties with the durability of the composite need to be more fully understood. Moreover, quantification of the environmental factors that contributes to the degradation of the composite needs to be developed. Analogous to the human body, we can estimate the remainder of lifespan by cholesterol levels or blood pressure, or by the number of additional low quality food items a system can sustain. The

cholesterol level and blood pressure are bond strength and material properties, while the low quality food items are freeze/thaw cycles or applications of deicing agents. All applicable “low quality food items” need to be identified and their effects on the system need to be quantified.

More understanding in regard to bond strength’s correlation to flexural or shear capacity could also benefit future designs. For instance, a maximum number of effective layers could possibly be determined by the pull-off or bond strength. Additionally, the amount of strengthening provided by FRP could be appropriately discounted as the bond strength decreased. Deriving this relationship through extensive studies, statistics of bond strengths could provide better guidelines than the existing recommendation of having bond strength of not less than 200 psi.

Improving testing techniques in the field is also a significant area in need of additional research to foster the collection of the necessary field data for the service life models discussed above. Thermal imaging has been done in laboratories to detect voids, but effective techniques to use in the field have yet to be established. Optimization of wavelengths used for thermal imaging combined with a standardized technique of heating or cooling could significantly improve the efficiency of void detection within FRP applications.

Establishing a standard approach for core drilling during the preparation for pull-off tests in the field that is practical without the use of core drill rigging system would provide consistency in the results collected at multiple sites. Core drilling induces

torsional and thermal stresses that could be quantified and techniques developed to minimize these induced stresses.

Differential scanning calorimetry may be explored for the ability to quantify the durability or aging process of a specimen. In addition, a standardized technique could be established to find the T_g while the specimen has the same water content during the testing that it had during service. In addition it would be beneficial to evaluate wet out in the field as a quality control measure. The degree of wet out and its correlation with durability could also be explored.

References

ACI 318-99, Building Code Requirements for Structural Concrete & Commentary. American Concrete Institute. ACI Committee 318. March 1999.

ACI 440.2R-08, Guide for the Design and Construction of Externally Bonded FRP Systems for Strengthening Concrete Structures. American Concrete Institute. ACI Committee 440. July 2008

ACI 503R-93, Use of Epoxy Compounds with Concrete (Reapproved 2008). American Concrete Institute. ACI Committee 503 and ACI Committee 548. July 1993.

ACI 515R, (1966). Guide for the Protection of Concrete Against Chemical Attack by Means of Coatings and Other Corrosion-Resistant Materials. American Concrete Institute. ACI Committee 515. Journal Proceedings, 63(NA) 1305-1392.

ACI 546R-96, Concrete Repair Guide (Reapproved 2001). American Concrete Institute. ACI Committee 546. October 1996.

American Society of Civil Engineers, (2009). *“Report Card for America’s Infrastructure, 2009.”*

<http://www.infrastructurereportcard.org/sites/default/files/RC2009_bridges.pdf>
(Apr. 12, 2011).

ASTM D3039/D3039M-08, Standard Test Method for Tensile Properties of Polymer Matrix Composite Materials. ASTM Subcommittee D30.04. American Society for Testing and Materials. Vol 15.03.

ASTM D4541-09e1, Standard Test Method for Pull-off Strength of Coatings Using Portable Adhesion Testers. ASTM Subcommittee D01.46. American Society for Testing and Materials. Vol 06.02.

ASTM D7522/D7522M-09, Standard Test Method for Pull-Off Strength for FRP Bonded to Concrete Structures. ASTM Subcommittee D30.05. American Society for Testing and Materials. Vol 15.03.

Bakis, C.E., Bank, L.C., Brown, V.L., Cosenza, E., Davalos, J.F., Lesko, J.J., Machida, A., Rizkalla, S.H., Triantafillou, T.C. (2002). Fiber-Reinforced Polymer Composites for Construction-State-of -the-Art Review. *Journal of Composites for Construction*, 6(2) 73-87.

Barlow, P. (2005). 10 Years of Seismic and Strengthening Case Histories using FRPs in the Northwest. *Materials and Processing Technologies for Revolutionary Applications, Fall Technical Conference (37th ISTC)*. October 31-November 3, 2005, Seattle, WA.

Bisby, L.A., Green, M.F., Kodur, V.K.R. (2005). Response to fire of concrete structures that incorporate FRP. *Progress in Structural Engineering and Material*. 7(3) 136-149.

Byars, E.A., Waldron, P., Dejke, V., Demis, S., Heddadin, S. (2003). Durability of FRP in concrete Deterioration mechanisms. *International Journal of Materials & Product Technology*, 19(1-2) 28-39.

Chen, Y., Davalos, J.F., Ray, I., Kim, H. (2007). Accelerated aging tests for evaluations of durability performance of FRP reinforcing bars for concrete structures. *Composite Structures*, 78(1) 101-111.

Chin, J.W., Nguyen, T., Aouadi, K. (1997). Effects of Environmental Exposure on Fiber-Reinforced Plastic (FRP) Materials Used in Construction. *Journal of Composites Technology & Research*, 19(4) 205-213.

Clarke, J., 2002. Installing, inspecting and monitoring FRP-strengthened concrete structures. *Concrete*, 36(2) 34-36.

Colorado Department of Transportation (CDOT), (2003). "Revision of Section 602." Fiber Bonded Polymer (FRP) Surface Reinforcing, not published. Construction Specification.

Coomarasamy, A., Goodman, S. (1999). Investigation of the Durability Characteristics of Fiber Reinforced Plastic (FRP) Materials in Concrete Environment. *Journal of Thermoplastic Composite Materials*, 12(3) 214-226.

Crawford, K. (2008). Evaluating long-term durability of FRP-structural systems applied to concrete bridges. *CSCCE 2008 Annual Conference*. Quebec, QC Proceedings, June 10-13.

De Sitter, W. R. (1984). "Costs for Service Life Optimization: The 'Law of Fives,'" *Durability of Concrete Structures, Workshop Report*, Ed. Steen Rostam, 18-20 May, Copenhagen, Denmark, pgs 131-134.

Fafach, D., Shing, B., Chang, S., Xi, Y. (2005). Evaluation of the FRP-Retrofitted Arches in the Castlewood Canyon Bridge. Colorado Department of Transportation Research Branch. Report No. CDOT-DTD-R-2005-01.

Federal Highway Administration, (2001). "Reliability of Visual Inspection for Highway Bridges." <<http://www.fhwa.dot.gov/publications/research/nde/01020.cfm>> (May 17, 2011).

Federal Highway Administration, (2004). "National Bridge Inspection Standards Regulation, 200." <http://frwebgate.access.gpo.gov/cgi-bin/getdoc.cgi?dbname=2004_register&docid=FHWA%E2%80%932001%E2%80%938954.pdf> (May 17, 2011).

Ghosh, K., Karbhari, V.M. (2005). Evaluation of environmental effect on FRP/concrete bond. *International SAMPE Symposium and Exhibition*, 50(Proceedings) 265-279.

Ghosh, K., Karbhari, V.M. (2006). A critical review of infrared thermography as a method for non-destructive evaluation of FRP rehabilitated structures. *International Journal of Materials & Product Technology*, 25(4) 241-266.

Ghosh, K., Karbhari, V.M. (2011). Use of infrared thermography for quantitative non-destructive evaluation in FRP strengthened bridge systems. *Materials and Structures*, 44(1) 169-185.

Hag-Elsafi, O., Alampalli, S., Kunin, J. (2004). In-service evaluation of a reinforced concrete T-beam bridge FRP strengthening system. *Composite Structures*, 64(2) 179-188.

Halabe, U.B., Vasudevan, A., Klinkhachorn, P., Gangarao, H.V.S. (2007). Detection of subsurface defects in FRP composite bridge decks using digital infrared thermography. *Nondestructive Testing and Evaluation*, 22(2-3) 155-175.

Harries, K.A., Porter, M.L., Busel, J.P. (2003). FRP Materials and Concrete: Research Needs. *ACI Conc. Inter*, 25(10) 69-74.

Hu, A., Ren, H., Yao, Q. (2007). Durability of Concrete Structures Strengthened with FRP Laminates. *Journal of Harbin Institute of Technology (New Series)*, 14(4) 571-576.

Hu, C.W., Shih, J.K.C., Delpak, R., Tann, D.B. (2002). Detection of air blisters and crack propagation in FRP strengthened concrete elements using infrared thermography. *InfraMation, The Thermographer's Conference*, (Aug. 1).

Karbhari, V.M., Chin, J.W., Reynaud, D. (2000). Critical gaps in durability of FRP composites in civil infrastructure. *International SAMPE Symposium and Exhibition*, 45(Proceedings, May 21-25) 549-563.

Karbhari, V.M. (2003). Durability of FRP Composites for Civil Infrastructure – Myth, Mystery or Reality. *Advances in Structural Engineering*, 6(3) 243-255.

Karbhari, V.M., Chin, J.W., Hunston, D., Benmokrane, B., Juska, T., Morgan, R., Lesko, J.J., Sorathia, U., Reynaud, D. (2003). Durability Gap Analysis for Fiber-Reinforced Polymer Composites in Civil Engineering. *Journal of Composites for Construction*, 7(3) 238-248.

Karbhari, V.M., Ghosh, K. (2009). Comparative durability evaluation of ambient temperature cured externally bonded CFRP and GFRP composite systems for repair of bridges. *Composites: Part A* 40(9) 1353-1363.

Karbhari, V.M., Lee, L.S., Hollaway, L.C. (2011). "Service Life Estimation and Extension of Civil Engineering Structures." Key Issues in the use of fibre reinforced polymer (FRP) composites in the rehabilitation and retrofitting of concrete structures. Woodhead, Cambridge, MA

LePatner, B. B. (2010). "Too Big To Fall." America's Failing Infrastructure and the Way Forward, Foster Publishing, New York, NY, 79

Levar, J., 2003. Nondestructive evaluation of carbon fiber-reinforced polymer-concrete bond using infrared thermography. *ACI Materials Journal*, 100(1) 63-72.

Miceli, M., 2002. Health monitoring of FRP Bridge Decks with infrared thermography. *Materials evaluation*, 60(10) 1245-1252.

No. 210.3-2004- Guide for Using In-Situ Tensile Pull-Off Tests to Evaluate Bond of Concrete Surface Materials (formerly No. 03739). International Concrete Repair Institute (ICRI)

No. 310.1R-2008- Guide for Surface Preparation for the Repair of Deteriorated Concrete Resulting from Reinforcing Steel Corrosion (formerly No. 03730). ICRI

No. 310.2-1997- Guideline for Selecting and Specifying Concrete Surface Preparation for Sealers, Coatings (formerly No. 03732). ICRI

No. 320.2R-2009- Guide for Selecting and Specifying Materials for Repair of Concrete Surfaces (formerly No. 03733). ICRI

Ozokwelu, E.D. (1990). Effects of temperature and catalyst level on the cure rate of fiber-reinforced plastic (FRP). *Journal of applied polymer science*, 41(11-12), 2603-2611.

Reay, J.T., Pantelides, C.P. (2006). Long-Term Durability of State Street Bridge on Interstate 80. *Journal of Bridge Engineering*, 11(2) 205-216.

Rytter, A., Brincker, R., Hansen, L.P. (1993). Vibration based inspection of civil engineering structures. *Bygningstekniske Meddelelser*, 62(4).

Saenz, N., Walsh, E.J., Pantelides, C.P., Adams, D.O. (2004). Long Term Durability of FRP Composites for Infrastructure Rehabilitation. *SAMPE 2004 – Long Beach, CA* May 16-20, 2004.

Sofge, E. (2009). “5 Engineering Lessons From the New, Reopened Minnesota Bridge, 2009.” *Popular Mechanics*, <<http://www.popularmechanics.com/science/4285220>> (Apr. 21, 2011).

Stallings, J.M., Tedesco, J.W., El-Mihilmy, M., McCauley, M. (2000). Field Performance of FRP Bridge Repairs. *Journal of Bridge Engineering*, 5(2) 107-113.

Starnes, M.A., Carino, N.J., Kausel, E. A. (2003). Preliminary thermography studies for quality control of concrete structures strengthened with fiber-reinforced polymer composites. *Journal of Materials in Civil Engineering*, 15(3) 266-273.

Superville, D. (2010). “Obama Blasts GOP, Calls For \$50 Billion Infrastructure Plan For Roads, Rail, Air Travel.” *Huffpost Politics*, <http://www.huffingtonpost.com/2010/09/06/obama-to-back-50-billion-_n_706452.html> (Apr. 12, 2011).

Tan, L., Liu, X., Zhu, M. (2011). Research on Factors Affecting Durability and Improvements for FRP Reinforced Concrete Structures. *Advanced Materials Research*, 189-193(NA) 847-852.

The Concrete Society, (2000). "Design Guidance for Strengthening Concrete Structures Using Fibre Composite Materials." Technical Report No. 55, Cromwell Press, Trowbridge, Wiltshire, UK

UserCom, (2000). Interpreting DSC Curves. Information for users of Mettler Toledo thermal analysis systems.

Vaysburd, A.M., McDonald, J.E. (1999). "An Evaluation of Equipment and Procedures for Tensile Bond Testing of Concrete Repairs." Technical Report REMR-CS-61. Army Corps of Engineers, Washington, DC

Zhang, J.S., Karbhari, V.M., Reynaud, D. (2002). Field exposure based durability assessment of FRP column wrap systems. *Composites: Part B*, 34(1) 41-50.

Appendix A: Voids, Defects, and Thermal Images

The following appendix is an account of the size and location of all notable defects, voids, cracks, and rust stains, found on the East arch during the field assessment of 2011. This documentation is intended to be a permanent record as opposed to the temporary physical markings left directly on the bridge. Details of the defects found are tabulated below. In addition, the available photographs and thermal images of the defects are organized with regard to the “bay” in which the defects were located.

Due to circumstances during the field assessment, there were a limited amount of thermal images and photographs. In some cases there was no photograph or thermal image of a particular defect. It is possible that defects with areas smaller than 5.1 cm x 5.1 cm (2” x 2”) exist on the extrados of the east arch and are not documented in the table or photographs below.

Sizes and distances were approximated in cases such as the rust spot found on the extrados in the 1NW bay, seen below in Figures A1 and A2.

Table A1. Summary of Voids on the Extradoses of the Entire East Arch and One Bay of the West Arch

Summary of Defects on the Extradoses of the East Arch				Location			
Void ID #	Bay	2007 Size, NS x EW Units: cm (in)	2011 Size, Measured : NS x EW Units: cm (in)	Reference Column	Distance from reference column Units: cm (in)	Edge Reference	Distance from edge Units: cm (in)
1	1NE		27.9 x 50.8 (11 x 20)	1NE	91.4 (36)	East	101.6 (40)
2	1NE		5.1 x 5.1 (2 x 2)	1NE	119.4 (47)	East	58.4 (23)
3,4,5	1NE		< 5.1 x 5.1 (2 x 2)	NA	NA	NA	NA
6	2NE		22.9 x 14 (9 x 5.5)	1NE	203.2 (80)	East	52.1 (20.5)
7	2NE		12.7 x 5.1 (5 x 2)	2NE	195.6 (77)	East	43.2 (17)
8	2NE		34.3 x 7.6 (13.5 x 3)	2NE	40.6 (16)	East	40.6 (16)
9	3NE		68.6 x 20.3 (27 x 8)	2NE	Near	West	15.2 (6)
10	3NE	7.6 x 12.7 (3 x 5)	24.1 x 25.4 (9.5 x 10)	2NE	195.6 (77)	West	68.6 (27)
11	3NE		52.1 x 68.6 (20.5 x 27)	2NE	256.5 (101)	West	61 (24)
12	3NE		27.9 x 30.5 (11 x 12)	2NE	317.5 (125)	West	45.7 (18)
	3NE	20.3 x 20.3 (8 x 8)	20.3 x 68.6 (8 x 27)	2NE	Near	West	15.2 (6)
13	3NE		50.8 x 10.2 (20 x 4)	3NE	152.4 (60)	East	8.9 (3.5)
14	4NE		10.2 x 3.8 (4 x 1.5)	3NE	61 (24)	West	45.7 (18)
15	6E		8.9 x 7.6 (3.5 x 3)	5NE	61 (24)	East	45.7 (18)
16	6E		10.2 x 20.3 (4 x 8)	5NE	62 (24)	West	63.5 (25)
17	4SE		29.2 x 17.8 (11.5 x 7)	4SE	Near	East	20.3 (8)
18	4SE	17.8 x 29.2 (7 x 11.5)	35.6 x 35.6 (14 x 14)	4SE	17.8 (7)	East	45.7 (18)
19	4SE		152.4 x 64.8 (60 x 25.5)	4SE	106.7 (42)	West	71.1 (28)
20	3SE		10.2 x 10.2 (4 x 4)	2SE	30.5 (12)	West	17.8 (7)
21	3SE		10.2 x 12.7 (4 x 5)	2SE	45.7 (18)	West	96.5 (38)
22	2SE		15.2 x 16.5 (6 x 6.5)	2SE	226.1 (89)	East	61 (24)
23	2SE		12.7 x 7.6 (5 x 3)	2SE	218.4 (86)	East	91.4 (36)

Table A1. Continued

Summary of Defects on the Extrados of the East Arch				Location			
Void ID #	Bay	2007 Size, NS x EW Units: cm (in)	2011 Size, Measured : NS x EW Units: cm (in)	Reference Column	Distance from reference column Units: cm (in)	Edge Reference	Distance from edge Units: cm (in)
24	2SE		5.1 x 10.2 (2 x 4)	2SE	165.1 (65)	East	91.4 (36)
25	1SE		14 x 16.5 (5.5 x 6.5)	1SE	68.6 (27)	West	16.5 (6.5)
26,27,28	1NW		< 5.1 x 5.1 (2 x 2)	NA	NA	NA	NA

Table A2. Summary of Cracks on the Extradoses of the Entire East Arch

Crack ID #	Bay	2007 Size, NS x EW Units: cm (in)	2011 Size, NS x EW Units: cm (in)	Reference Column	Distance from reference column Units: cm (in)	Edge Reference	Distance from edge Units: cm (in)
1	1NE	Crack identified, length unknown	Section removed	1NE	91.4 (36)	East	101.6 (40)
2	2NE	Crack identified, length unknown	88.9 (35)	2NE	101.6 (40)	East	88.9 (35)
3	3SE	Crack identified, length unknown	NA	NA	NA	NA	NA

Table A3. Summary of Rust on the Extradoses of the Entire East Arch and One bay of the West Arch

Rust ID #	Bay	2007 Size, NS x EW Units: cm (in)	2011 Size, NS x EW Units: cm (in)	Reference Column	Distance from reference column Units: cm (in)	Edge Reference	Distance from edge Units: cm (in)
1	1NW	Rust identified, Size unknown	25.4 x 45.7 (10 x 18)	1NW	101.6 (40)	East	25.4 (10)

Bay 1NW: 3 Voids, 1 Rust Spot



Figure A1. Bay 1NW, 2 of the 3 small voids and rust spot

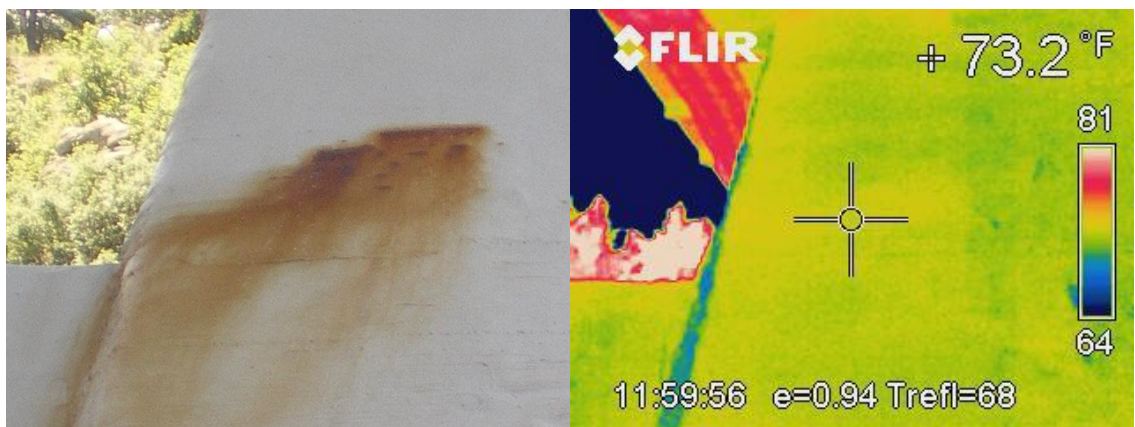


Figure A2. Photograph and thermal image of rust spot

Bay 1NE: 5 Voids, 1 Crack



Figure A3. Bay 1NE, 5 voids

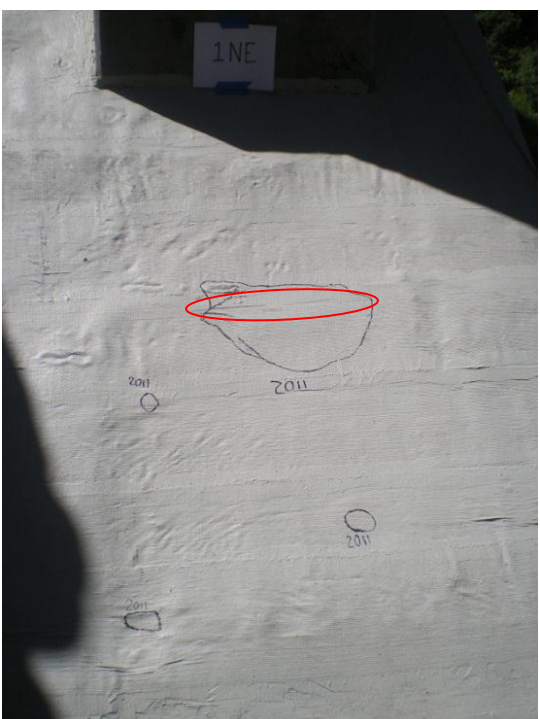


Figure A4. Bay 1NE, 4 of the 5 voids; Crack exists, enclosed in red oval, in the top of the largest void

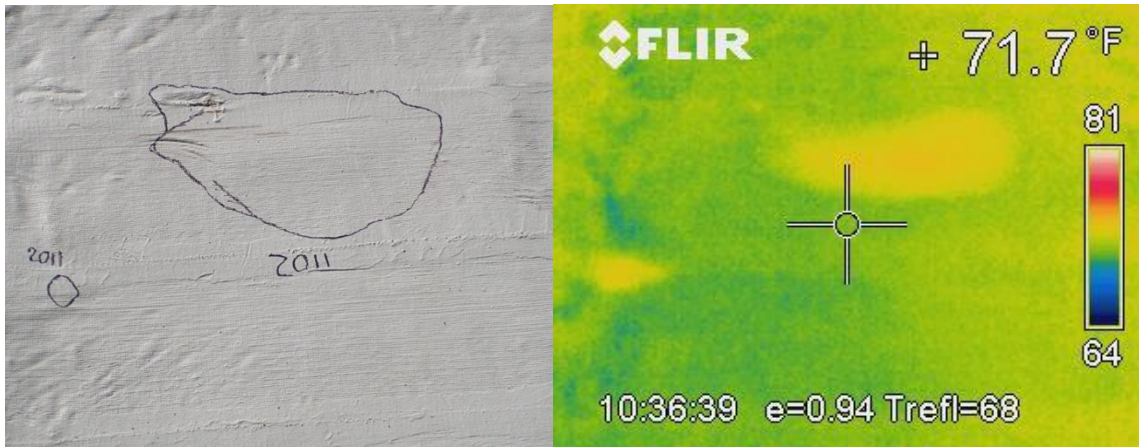


Figure A5. Photograph and thermal image of two voids in Bay 1NE

Bay 2NE: 3 Voids, 1 Crack



Figure A6. Bay 2NE, 3 Voids



Figure A7. Bay 2NE, Crack enclosed in red oval was identified in 2007



Figure A8. Previously identified in 2007, a crack enclosed in the red oval, no debonding at the location of the crack

Bay 3NE: 5 Voids, 2 Were Identified in 2007



Figure A9. Bay 3NE with 1 of the 2 defects found in 2007 shown



Figure A10. 4 of the 5 voids found in 2011



Figure A11. Enclosed in the red circle is 1 of the 2 voids found in 2007

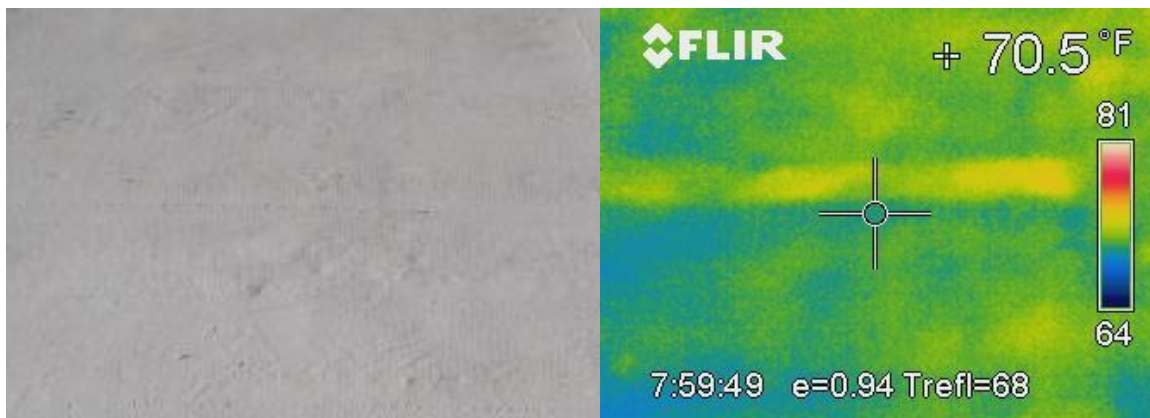


Figure A12. Photograph and thermal image of a seam in the CFRP sheets, no void present

Bay 4NE: 1 Void



Figure A13. Bay 4NE, V-shaped silicone bead water diverter

Bay 5NE: No Defects Found



Figure A14. Bay 5NE

Bay 6E: 2 Voids

No photos available.

Bay 5SE: No Defects Found



Figure A15. Bay 5SE

Bay 4SE: 3 Voids, 1 Was Identified in 2007



Figure A16. Bay 4SE



Figure A17. Void from 2007 has grown and a new void developed

Bay 3SE: 2 Voids, 1 Crack



Figure A18. Bay 3SE

No photograph available for the previously identified cracks in 3SE or the two small voids, but the thermal image is below.

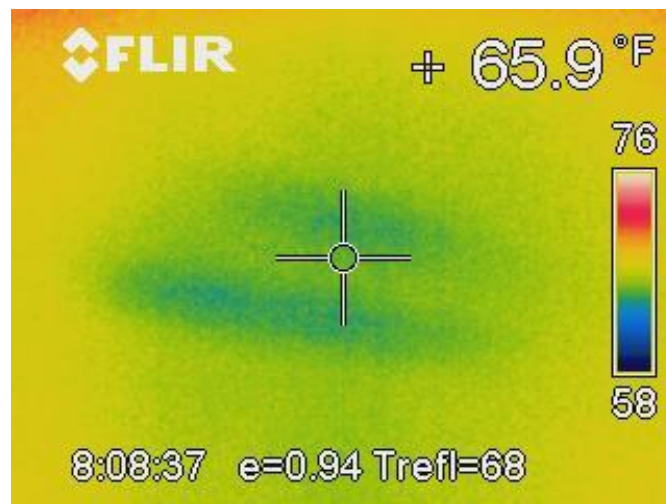


Figure A19. Thermal image of cracks previously identified in 2007

Bay 2SE: 3 Voids



Figure A20. Bay 2SE

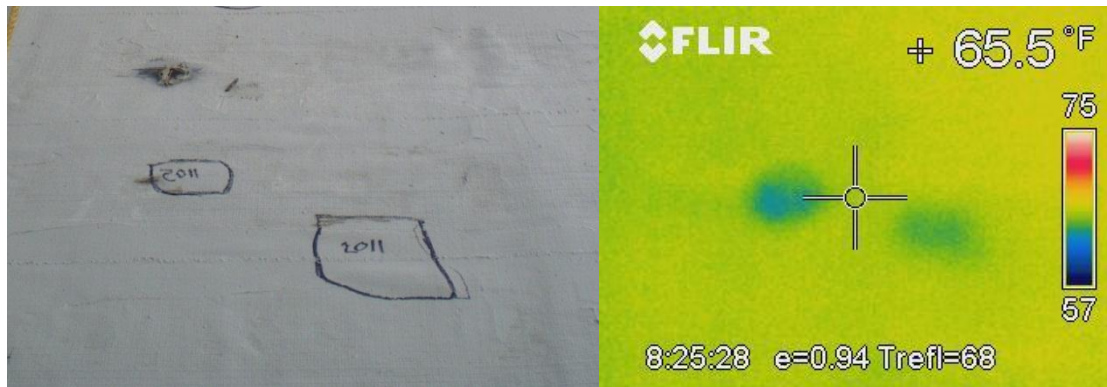


Figure A21. Photograph and thermal image of two voids

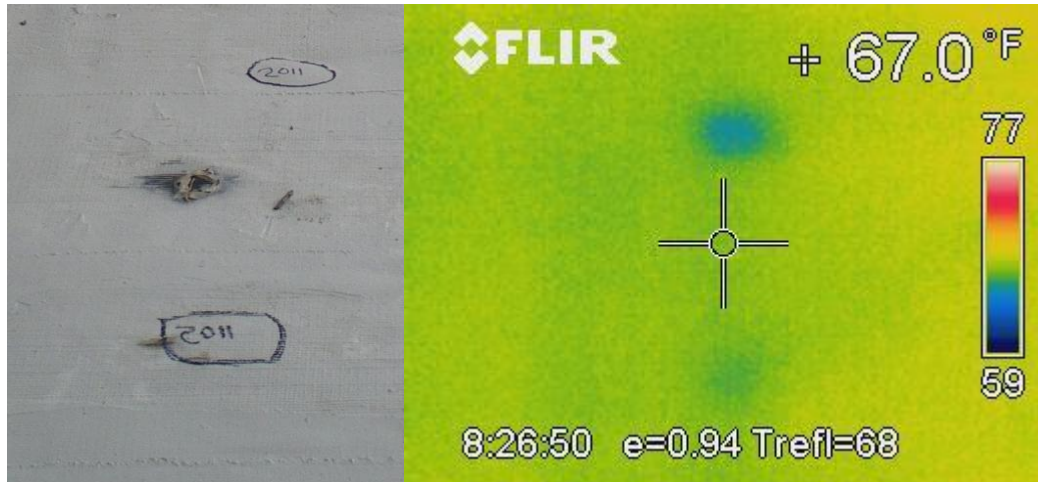


Figure A22. Photograph and thermal image of two voids, the black color in the photograph is left over strain gauges from the work done by Colorado University of Boulder

Bay 1SE: 1 Void



Figure A23. Bay 1SE, 1 void

Bay 1SW: 1 Defect



Figure A24. Photograph and thermal image of a defect found in Bay 1SW

Appendix B: Pull-off Tests

Table B1. Pull-off Test Results from 2011

Global Test Number	Date	Test No.	Core Diameter		Tensile Bond Strength		Failure Mode (ASTM A-G)
			mm	in	MPa	psi	
Test Location: North End of East Arch (1NE)							
1	7/11/2011	1	50	2	1.63	237	F
2	7/11/2011	2	50	2	2.07	300	A
3	7/11/2011	3	50	2	2.93	425	A
4	7/11/2011	4	50	2	1.54	224	E
5	7/12/2011	5	50	2	1.92	279	F
6	7/12/2011	6	50	2	2.39	346	F
7	7/12/2011	7	50	2	2.25	327	F
8	7/12/2011	8	50	2	1.15	167	E
9	7/12/2011	9	50	2	1.35	196	F
Test Location: North End of West Arch (1NW)							
10	7/12/2011	1	50	2	1.03	150	E
11	7/12/2011	2	50	2	NA	NA	NA
12	7/12/2011	3	50	2	1.03	150	E
13	7/12/2011	4	50	2	0.83	120	E
14	7/12/2011	5	50	2	1.15	167	E
15	7/12/2011	6	50	2	0.52	76	E
16	7/12/2011	7	50	2	NA	NA	NA
17	7/12/2011	8	50	2	3.81	553	G
18	7/12/2011	9	50	2	3.42	496	F

Table B1. Continued

Global Test Number	Date	Test No.	Core Diameter		Tensile Bond Strength		Failure Mode (ASTM A-G)
			mm	in	MPa	psi	
Test Location: Center of East Arch (6E)							
19	7/12/2011	1	50	2	3.35	486	B/F
20	7/12/2011	2	50	2	3.09	448	B/F
21	7/12/2011	3	50	2	2.55	370	G
22	7/12/2011	4	50	2	1.98	287	G
23	7/12/2011	5	50	2	0.74	108	G
24	7/12/2011	6	50	2	1.79	260	G
25	7/12/2011	7	50	2	3.08	446	G
26	7/12/2011	8	50	2	0.13	19	G
27	7/12/2011	9	50	2	2.50	363	G

Table B2. Pull-off Test Results from 2003

Global Test Number	Date	Test No.	Core Diameter		Tensile Bond Strength		Failure Mode (ASTM A-G)
			mm	in	MPa	psi	
Test Location: 1SE							
1	6/10/2003	1	50	2	2.59	375	A
2	6/10/2003	2	50	2	3.43	498	A
3	6/10/2003	3	50	2	4.12	597	G
4	6/10/2003	4	50	2	NA	NA	NA
5	6/10/2003	5	50	2	4.09	593	G
6	6/10/2003	6	50	2	3.24	470	G
Test Location: 1SW							
7	6/10/2003	1	50	2	4.07	590	G
8	6/10/2003	2	50	2	3.52	510	G
9	6/10/2003	3	50	2	3.50	508	E
10	6/10/2003	4	50	2	3.34	485	G
11	6/10/2003	5	50	2	3.03	439	A
12	6/10/2003	6	50	2	3.03	440	G

Table B2. Continued

Global Test Number	Date	Test No.	Core Diameter		Tensile Bond Strength		Failure Mode (ASTM A-G)
			mm	in	MPa	psi	
Test Location: 1NW							
13	6/13/2003	1	50	2	3.54	513	A
14	6/13/2003	2	50	2	3.54	514	G
15	6/13/2003	3	50	2	3.94	572	A
16	6/13/2003	4	50	2	3.76	545	A
17	6/13/2003	5	50	2	3.45	501	A
18	6/13/2003	6	50	2	3.25	471	A
Test Location: 6E							
19	6/30/2003	1	50	2	3.03	439	G
20	6/30/2003	2	50	2	3.12	452	G
21	6/30/2003	3	50	2	3.25	471	G
Test Location: 6W							
22	6/30/2003	1	50	2	3.30	478	G
23	6/30/2003	2	50	2	2.72	395	G
24	6/30/2003	3	50	2	2.99	433	G
Test Location: 5SE							
25	7/9/2003	1	50	2	1.32	191	A
26	7/9/2003	2	50	2	1.50	217	G
27	7/9/2003	3	50	2	1.67	242	G
Test Location: 5SW							
28	7/9/2003	1	50	2	2.81	408	E
29	7/9/2003	2	50	2	2.72	395	G
30	7/9/2003	3	50	2	2.90	420	G
Test Location: 5NE							
31	7/17/2003	1	50	2	2.94	427	G
32	7/17/2003	2	50	2	2.76	401	G
33	7/17/2003	3	50	2	NA	NA	NA
Test Location: 5NW							
34	7/17/2003	1	50	2	1.76	255	G
35	7/17/2003	2	50	2	1.89	274	G
36	7/17/2003	3	50	2	NA	NA	NA

Table B2. Continued

Global Test Number	Date	Test No.	Core Diameter		Tensile Bond Strength		Failure Mode (ASTM A-G)
			mm	in	MPa	psi	
Test Location: 4NE							
37	7/17/2003	1	50	2	2.24	325	G
38	7/17/2003	2	50	2	3.03	439	G
39	7/17/2003	3	50	2	2.19	318	G
Test Location: 4NW							
40	7/17/2003	1	50	2	2.68	389	F
41	7/17/2003	2	50	2	2.72	395	F
42	7/17/2003	3	50	2	3.56	516	F

Table B3. Average Values of Bond Strength

Averages	MPa	psi
2003 Tests	2.99	433.36
2011 Tests	1.93	280.00
% Decrease	35.4	

Corresponding photographs to the 2011 pull-off tests:

Bay 1NE



Figures B1 and B2. Tests No.1 and 2



Figure B3. Test No.3, Photograph of Test No.4 is not available



Figures B4 and B5. Test No.5, note puck slid off of center while epoxy was setting, and Test No. 6



Figures B6 and B7. Test No.7 and Test No.8, weak bond strength



Figure B8. Test No.9, weak bond strength

Bay 1NW

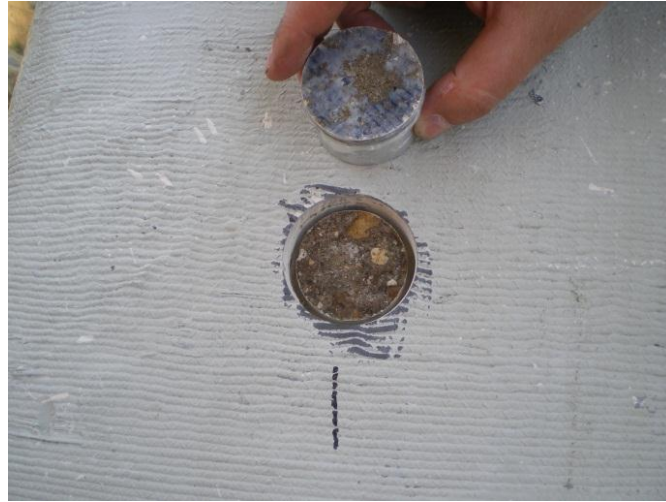


Figure B9. Test No.10, weak bond strength, and Test No.11 not available, cored area failed during drilling

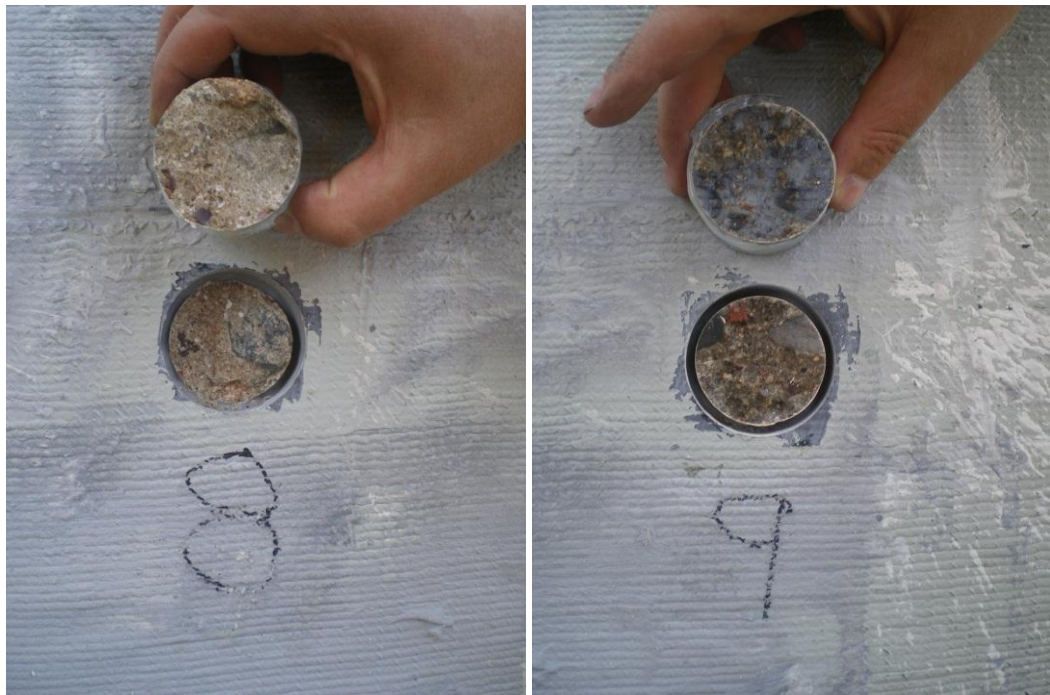


Figures B10 and B11. Test No.12, weak bond strength, and Test No.13, weak bond strength



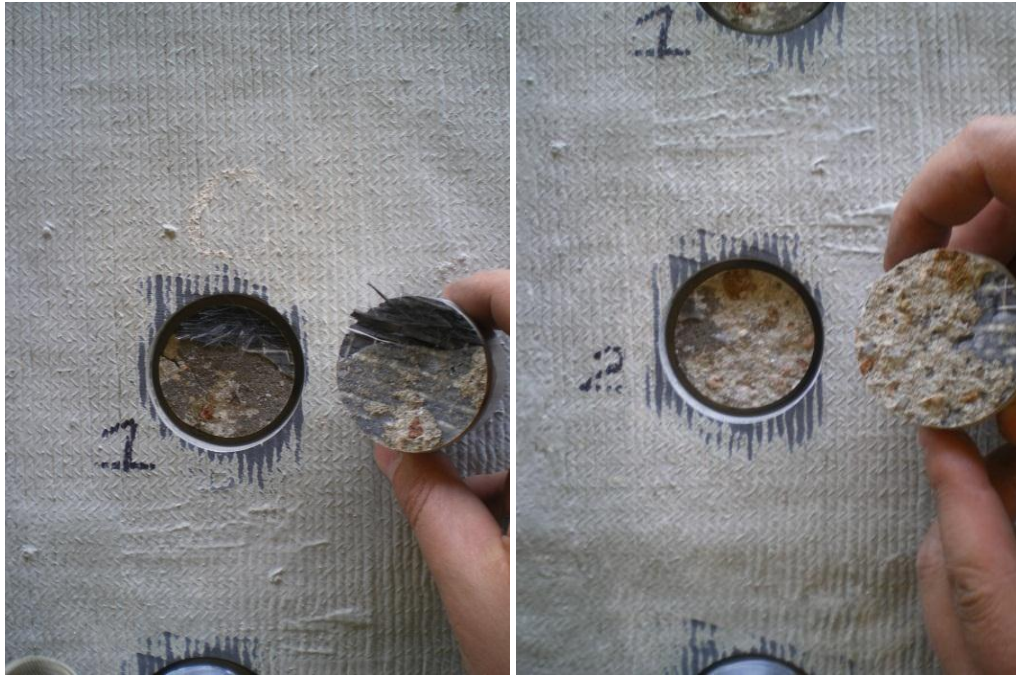
Figures B12 and B13. Test No.14, weak bond strength, and Test No.15, weak bond strength

Test No.16 Not available, puck had faulty threads

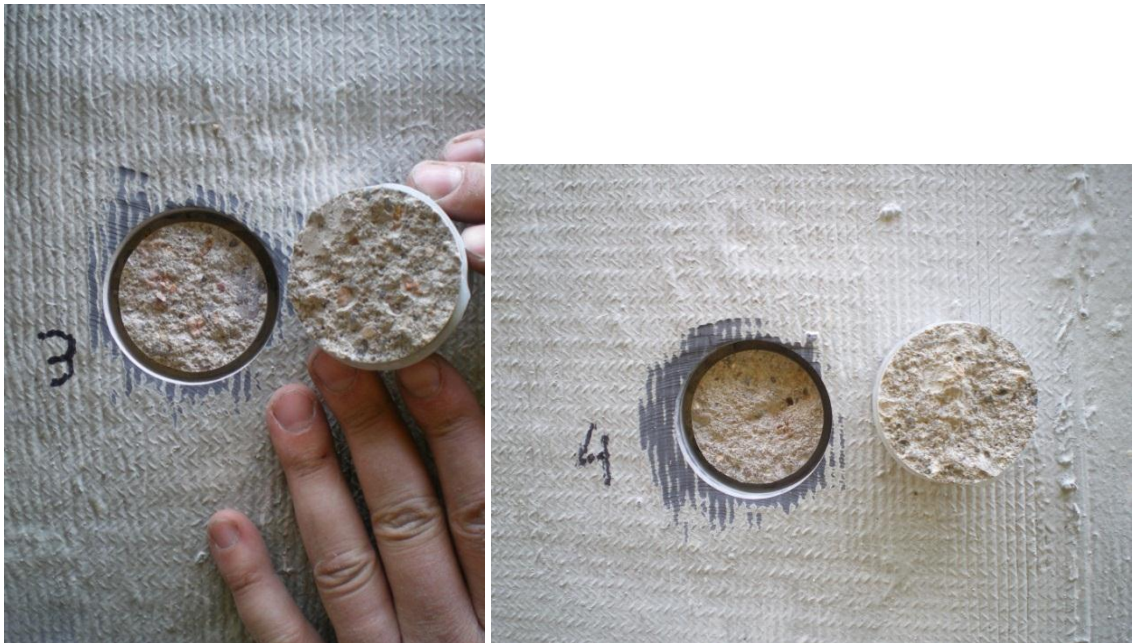


Figures B14 and B15. Tests No.17 and 18

Bay 6E



Figures B16 and B17. Tests No.19 and 20



Figures B18 and B19. Tests No.21 and 22



Figures B20 and B21. Test No.23, weak bond strength (poorly mixed concrete?), and Test No.24



Figures B22 and B23. Test No.25 and Test No.26, note very weak bond strength (poorly mixed concrete?)



Figure B24. Test No.27

Appendix C. Tensile Tests

Table C1. 2011 Tensile Tests

Specimen ID	Width		Thickness		Actual Area of 1 Layer		Normalized Area of 1 Layer	
	mm	in	mm	in	mm ²	in ²	mm ²	in ²
Small Patch from Bay 1NE								
1	25.7	1.01	2.39	0.09	61.3	0.10	26.1	0.040
2	25.9	1.02	2.95	0.12	76.2	0.12	26.3	0.041
3	27.0	1.06	3.23	0.13	87.0	0.13	27.4	0.042
4	25.9	1.02	3.20	0.13	82.9	0.13	26.3	0.041
5	25.8	1.02	2.87	0.11	74.1	0.11	26.2	0.041
6	26.0	1.02	2.79	0.11	72.6	0.11	26.4	0.041
7	25.9	1.02	2.67	0.11	69.0	0.11	26.3	0.041
8	25.9	1.02	2.54	0.10	65.7	0.10	26.3	0.041
9	25.9	1.02	3.15	0.12	81.5	0.13	26.3	0.041
10	25.2	0.99	3.63	0.14	91.6	0.14	25.6	0.040
11	25.8	1.02	3.53	0.14	91.1	0.14	26.2	0.041
12	25.9	1.02	3.11	0.12	80.5	0.12	26.3	0.041
Large Patch from Bay 3NE								
1	26.1	1.03	3.15	0.12	82.2	0.13	26.5	0.041
2	26.5	1.04	3.33	0.13	88.2	0.14	26.9	0.042
3	26.0	1.02	3.56	0.14	92.4	0.14	26.4	0.041
4	26.2	1.03	3.53	0.14	92.5	0.14	26.6	0.041
5	26.0	1.02	3.48	0.14	90.5	0.14	26.4	0.041
6	26.6	1.05	3.33	0.13	88.5	0.14	27.0	0.042
7	25.5	1.00	3.48	0.14	88.6	0.14	25.9	0.040
8	26.5	1.04	3.58	0.14	94.9	0.15	26.9	0.042
9	26.5	1.04	3.35	0.13	88.7	0.14	26.9	0.042
10	25.9	1.02	3.51	0.14	90.9	0.14	26.3	0.041
11	26.4	1.04	3.12	0.12	82.5	0.13	26.8	0.042
12	26.4	1.04	3.61	0.14	95.3	0.15	26.8	0.042
Manufacturer's Data			1.01 6	0.04				

Table C1. Continued

Specimen ID	Tensile Force		Normalized Tensile Strength		Normalized MoE		Rupture Strain	Failure Mode
	N	lb (f)	MPa	ksi	GPa	ksi		
Small Patch Removed from Bay 1NE								
1	1197	5324	36.7	5.3	79.3	11506	0.00046	SGM
2	1100	4892	16.9	2.4	87.7	12714	0.00019	LAT
3	1064	4732	10.9	1.6	74.8	10852	0.00015	LAB
4	1039	4621	8.0	1.2	88.2	12795	0.00009	LWB
5	939	4176	5.8	0.8	84.6	12272	0.00007	SGM
6	1123	4996	5.7	0.8	82.7	11998	0.00007	SGM
7	1305	5807	5.7	0.8	72.2	10476	0.00008	XGM
8	1115	4960	4.3	0.6				SGM
9	1106	4920	3.8	0.5	103.3	14982	0.00004	MAB
10	907	4035	2.8	0.4	66.5	9649	0.00004	LGM
11	1050	4669	2.9	0.4	71.3	10335	0.00004	LGM
12	1149	5110	2.9	0.4				AWT
Large Patch Removed from Bay 3NE								
1	878	3906	26.9	3.9				SAB
2	1115	4961	17.1	2.5	75.4	10942	0.00023	LWB
3	840	3737	8.6	1.2	61.1	8855	0.00014	LAB
4	1041	4632	8.0	1.2	69.8	10123	0.00011	LAT
5	756	3365	4.6	0.7	88.1	12779	0.00005	SGM
6	1164	5179	6.0	0.9	72.2	10477	0.00008	MGM
7	933	4151	4.1	0.6	91.4	13255	0.00004	SAT
8	1274	5666	4.9	0.7	85.5	12397	0.00006	LAT
9	960	4269	3.3	0.5	102.3	14843	0.00003	LAT
10	1078	4795	3.3	0.5	61.6	8929	0.00005	LWB
11	781	3474	2.2	0.3	54.8	7955	0.00004	LAB
12	297	1320	0.8	0.1	51.3	7437	0.00001	LAB
Manufacturer's Data			875.6	127	72.4	10500	0.01210	

Table C2. Average Values for each Sample

Averages	Tensile Force		Normalized Tensile Strength		Normalized MoE		Rupture Strain
	N	lb(f)	MPa	ksi	GPa	ksi	
Bay 1NE	1091	4854	820	119	81	11758	0.010121
Bay 3NE	926	4121	688	100	74	10726	0.009306
Total	1009	4487	754	109	78	11242	0.009713

Appendix D: Differential Scanning Calorimetry (DSC)

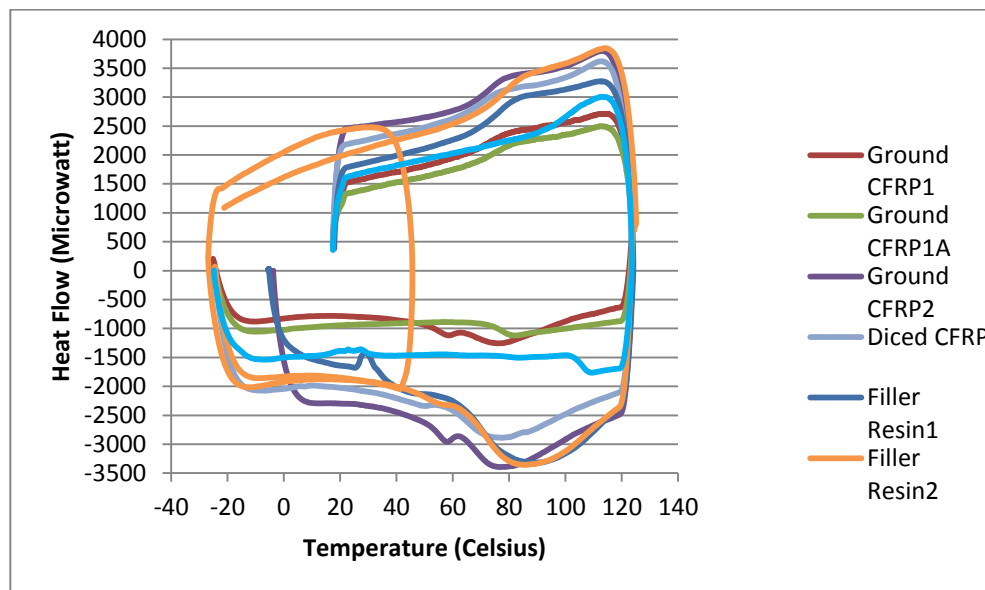


Figure D1. Differential Scanning Calorimetry Curves

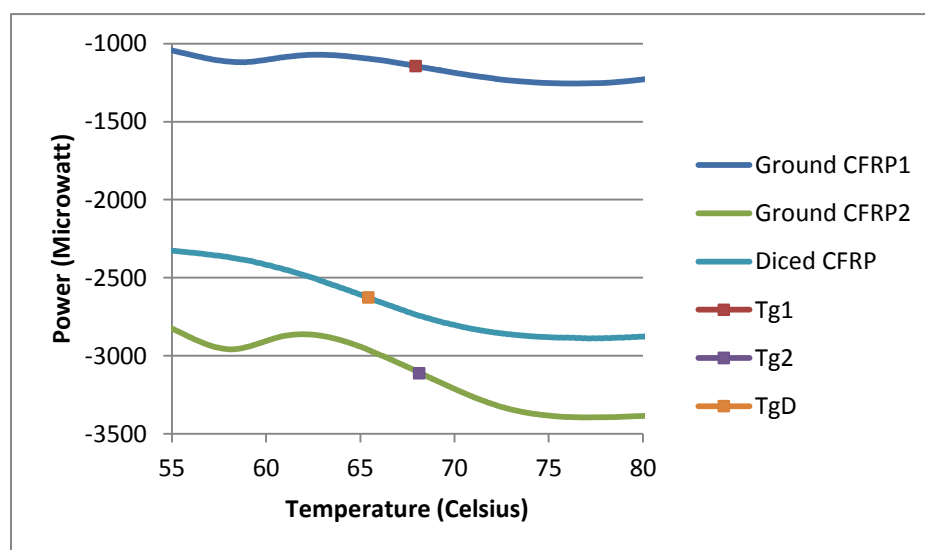


Figure D2. Close up of T_g Regions

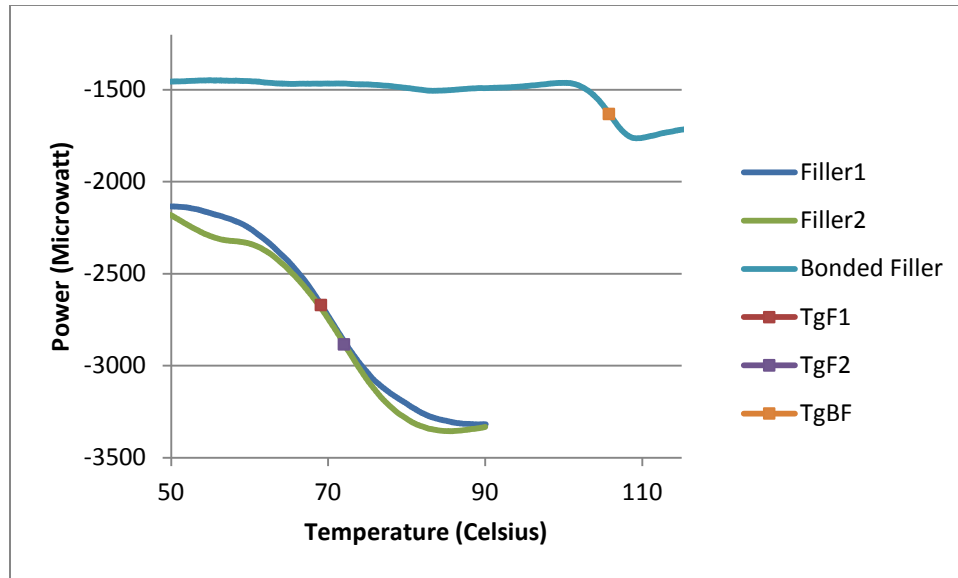


Figure D3. Close up of T_g Regions